Launch Vehicle First Stage Reusability

Technische Universiteit Delft

Launch Vehicle First Stage Reusability

a study to compare different recovery options for a reusable launch vehicle

M. D. Rozemeijer

Launch Vehicle First Stage Reusability

a study to compare different recovery options for a reusable launch vehicle

by

M. D. Rozemeijer

to obtain the degree of Master of Science
at the Delft University of Technology,
to be defended publicly on **Tuesday December 1st, 2020 at 09:00**.

Student number:	4141733	
Project duration:	April 23, 2019 – December 1, 2020	
Thesis committee:	Ir. B. T. C. Zandbergen,	TU Delft, supervisor
	Dr. A. Cervone,	TU Delft
	Ir. M. C. Naeije,	TU Delft

TU Delft

Preface

This report concludes, and is the culmination of, my Master thesis to complete the master curriculum in the field of Aerospace Engineering. Besides this, it also, hopefully, answers part of the question on how to make access to space easier.

I have been working in the field of entry descent and landing since the start of the Stratos III project in 2016. This is also the start of the ParSim tool, which is the base of my thesis tool. Back then it was only able to recover part of the Stratos III rocket. This tool expanded to encompass the demands for the other projects I have been working on within Delft Aerospace Rocket Engineering (DARE), which are Project Aether and the Supersonic Parachute Experiment Aboard Rexus (SPEAR) all within the Parachute Research Group. Besides the tool, working on these projects increased my knowledge of Entry, Descent and Landing tremendously. This all led to the publication of several articles at the AIAA 2018, IAC 2018 and EUCASS 2019.

I would like to thank B.T.C. Zandbergen for supervising my thesis, giving me the push to look a bit further sometimes and other times getting me back on the right course with his feedback and ideas. I would like to thank my teammates from the Parachute Research Group for the research over the years. As well as for some of the data used in this research.
In particular, I would like to thank Lars Pepermans & Thomas Britting for helping in developing ParSim which is the basis of the tool build for this research.
Lastly, I would like to thank my friends and family for supporting me during the whole of my studies and pushing me to where I am now and supporting me through the tough and difficult year that was 2020.

M. D. Rozemeijer
Delft, November 4th, 2020

Summary

Going to space is an expensive endeavour, even the cheapest option costs €2719 per kilogram of payload to a low earth orbit (LEO). Since the cost of satellites is decreasing, the demand for low-cost launches is increasing. Currently, for most of the launchers, the first stage is expendable, meaning they are only used once. This seems a waste of such an expensive element costing in the millions of euros. Literature indicates that potentially the launch cost be driven down by at least 30% when reusing the first stage at least ten times, but proof is not yet substantial. In addition, although many investigations have been previously performed they mostly focused on only one option. In this research more than one option will be considered. Questions tackled in this work are: What the best method is to decelerate the stage? What is the best way for a landing the stage? Is it better to only recover the engine or the complete stage and does the target orbit make a difference?

To make a stage reusable several elements are needed. First, a deceleration system is needed. In this research four systems are considered including parachutes, both sub- and supersonic, a hypersonic inflatable aerodynamic decelerator, grid fins and/or propulsive landing. For the landing system, both airbags and landing legs are used. To do so, a tool is made that encompasses multiple models. These are mostly mass and cost models for the various deceleration and landing systems. But also models to be able to increase the propellant tank and to predict the thrust and the drag forces accurately. All these models are included in a tool for which a surrogate optimisation is used to determine which deceleration and landing system produces the cheapest option. Thereby taking into account not only the production cost but also refurbishment and retrieval costs.

For design optimisation, surrogate optimisation method is used. The surrogate optimisation is a relatively new optimisation algorithm that creates a surrogate function which is minimised and evaluated in order to find the global optimum. Although less accurate than the genetic optimisation, which is the benchmark global optimisation algorithm, it can produce a result in 20% of the time. Although it is significantly faster, it does not produce the same result as the genetic algorithm but a solution within 1% of the genetic optimisation algorithm. The difference in the objective function is accepted, because of the difference between the computation time which is 20min-60min for the surrogate optimisation and 2-26hrs for the genetic optimisation.

Two vehicles are investigated for two different target orbits. These are the Falcon 9, which is designed with reusability in mind, and a modified version of the Delta IV, the Delta IV+, which is an expendable launcher. The two orbits are a circular low earth orbit and a geostationary transfer orbit. The payload mass for the Falcon 9 is 15600 kg and 6500 kg, for LEO and GTO respectively and the payload masses for the Delta IV+ are 9000 kg and 4500 kg for the LEO and GTO respectively. These payloads are the highest proven payloads flown. For the four combinations of vehicle and orbit, three separate cases are investigated. Two cases where the complete stage is recovered, using either retro-propulsion or non-propulsive means. The last case is one where only the engine is recovered using non-propulsive means. For all of the cases, the descent deceleration needs to be lower than 10 g and have a maximum dynamic pressure below 200 kPa.

For all the cases, it was found that 30% cost savings could not be achieved. For the Falcon 9 the savings came closest to the 30% but did not reach it. This 28% cost saving was achieved by reusing the complete stage, the difference between non-propulsive and retro-propulsion was minimal, but the non-propulsive way was slightly cheaper. There was no significant difference between LEO and GTO missions since for the Falcon 9 the second stage produced more than 50% of the ΔV of the launcher. This leads to a separation velocity around 2000-3000 m/s where the orbital velocity is 7700 m/s for a LEO and 10100 m/s for a GTO.

For the Delta IV it was seen that reusing the complete stage becomes more expensive than reusing only the engine. This is due to the high separation velocity, which is in the range of 3500-5000 m/s, these are significantly higher than for the Falcon 9. Recovering from these separation velocities, requires a larger and therefore heavier system to decelerate the first stage. But by making the system larger it becomes more expensive. Furthermore by making it larger the risk of going over the deceleration limit is higher. The maximum savings achieved for the Delta IV is 20%, this is for recovering only the engine. Again here there was little difference between the solution for LEO and GTO.

So overall, 30% cost savings could not be achieved. However, there can still be significant savings by reusing the first stage. From the results, it became clear that using a Hypersonic Inflatable Aerodynamic Decelerator and a Ringsail parachute is the best option to decelerate the system. For the landing system, both airbags and mid-air retrieval were used for the optimal solution. Furthermore, it was seen that the deceleration constraint is the leading constraint, and the dynamic pressure limit comes close to the limit when the stage has a small reference area for the drag. There was little difference between LEO and GTO for the two vehicles. However, there were substantial differences between the two vehicles. Interestingly, the maximum savings are achieved between 8-15 reuses meaning that more reuses is not always better. The reason for this minimum is because the expendable case decreases in cost the more launchers are produced. On top of this, the refurbishment cost increases with the number of reuses. This results in the minimum point around ten reuses.

Contents

List of Figures

List of Tables

Nomenclature

Abbreviations

AIT	Assembly Integration and Test.
DLR	German Aerospace Center (Deutsches Zentrum für Luft- und Raumfahrt).
DRL	Down-range landing.
FRT	First stage reusable tool.
GA	Genetic algorithm.
GTO	geostationary transfer orbit.
GTOW	Gross take-off weight.
HIAD	Hypersonic Inflatable Aerodynamic Decelerator.
LEO	Low earth orbit.
MAR	Mid-air Retrieval.
PSO	Particle Swarm Optimisation.
RLS	Return to launch site.
RSME	Root-square-mean-error.
SO	Surrogate Optimisation.
TSTO	Two stage to orbit.
ULA	United Launch Alliance.

Conversion Factors

1 $[kg/m^3]$	0.001940320 $[slug/ft^3]$
1 $[kg]$	2.20462262 $[lbs]$
1 $[m]$	3.2808399 $[ft]$
1 $[W/m^2]$	8.805509170e-05 $[Btu/(ft^2 s)]$

Greek Symbols

Γ	Vandenkerckhove function	$[-]$
γ	Specific heat ratio	$[-]$
μ	Standard gravitational parameter	$[m^3/s^2]$
Ψ	Thrust-to-Weight ratio	$[-]$
ρ	Density	$[kg/m^3]$
ρ_0	Density at sea-level	$[kg/m^3]$
ρ_p	Propellant density	$[kg/m^3]$

σ_{ult}	Ultimate strength	$[Pa]$
θ	Pitch angle	$[deg]$
φ	Flight path angle	$[deg]$

Latin Symbols

Δm_{empty}	Difference between empty masses	$[kg]$
$\dot{m}$	Mass flow	$[kg/s]$
a	Semi-major axis	$[m]$
A_e	Nozzle exit area	$[m^2]$
A_t	Nozzle throat area	$[m^2]$
$A_{parachute}$	Parachute reference area	$[m^2]$
C	Cost	[Man-Year]
c	Material cost	$[\$/unit]$
$C(B)$	Production cost of the hardware to be reused	[$]
$C(RHW)$	Reused portion of the cost to recover and reuse	[$]
$C(RR)$	Expended portion of the cost to recover and reuse	[$]
C_D	Drag coefficient	$[-]$
C_k	Opening shock factor	$[-]$
C_x	Opening force coefficient at infinite mass	$[-]$
C_{MY}	Cost of a Man-year of work	[€]
D	Diameter	$[m]$
D_0	Parachute reference diameter	$[m]$
F	factor representing increase in unit production cost with decreasing production rate	$[-]$
F_D	Drag force	$[N]$
F_T	Thrust force	$[N]$
$F_{ATM,final}$	Ratio between the different tank masses after final correction	$[-]$
$F_{ATM,new}$	Ratio between the different tank masses after one correction	$[-]$
F_{ATM}	Ratio between original and modified tank mass	$[-]$
g	Gravitational acceleration	$[m/s^2]$
H	Altitude	$[m]$
I_{sp}	Specific impulse	$[s]$
k	fraction of the production cost that is reused	$[-]$
M	Molar mass	$[g/Mol]$
m	Mass	$[kg]$
n	Number of reuses	$[-]$

$n_{flotation}$	Amount of flotation devices	$[-]$
p	Ratio of payload loss of the reusable compared to the expendable launcher	$[-]$
P_a	Atmospheric pressure	$[Pa]$
p_c	Chamber pressure	$[Pa]$
p_e	Exit pressure	$[Pa]$
P_{hyd}	Hydrostatic pressure	$[Pa]$
P_{MEOP}	Maximum operating pressure	$[Pa]$
P_{vapour}	Vapour pressure	$[Pa]$
q	Dynamic pressure	$[Pa]$
q_s	Convective heat flux	$[W/m^2]$
R	Radius	$[m]$
R_E	Earth radius	$[m]$
R_N	Nose tip radius	$[m]$
r_{pe}	Radius of periapsis	$[m]$
$R_{specific}$	Specific gas constant	$[J/(kg \cdot K)]$
RI	Reuse Index	$[-]$
S	Surface area	$[m^2]$
T	Temperature	$[K]$
t	Thickness	$[m]$
t	Time	$[s]$
T_c	Flame temperature	$[K]$
t_f	Parachute inflation time	$[s]$
T_{MYrH}	Hours in a working year	$[hr]$
t_{travel}	Travel time	$[s]$
V	Velocity	$[m/s]$
v_1	Velocity at parachute inflation	$[s]$
V_e	Exit velocity	$[m/s]$
$V_{displacement}$	Displacement volume	$[m^3]$
V_{eq}	Equivalent exhaust velocity	$[m/s]$
$v_{landing}$	Landing velocity	$[m/s]$
V_{sphere}	Sphere volume	$[m^3]$
X_1	Opening force reduction factor	$[-]$
u	The circumferential velocity component normal to the radius vector	$[m/s]$

Subscripts

∞	At free stream conditions.

1 Introduction

Space travel is hard enough without worrying about the cost of it. However, reducing the cost seems to be the driving factor of space travel today. The cheapest launch of a satellite per kilogram of payload is €2719[101]. This is for the Falcon 9 fully expendable launcher to a low earth orbit (LEO). To go higher is only more expensive.

Two things can be done to drive the specific payload cost down. Either elements of the first stage can be recovered, or the production of the launcher can be made cheaper. Reducing the production cost is most likely achieved through standardising and mass production of parts. However, this is hard for a field in which the total number of launches per year is around 100 divided over multiple competitors[55]. For recovering elements, a balancing act will have to be performed where the increased initial cost, the reduced learning curve and the extra mass have to weigh against the number of reuses the system can handle. For recovering elements of the rocket again a couple of avenues can be pursued. This can be either recovering the first stage of the launcher or recovering the second stage of the launcher. For this work, the focus will be on the recovery of the first stage. The reusability of the second stage was done by L. Pepermans[77]. For the first stage recovery, a division can be made of recovering only the engine or the entire stage. The first option can be advantageous since according to ULA [4] the cost of the engine can be 60% of the cost but only 25% of the weight for the first stage. However, there is no distinct method of when to use which element to recover. As well as what recovery method is best and how many reuses are required to make reusable first-stages an advantageous option.

As this is not entirely a standalone work, it should be discussed in what frame this work fits. First of all the works of F. Miranda and M. van Kesteren [68, 112]. They worked on the trajectory optimisation of small launchers. This was mostly focused on the comparison between air-launched and ground launched solid and hybrid rockets. They both concluded that about 70% of the Gross Take-Off Weight (GTOW) could be saved by air-launching for a payload of 10kg [68, 112]. The save in GTOW would, however, decrease when the payload mass is increased. From these works, the ascent optimisation for minimum mass can be used. The work of L. Pepermans [77], which focused on reusing the upper stage of launchers and looking at what the best system is to return upper stages to earth and reuse them in the most commercially viable manner. S. Constant investigated the commercial viability of creating a reusable small orbital launcher[31]. This launcher is landed using only propulsive means. On top of that M. Snijders investigated the reusability of the small innovative launcher for Europe, which is also a small satellite launcher[99]. Finally, T. Haex investigated the design of a small satellite two-stage to orbit spaceplane concept, which is semi-reusable [45]. From these various mass and cost models can be used as well as their methodology and recommendations.

From the literature study, done before the thesis, it became clear what the options are for recovering the first stage but not what the best option is[95]. Therefore an investigation should be done into how to best recover the first stage of a rocket. For this reason, the following research question is proposed:

Is it feasible to reduce the launch cost with 30% by recovering the first stage of an existing launcher, given a launch rate of 10 launches per year?

Existing launchers are used since the development cost of a launcher is significant[95]. The 30% is chosen because of the claims made by Ariane[6, 32], and it should at least match these savings. The 10 reuses comes from a statement made by Elon Musk that Falcon 9 is completely reusable for at least 10 relaunches, after which according to Musk "heat shields and a few other items" need to be replaced[72]. This serves than as the main point of interest for the amount of reuses. This main research question can be divided into multiple parts:

1. ***What is the best deceleration method to have a minimal first-stage cost?*** - Which deceleration method would be optimal for recovering the first stage of a launcher. This would concern not only the production cost but also the operational cost.

2. ***What is the impact of the landing method on the launch cost per kilogram of payload?*** - What is the difference concerning the launch cost when using different landing methods (landing gear, mid-air retrieval or airbags).

3. ***What is the additional mass/cost that is needed to make an expendable first stage into a reusable first stage?*** - By changing an expandable first stage into a reusable one, mass in the form of a deceleration system and a landing system are needed. What is the required mass/cost in order to achieve a landing?

4. ***What is the effect of the number of launches on the cost savings?*** - When does a launcher become cost-effective, since adding a recovery system would increase the initial cost however reusing it will decrease the launch cost.

5. ***Is it better to recover only the engine or the entire stage?*** - Would recovering only the engine be better than recovering the entire stage with regard to the cost per launch.

6. ***What is the influence of the target orbit?*** - Does it matter to which orbit the payload needs to be delivered? If so, how much is the influence of the orbit?

The research will be limited to only investigating restartable bi-propellant engines to be able to use the same engine for the ascent as for descent if required. As well as using an existing launcher a a base. This is done for two reasons, first is to be able to focus on the reusability of the launcher and not designing the launcher, only modifying it. The second reason is that it is expensive to develop a launcher. The estimated development cost for the Falcon 9 is around 400 M$ [31, 38]. For this reason it is more economical to modify the existing launcher to be reusable instead of developing a completely new launcher.

Within the TU Delft the research is mostly focused on the small launcher market. The rest of the research on reusable launcher is either focused on propulsive landing, like the Falcon 9, or on winged vehicles either fully or partially. The winged vehicle can either be only recovering the engine, as with the Adeline concept, or recovering the complete stage as can be found in research performed by DLR [32, 98, 103]. Although these concepts are being researched scientific publications are limited. The research from DLR although published focuses mostly on the mass and the trajectory of the launcher and does not focus on the cost of the launcher. These researches usually only examine one or two of the options, but they do not compare the whole field. They mostly focus on the mass and the trajectory and not the cost of the launcher. This research will focus on comparing various concepts for the reusability of the first stage on the basis of cost as well as the trajectory flown

The report is divided into seven chapters, of which this is the first. Next, background information to create a full view of what is required to reuse a stage. After this, in chapter 3, various mass models and physics models are discussed in order to cover the various elements encountered during the descent flight. The cost models are discussed in chapter 4 these are the cost models for the entire launch vehicle, the various deceleration systems and the refurbishment. In chapter 5, the tool is discussed that is made to answer the research question. For the tool, the inputs are discussed as well as the optimisation loops that are involved. Then using the tool various cases will be examined in chapter 6. The cases will be for the Falcon 9 and for a modified version of the Delta IV. Finally in chapter 7 the conclusion and recommendations are given.

2

Background

What does an expendable stage need to make it reusable and what goes into discovering what the best solution is. In this chapter, first, a brief overview is given of what is required for a reusable launcher. This is followed by the previous missions to give an overview of the current reusable concepts. Following this, there are some notes on the optimisation algorithms that will be required for both vehicle design and trajectory. Finally, there will be some information on the sensitivity analysis that will be performed.

2.1. Reusable First Stage Overview

To see how much the flight cost is decreased, multiple elements need to be thought of. Besides needing something to land the stage safely, other elements are required. An overview can be seen in Figure 2.1. All elements in Figure 2.1 are covered in the section below, with the exception of the launch preparations and separation.

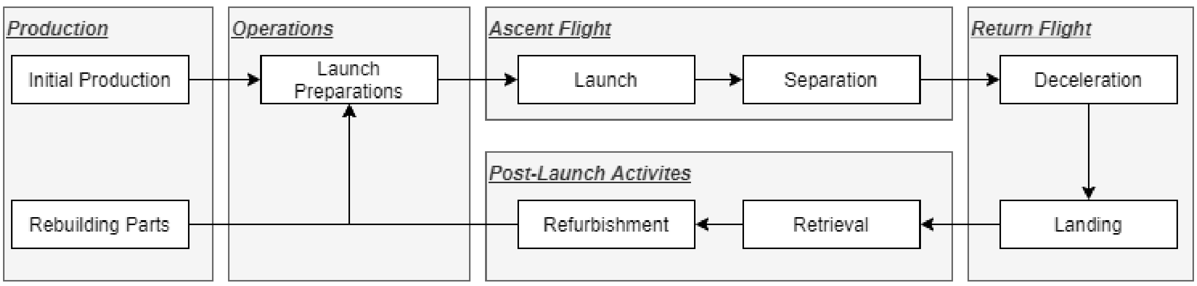

Figure 2.1: Overview of a life cycle of first stage reusable launcher

2.1.1. Launch

The first stage itself does not reach orbit, but it does need to give the required ΔV to reach the target orbit. Two orbits will be used in this study to compare the different requirements for a reusable launcher. The first is a circular low earth orbit (LEO), this is a relatively standard orbit used for most satellites[55]. The second orbit is a geostationary transfer orbit (GTO), this orbit is highly elliptical that has its perigee altitude usually around 200-500 km and an apogee altitude that is around 35000 km. The two target orbits that will be used in this research can be found in Table 2.1. These orbits are used because they have a different ΔV requirement and different inclination.

Table 2.1: Overview of the orbits flown

Mission	Apoapsis - Periapsis altitude [km]	Velocity at Periapsis [m/s]	Inclination [deg]
LEO	290 - 290	7736	53
GTO	32827 - 218	10162	28

2.1.2. Deceleration Systems

A deceleration system is one which performs everything between separation and the final landing phase that decreases the velocity. The landing phase only has to put the system safely on the ground coming from its final velocity. To recover a first stage one needs to decelerate the system from velocities at separation which can be in the order of 4km/s [3] to a landing velocity. The drag from the body itself already dissipates much energy; however, this is not enough. Therefore an additional deceleration system is needed. However, that is not all that is needed. Next to a deceleration system, also a landing system is needed as well as a place to land. This is discussed in subsection 2.1.3

Six main types of deceleration systems have been identified during the literature study [95]. These are parachutes, inflatables, deployables, rotor system, winged system and retro propulsion. However, not all fall within the scope of this research. First of all, the winged systems this is a field of itself and could be a separate research as was done by Haex[45]. Furthermore, this would alter the stage too much as was seen in the literature study [95]. Next is rotor systems which on the surface is promising, but the TRL system is not yet at the level that it can be used[95]. All the other systems will be discussed briefly.

Parachutes are the standard system to decelerate something. It is used from skydiving to the Apollo capsule. Parachutes usually come in two main categories. The main distinction between these categories is if the parachute can be used in supersonic conditions. Within these categories, there are differences until which Mach number they can be used, but this is the critical distinction. Therefore for this research also two parachutes will be used one capable of supersonic flight and one that can function only in subsonic conditions. These parachutes are the Ringsail parachute, Figure 2.2, which is a subsonic parachute capable of going to Mach 0.5[52]. This is also the main parachute used on Mercury, Gemini and Apollo missions[35]. The second parachute is the Hemisflo Ribbon Parachute, Figure 2.3. This parachute can handle high dynamic pressure and has a large operational range being capable of handling speeds up to Mach 3[52, 80].

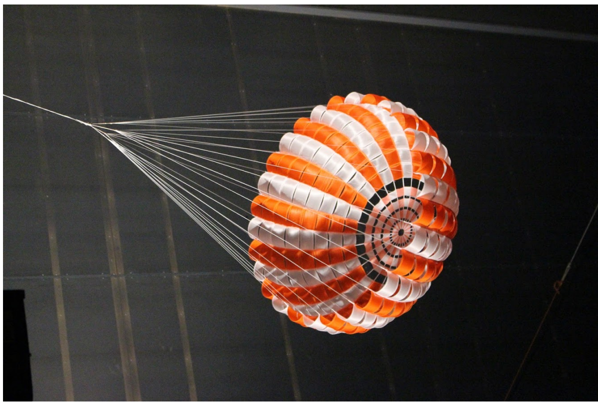

Figure 2.2: Figure of a Ringsail parachute being tested by DARE in the TU Delft Open Jet Facility

Figure 2.3: Figure of a Hemisflo Ribbon parachute being tested by DARE in the TU Delft Open Jet Facility

Besides the differences in maximum Mach number the Hemisflo ribbon parachute has a lower base C_D value, 0.3 compared to the 0.5 for the Ringsail [52]. Also, because the Hemisflo Ribbon parachute is used in supersonic conditions, it will most likely meet higher temperature during the descent. Therefore the Hemisflo Ribbon parachute will be made out of Aramids, rather than the nylon for the Ringsail.

Inflatables are systems that are stored safely during launch when they are not needed and can be inflated upon command. Recently ULA together with NASA have been investigating a Hypersonic Inflatable Aerodynamic Decelerator (HIAD) for possible use on Mars. However, there are also possibilities to be used for reusable stages[34, 77, 83]. These can be designed to work in hypersonic regimes and can also act as a heat shield during re-entry. The advantage of a HIAD over a supersonic parachute is that the HIAD does not need air to inflate as it has its own inflation mechanism. This means it can be deployed in vacuum conditions before re-entry whereas a parachute cannot.

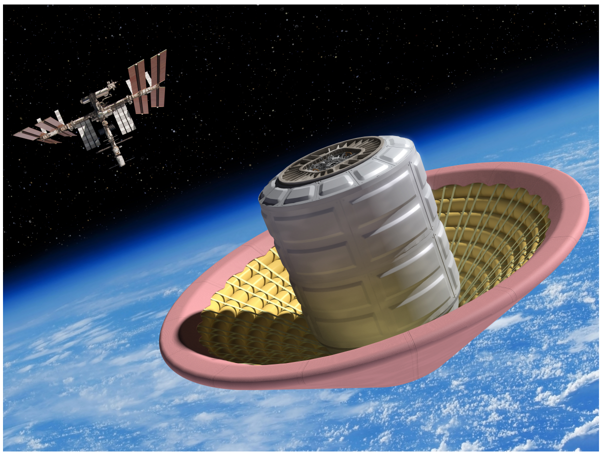

Figure 2.4: Overview of a HIAD system

Deployables are, much like inflatables, stored until they are needed. However, the main difference between the two is that deployables consists of rigid elements that are stored. This means deployables usually do not change their shape that significantly compared to inflatables. The prime example of deployables is the grid fins used by SpaceX on their Falcon 9 launcher, Figure 2.5.

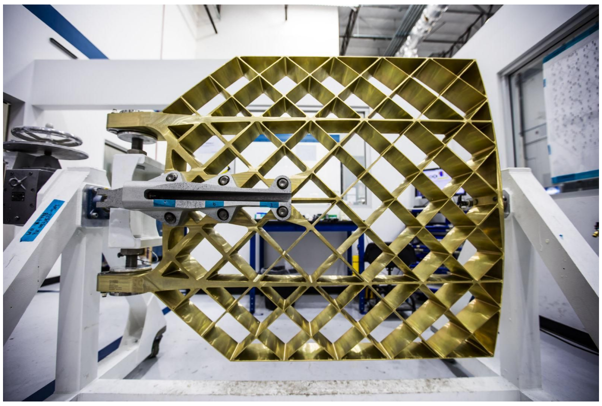

Figure 2.5: The Falcon 9 Grid Fin [31]

Retro propulsion, or propulsive landing, is the method where the main engine is used to land the system. The primary example is again the Falcon 9 launcher. Propulsive landing has the advantage that no other system has to be built to decelerate the launcher. However, this means taking either extra propellant or reserve a certain amount of propellant for the descent of the launcher. This propellant needs to cover a possible deceleration before re-entry to limit the heating and to land the system safely. The fact that extra propellant needs to be reserved means this propellant cannot be used for the ascent.

2.1.3. Landing & Retrieval

For the landing, there are two separate issues. The first is the landing system; the second is the landing location. For the landing system, a couple of methods can be used to bring the vehicle to a standstill. This can be done through a couple of methods. First is mid-air capture, this is where usually under a parachute, an aeroplane/helicopter is used to catch the system in mid-air and return it to land. This is proposed for the new Vulcan launcher[83]. This option is limited by the carrying capacity of the aeroplane/helicopter, which is used. Another method is to use landing legs. This option is being used for the Falcon 9 rocket [100]. With landing legs, the system is deployed and locks into place after which the suspension of the landing legs absorbs the last bit of energy. The final option is airbags which are placed on the bottom surface of the system. Once the system comes close to the ground, the airbags deploy, creating a cushion absorbing the force. This is currently being used on the new crew vehicle made by Boeing [82]. If the stage lands on water without the benefit of a platform, the stage will need a flotation device to keep the stage afloat in the water.

For the landing location, there are two options. The first is to land in the direction of travel of the first stage, down-range landing (DRL). This has the advantage that the first stage does not have to alter its course significantly but can continue on its way. The second option is to return to the launch site (RLS), this option saves on a transport system that is needed for the DRL, but it requires the first stage to make a u-turn to get back to the launch site. This costs a significant amount of propellant, leading to a payload mass loss that can be as high as 40-65% for LEO missions[39, 104]. This change in payload mass can only be defended if the boat cost is also significantly high. However, Snijders[99] found that the boat cost is below 1 million euros where the launch cost is higher than 10 million euros. Therefore the losses for RLS do not outweigh the benefits, and it will not be used within this study. It should be said that RLS is beneficial if only masses are flown that are 40-65% lower than the maximum payload capability. But this will not be the case for this research.

2.1.4. Refurbishment

The refurbishment is one of the least known aspects of the economics of reusable launch vehicles [103]. DLR even goes so far as to say that a demonstrator mission is needed to give a good insight into the refurbishment costs. Nonetheless, multiple efforts have been performed in order to get an estimate. Although all models are given as a percentage of the production cost of the stage, no clear solution is found when comparing these efforts. Wertz gives a range between 7-50% this range varies significantly because a 'learning curve', of 105-115%, is used, which increases the refurbishment cost per flight logarithmically[119]. Koelle gives the refurbishment cost model as a linear increase of 1-2% per flight [56]. The lower estimation of 1% for Koelle compares to the highest estimate of Wertz at 100 reuses of 50%. Another figure given by Hermann gives a flat rate of 10-20% based on historical data [46]. However, it is unclear what this historical data is. From these studies, it is clear that the refurbishment is still unclear to what the specific costs are although two conclusions are drawn. First is that the refurbishment costs increase with the number of flights. This also feels logically compared to other vehicles, as was also mentioned in [119]. Second is that the refurbishment cost will be somewhere between 5-50% of the production cost.

2.1.5. Production

When talking about a reusable first stage, it means that the production of part of the launcher is limited. When recovering only the engine or the complete stage, the engine for the first stage does not have to be produced for every launch. However, the second stage does have to be rebuilt every time. As will be discussed in section 2.3 and in chapter 4, the cost for production becomes cheaper the more times the stage is produced. This holds for both the initial production and for the parts that need to be rebuild. This decrease in cost is due to increases in experience; this is called the learning curve. This learning curve is a logarithmic function [38, 57]:

$$\text{Learning Curve} = k^{\frac{log(f)}{log(2)}} \tag{2.1}$$

With k, the number of units produced and f the learning curve coefficient. This coefficient is for stage production around 80-90%[38, 57, 119].

2.1.6. Complete Overview

To put everything back together a complete overview is given in Figure 2.6. This is all the elements that are either varied or used in the optimisation in order to answer the research questions. However not all combination are possible, this will be discussed in subsection 5.4.3.

<table>
<tr><th colspan="30">Reusable First Stage</th></tr>
<tr><td colspan="30">Mission</td></tr>
<tr><td colspan="15">LEO Mission</td><td colspan="15">GTO Mission</td></tr>
<tr><td colspan="30">What to Recover</td></tr>
<tr><td colspan="15">Engine Only</td><td colspan="15">Complete Stage</td></tr>
<tr><td colspan="30">Deceleration Hardware</td></tr>
<tr><td colspan="6">Subsonic Parachutes</td><td colspan="6">Supersonic Parachutes</td><td colspan="6">HIAD</td><td colspan="6">Grid Fins</td><td colspan="6">Propulsive Landing</td></tr>
<tr><td colspan="30">Landing & Retrieval</td></tr>
<tr><td colspan="10">Landing Legs</td><td colspan="10">Airbags</td><td colspan="10" rowspan="2">Mid-Air Retrieval</td></tr>
<tr><td colspan="20">Boat Retrieval</td></tr>
</table>

Figure 2.6: Overview of the elements in a first stage reusable system

2.2. Comparable Launchers

Although there is only one operational reusable launcher, at the time of writing, there are some concepts that are applicable to this research. Most notable vehicles are the SpaceX Falcon 9 and Blue Origin New Glenn who are designed to be reusable. They use the propulsive system for a soft landing. Although this seems like an easy system to implement it also carries a great loss with it. According to a NASA study[104], and also investigated during the literature study [95] on the matter, the payload loss is at least 40% compared to a fully expendable launcher. Meaning that by not changing the total mass of the launcher, 40% of the payload mass is lost to recovering the first stage. Furthermore, Dumont[39] did an investigation on the Falcon 9 and showed that for landing on a barge down-range, the loss is between 30-35%. However, when returning to base, the payload loss can be as high as 60% to 65% for LEO missions.

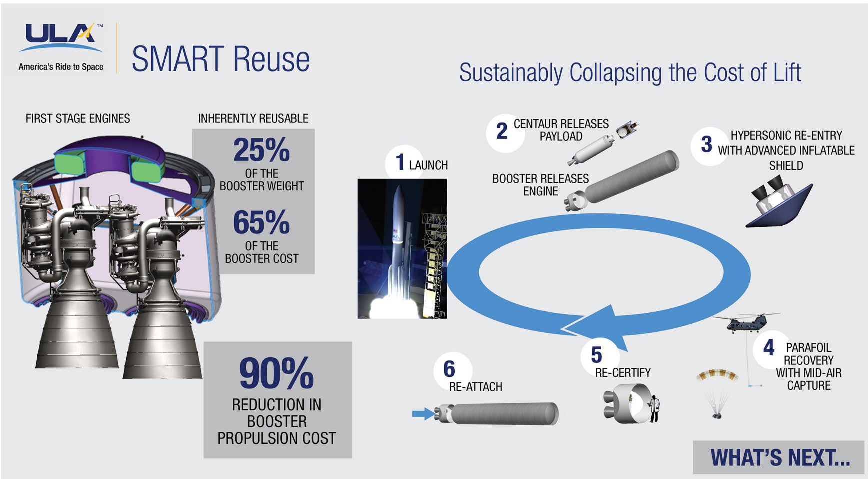

Figure 2.7: Overview of the SMART reuse system for the ULA Vulcan Launcher[111]

For the new generation of launchers which is coming to the market, they are investigating only to recover the engine. These are the Vulcan launcher and the Ariane VI. The Vulcan uses a Hypersonic Inflatable Aerodynamic Decelerator and a lift generating parachute, but as mentioned before only the engine is recovered[83]. An overview of the Vulcan system can be found in Figure 2.7. The Ariane VI uses wings and small propellers to return the engine to a landing strip[33].

2.3. Reuse-index

The Reuse index (RI) is something mentioned in an article published by ULA[83]. They use the equation:

$$RI = p\left(k\left(\frac{F}{n} + \frac{1}{n}\left(\frac{C(RHW)}{C(B)}\right) + \frac{C(RR)}{C(B)}\right) + (1-k)\right) \tag{2.2}$$

Where:

- RI is the reuse index
- p is the ratio of payload loss of the reusable compared to the expendable launcher
- k is the fraction of the production cost that is reused
- F is a factor representing the production unit cost increase when the production rate is decreased
- n is the number of reuses
- C(RHW) is the reused portion of the cost to recover and reuse such as the cost of the recovery hardware that will be reused
- C(B) is the production cost of the hardware to be reused
- C(RR) is the expended portion of the cost to recover and reuse such as recovery operations and refurbishment cost

However, this is nothing more than the ratio of payload specific cost of the expendable and reusable launcher. This fact will be used, as the cost savings will be calculated not from Equation 2.2, but from the cost model, which is discussed in chapter 4. The model used, gives a cost per flight for both the expendable and reusable version of the launcher, which then combined with the payload mass gives the same result as Equation 2.2.

There are some drawbacks from the RI that need to be mentioned. This has to do with the economics of the launcher. The RI compares the expendable to the reusable. However, it does this using two different payload masses. From a customer perspective, this causes some problems since the customer has a fixed payload mass as the satellite will not primarily be designed for a specific launcher. So the payload reduction fraction p becomes less of a factor. Besides this, the RI does not take a variable payload mass into account and assumes that the launcher works at maximum capacity all the time. This is contrary to realistic launcher operations where various payload masses are used on the same launcher during its lifetime. For these reasons, the RI will not be used on its own, but the total cost per flight will also be used. This is done to give a better overview of the costs.

2.4. Optimisation Algorithm

For optimisation algorithms, there are usually two categories. The first category is gradient-based optimisation which differentiates the function and tries to find a local optimum. This, therefore, requires a smooth differentiable function. Either it needs to be known if the function has only one optimum or roughly in what range the required optimum is. The other category is heuristic optimisation; these are mostly based on randomly changing the input parameters to find the global optimum. As they do not need to differentiate the objective function, they can be used in more situations. Though the last category seems better due to the heuristical nature of the algorithms, they require more function evaluations to reach the result and therefore cost more time[31]. Because the optimisation needs to choose between deceleration elements for this research, the latter category will be used for the design optimisation. Within the heuristical category, three optimisation algorithms will be considered:

- Genetic Algorithm (GA)- The Genetic Algorithm borrows from real-life genetics where random mutations are applied to a set population. With this usually, the best solutions of each generation are carried over to the next [31]. Whereas the others in the population get new mutations. This is also the algorithm used by Pepermans and Contant.

- Particle Swarm Optimisation (PSO)- The particle swarm optimisation is also based on a population; however, here the point moves through the search space with a random speed and velocity. This is, however, not entirely random as they will gravitate towards the best neighbour within a certain range [31].
- Surrogate Optimisation (SO) - Surrogate optimisation is meant for functions which are expensive to calculate. Here random points throughout the search space will be used to create a simplified function. This function will then be used to direct the search towards the lowest point. The next point is chosen randomly within a decreasing range until the minimum value distance is reached. After this, the search partially resets and search for a new minimum point[66].

Because of the way the SO is set-up, this is generally the fastest, followed by PSO and GA. However, only SO and GA can optimise discrete variable problems, where PSO does not. Therefore the SO and GA will be used for the main loop and PSO will be used when a global optimum is required and the function does not contain discrete variables.

3 Models

To create a tool to calculate what the best solution is to reuse a first stage, multiple models are needed. First, the mass models of the various elements for the launcher are discussed, these are the mass models for increasing the tank size, the landing systems and the deceleration systems. Following this, the thrust model will be discussed to put the launcher into orbit. After this, the drag models will be discussed. This is for the general drag model but also some specific elements for parachutes. Finally, the aerothermal heating model is discussed.

3.1. Extra Tank Mass

To allow for extra propellant a model is needed to extend the tank and calculate the resulting extra mass. For this, the choice was made to not only use historical data. This model compares the mass before and after extension. From this, a factor is created that is applied to the inputs. Since there is some historical data, the model is corrected and validated based on this.

3.1.1. Model

Since existing launchers are used and modified to create a reusable launcher, there should be a model to calculate the extra tank mass when extra propellant is added to the tank. Since the thickness and specific material of the existing launcher are not known a model needs to be created that also does not require this information. This is done by using a design model found in Zandbergen [124] and assuming that the material is aluminium. Using this design model first the mass is calculated for the existing launcher, then for the tank with the extra propellant. From this, a fraction is created which represents the increase in tank mass. This is similar to the approach of Pietrobon who created a model for the stage mass as a function of the propellant mass based on historical data[81]. This model does not depend on the geometry of the stage whereas this is taken into account for the model found in Zandbergen. This has the benefit that it requires a limited amount of inputs. All that is needed is:

- propellant type
- current propellant mass
- propellant mass added
- current tank mass
- engine mass
- Stage diameter and length

The engine mass is only needed to make sure the calculated factor will only apply to the tank and not to the entire stage.

To determine the masses of the two tanks, first, the vapour pressure is calculated for both the oxidizer and the fuel. Which is done by using [124]:

$$P_{vapour} = e^{\frac{(A-B)}{(T+C)}} \tag{3.1}$$

Where A, B and C are coefficients of the vapour pressure at the storage temperature T. In Table 3.1 the various coefficients for fuels and oxidisers can be found. By using the temperature in Table 3.1 it is assumed that the propellants are actively cooled to that temperature to the temperature given.

Table 3.1: Overview of the propellants which can be used for the tank extension model

Propellant Component	A	B	C	T [K]	ρ [kg/m^3]
LOX [116, 124]	3.95	340	-4.14	104.35	1141
LH2 [115]	3.54	99.40	7.72	21	71
RP1 [117]	4.05	1355.13	-63.63	362.9	915
N2O4 [61]	21.98	6615	86.88	284.3	1440
UMDH [118]	4.71	1388.51	-40.61	265.41	793

Added to that is the hydrostatic pressure which is the pressure caused by the weight of the amount of propellant against the tank which is calculated by:

$$P_{hyd} = \rho_p \Psi g H \tag{3.2}$$

Where ρ_p is the density of the fluid, Ψ is the thrust-to-weight ratio, g is the gravitational acceleration, and H is the height of the fluid between the upper level of the liquid and the tank wall. It is assumed that the pressure is at its highest during launch. These pressures are summed together to get the maximum design pressure [124] and increased first by a factor of 10% for any non-ideal gasses in the tank. Finally, the maximum operating pressure is determined by getting the total expected pressure and multiplying it with a safety factor of 2[124].

The thickness of the tank is calculated by using the maximum expected operating pressure P_{MEOP}, the launcher radius R and the ultimate strength of the tank material σ_{ult}, which for aluminium 7075 is 483 MPa[67]. This thickness is calculated for a cylindrical tank as this is the critical part for the tank.

$$t = \frac{P_{MEOP} R}{2\sigma_{ult}} \tag{3.3}$$

After the thickness is known the length of the tank is calculated. This is done by assuming that both the oxidiser and the fuel are stored in individual tanks with semi-spherical bulkheads. For this first, the required volume for the tank is calculated, which is done by simply dividing the mass by the density of the propellant. The length of a cylinder can be calculated by deducting one sphere (both bulkheads) from the total volume and calculating the cylinder that is needed for the remainder. Then using a thin-walled approach, the mass of the tank is calculated:

$$m = \rho S t \tag{3.4}$$

Where S is the surface area of the tank ρ is the density of the material and t is the thickness calculated in Equation 3.3. After which the mass is increased by 25% for added plumbing and systems needed for propellant management.

This is done for both the old tank as well as for the tank with increased propellant after which a ratio is calculated between the two, which is then applied to the actual empty mass of the launcher.

$$F_{ATM} = \frac{M_{new}}{M_{old}} \tag{3.5}$$

For this model the engine will not be taken into account. However the separation system cannot be separated that easily as it is not known what the mass of this system is for most launchers. The accuracy of this model will be discussed next.

3.1.2. Model Validation

For the validation, seven different data points are used for stages of launchers which were changed while still keeping the same engine. In order to calculate the factor which corresponds to the one calculated by the model in Equation 3.5 the following equation is used:

$$F_{ATM,actual} = \frac{M_{empty,new} - M_{engine}}{M_{empty,old} - M_{engine}} \tag{3.6}$$

Table 3.2: Validation Data used for the extra tank mass model

Launcher Case	Old-New	Original Propellant Mass[kg]	Added Propellant Mass [kg]	Error [%]	Actual Mass Fraction [-]	Model Mass Fraction [-]
Falcon 9 1st Stage [87]	V1.1 - V1.2	385000	26000	-22.47	1.371	1.063
Falcon 9 2nd Stage [87]	V1.0 - V1.2	67400	44100	17.58	1.342	1.578
Centaur [18, 19]	II-III	16780	3900	6.34	1.053	1.120
DCSS [85, 86]	DCSS III - DCSS IV	16820	4500	-5.06	1.138	1.080
LM 3 1st Stage [88]	CZ-3A - CZ-3BE	18200	14400	-1.88	1.094	1.074
LM 3 Booster [88]	CZ-3B- CZ-3BE	37700	376.4	-12.65	1.232	1.076
LM 2 2nd Stage [88]	CZ-4A - CZ-2E	183200	50450	27.72	1.456	1.860

As can be seen in Table 3.2, the model fits for some stages but not for all stages. The Delta Cryogenic Second Stage (DCSS), Centaur upper stage and the Long March (LM) 3 1^{st} stage fall within 10%. The rest fall outside and not to only one side. So the model needs some more investigation in order to get the error more manageable. First the error of the model as a function of the function value is plotted. Here, in Figure 3.1 the

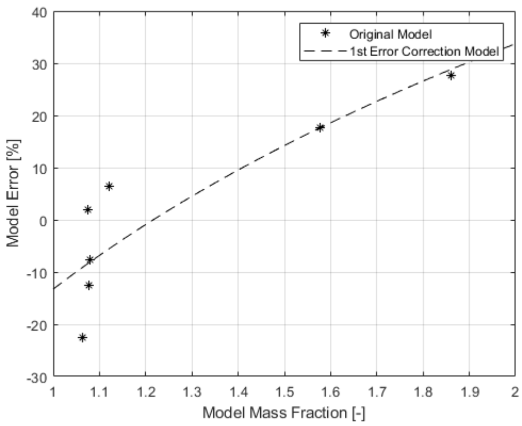

Figure 3.1: Model error as a function of the mass fraction

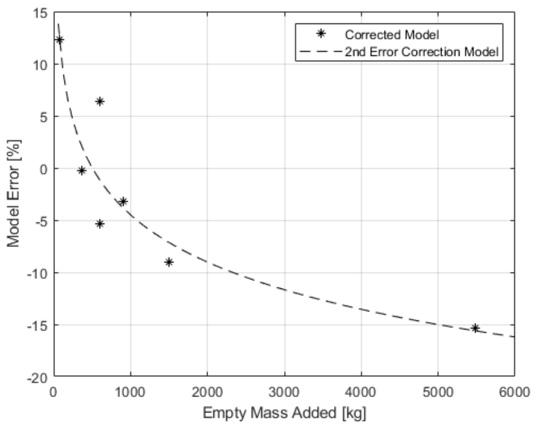

Figure 3.2: Modified Model error as a function of the added empty mass

data is plotted with a logarithmic fit through it. This fit follows the following equation:

$$f_{error}(F_{ATM}) = 66.698 ln(F_{ATM}) - 12.664 \tag{3.7}$$

This error is than applied to the model as follows:

$$F_{ATM,new} = F_{ATM} \frac{100 - f_{error}(F_{ATM})}{100} \tag{3.8}$$

This modification already produces positive results. Where the initial model had a root mean squared error (RMSE) of 16.1% this new model has a RMSE of 7.1%. A second correction is performed on the basis of the extra empty mass that is added from the validation data. When looking at Figure 3.2 also in this case a second error model can be found as a function of the extra empty mass.

$$f_{error,2}(\Delta m_{empty}) = -6.527ln(\Delta m_{empty}) + 41.46 \tag{3.9}$$

This model is applied in the same manner as before leading to:

$$F_{ATM,final} = F_{ATM,new}\frac{100 - f_{error,2}(\Delta m_{empty})}{100} \tag{3.10}$$

This final correction produces a model with a RSME of 6.1%. The reason for this correction being less impactfull than the previous one is because for the validation data the added empty mass is known in advance. In the use of the model this is a result of the model. Any other significant correlation could not be found. The final results can be found in Table 3.3.

Although the final results are better than the uncorrected model, there are still some errors. When looking

Table 3.3: Validation Data used for the extra tank mass model

Launcher Case	**Old**	**New**	**Added Propellant Mass [kg]**	**Final Model Error [%]**	**Actual Mass Fraction [-]**	**Final Mass Fraction Model [-]**	**Old Mass Fraction Model [-]**
Falcon 9 1st Stage	V1.1	V1.2	26000	-8.22	1.371	1.258	1.063
Falcon 9 2nd Stage	V1.0	V1.2	44100	-1.35	1.342	1.324	1.578
Centaur	Centaur 2	Centaur 3	3900	5.93	1.053	1.116	1.120
Delta DCSS	DCSS III	DCSS IV	4500	-1.18	1.138	1.124	1.080
Long March 3 1st Stage	CZ-3A	CZ-3BE	14400	9.78	1.094	1.202	1.074
Long March 3 Booster	CZ-3B	CZ-3BE	376.4	-7.87	1.232	1.135	1.076
Long March 2 2nd Stage	CZ-4A	CZ-2E	50450	-5.26	1.456	1.380	1.860

at the model itself, there could already be some explanations. These inputs are all linked to the calculation of the maximum operating pressure. If the maximum operating pressure increases the corresponding tank mass also increases with the same factor when looking at Equation 3.3 and Equation 3.4.

The first is the coefficients in Equation 3.1. These are experimentally determined but are not set because for some compound, such as for LOX[116], there are two sets. For this one set is chosen as mixing or averaging would create problems with the temperature ranges given for the coefficients. To continue with the temperature, the storage temperature, T in Equation 3.1, is assumed to be the middle of the range given for the vapour pressure coefficients. However, when increasing or decreasing the temperature, the vapour pressure correspondingly increases and decreases.

For the calculation of the hydrostatic pressure, it is assumed that the maximum pressure occurs at lift-off when the most mass is accelerated. This does not have to be the case for the various launchers where it could occur during the flight when the Thrust-to-Weight ratio increases more than the maximum height of the propellant decreases. All these reasons could alter the masses of the tank both to increase and decrease.

Besides the pressure calculation, there could be some other reasons that alter the mass calculation. Since most of these propellant tanks also serve as the primary load-carrying structure of the launcher, this could impose additional requirements on the tank not having to do with the propellant storage, as was also suggested in [124]. This would most likely increase the mass of the tank to cope with, for example, bending moments. Finally, for the model, it was assumed that the thickness of the tank is uniform for the entire tank. This does not have to be the case. Because the tank will then be designed for the maximum pressure at the bottom of the tank; however, at the top, it has to cope with the vapour pressure alone. Therefore, since in a launcher, every excessive kilogram means less payload capability, it is conceivable that tanks have a variable thickness along the length of the tank. This could decrease that mass of the tank.

Linking all this back to the model, since the tank increases in length due to the increase in propellant mass, the bending moments on the tank are also probably increased. This could increase the tank mass even more because it now also has to handle the increase in forces from the flight. Finally, if a variable thickness is applied, this distribution would change with the new increase in height changing the mass with it.

3.2. Landing System

The landing system is divided into two parts the system that is needed during touchdown and the flotation system to keep it afloat if landing on water.

3.2.1. Landing Legs

For landing legs, there are not many examples for launchers. The Falcon 9 is the only launcher currently in operation with landing legs. The New Glenn launcher is currently being designing to have landing legs, just as the Callisto demonstrator being designed by CNES, DLR and JAXA[75, 105]. However, both of these launchers did not have their first launch yet, and information about them is limited. On top of that, detailed information about the Falcon 9 is also limited [21]. The model that will be used for the landing legs will be from historical data. This will be a percentage of the empty mass.

Although there is some data on the Falcon 9, it is unclear. The mass of the landing legs for the first stage is somewhere between 2300-2400 kg [51, 84, 106]. It is, however, unclear how much propellant is left at landing. If assuming that all the propellant is gone at the exact moment of touchdown than the landing mass is 27200 kg. A simulation run by Murphy gives for the Starlink mission that 4.49t of propellant is left bringing the landing mass to 31690 kg [71]. The amount of left-over propellant cannot be confirmed from another source. Having a little reserve when landing under nominal conditions would be logical though. This reserve would be to account for possible different wind conditions and small errors in the flight path that needs to be corrected.

So if the Falcon 9 is not going to give a conclusive answer to the weight of the landing legs, other vehicles should be examined, focusing on landers from space exploration missions. The Apollo moon lander (LM) and the surveyor spacecraft[37, 93]. For these missions, extensive documentation is available specifically the landing mass history as well as the vehicle mass history for the Apollo lunar lander. The overview of the mass percentage of the landing mass and the landing leg system mass can be found in Figure 3.3. The final point of the graph is the Apollo 11 lander which will also be used.

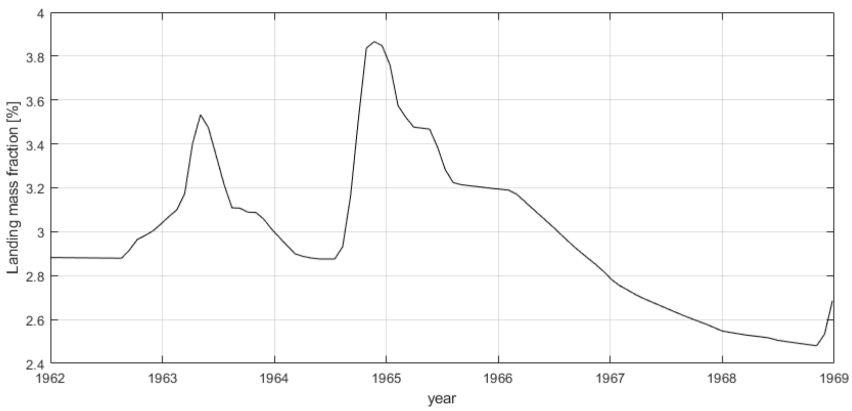

Figure 3.3: Landing system mass as a percentage of the landing mass for the development of the Apollo lander[93]

For the surveyor spacecraft, a detailed mass breakdown is given. The final lander which is used is the Philae lander for the Rosetta mission [94]. Finally, NASA performed a study on creating a Two-stage-to-Orbit (TSTO) fully reusable launcher. They set the mass for the landing legs at 10% of the stage mass [104]. All the data from the sources are given in Table 3.4. Here the landing mass of the vehicle is given as well as the landing leg system and the percentage of the landing leg system mass to the landing mass.

Table 3.4: Landing leg mass for various landers and launchers

Vehicle/Study	Landing Mass	Landing Legs Mass	percentage [%]
Falcon 9 (empty)	27200	2300	8.46
Falcon 9 (empty)	27200	2400	8.82
Falcon 9 (reserve propellant)	31690	2300	7.26
Falcon 9 (reserve propellant)	31690	2400	7.35
Apollo max	14455	558.9	3.87
Apollo min	16111	399.7	2.48
Apollo 11	16167	434.3	2.69
Surveyor	624.72	38.28	6.13
Philae	97.6	11.1	11.37
NASA study	-	-	10
Average			6.86
Standard Deviation			2.89

For the landers it should be noted that they do not land on earth. This means that although the momentum they need to absorb remains the same when comparing to an earth landing. However, the ultimate force they need to be able to handle is lower due to the reduced gravitational acceleration. Switching from the actual landing location to an earth landing most likely means the weight increases but by how much is unclear.

In order to take the variation into account and assume a conservative value for the landing leg mass the average plus one standard deviation is used and rounded to the nearest integer. This means the landing leg system mass will be 10% of the empty mass. Using the empty mass instead of the landing mass does mean that for larger remaining first stage propellants the landing leg system mass will be underestimated. But the conservative value will compensate for this slightly.

3.2.2. Airbags

Airbags are used to decelerate an object and to cushion the impact. This is true for the airbags in cars, as well as the airbags that can be used for landing a stage. The model for the mass comes from Knacke[52].

$$m_{airbags} = m_{stage} * (4.57e-6 * v_{landing}^3 - 2.11e-4 * v_{landing}^2 + 0.0032 * v_{landing}) \quad (3.11)$$

It should be noted, however, the model given in Knacke gives the ratio between the landing mass and the airbag mass. Although in Knacke all inputs are given in imperial units, using that the output is a ratio the input stage mass can be supplied in any unit. However since this is an empirical relation the landing velocity does have to be given in ft/s. An overview of the model can be seen in Figure 3.4 What can be seen is that the mass of the airbags increases rapidly with velocity as expected from the equation. Still, the effect from the stage mass is dominant below a landing velocity of 10m/s and below a stage mass of 10-15 tons. This L-shaped zone is when the stage mass determines mostly the airbag mass, and otherwise, the landing velocity is the dominant factor. For the airbag system validation data was found in Knacke, but also from the Kistler K-1 which used airbags to land the first stage[42, 52].

Table 3.5: Validation of the airbag mass model

Vehicle	Landing Mass[kg]	Landing Speed [m/s]	Airbag Mass		Difference [%]
			Actual Mass [kg]	Model Mass [kg]	
Kistler K-1 LAP [9, 42]	20500	6.1	181.44	331.12	82.5
CL-289 [52, 114]	215.45	9.4	3.99	6.35	59.15
USD-5 [52, 53]	2177.2	7.9	50.08	45.47	-9.20
CL-89 [52, 114]	136.07	11.0	9.39	7.48	-20.33
Mean Error					28.03
Error Standard deviation					43.76

The large errors in the model are probably due to the simplicity of the model. In the model the allowable

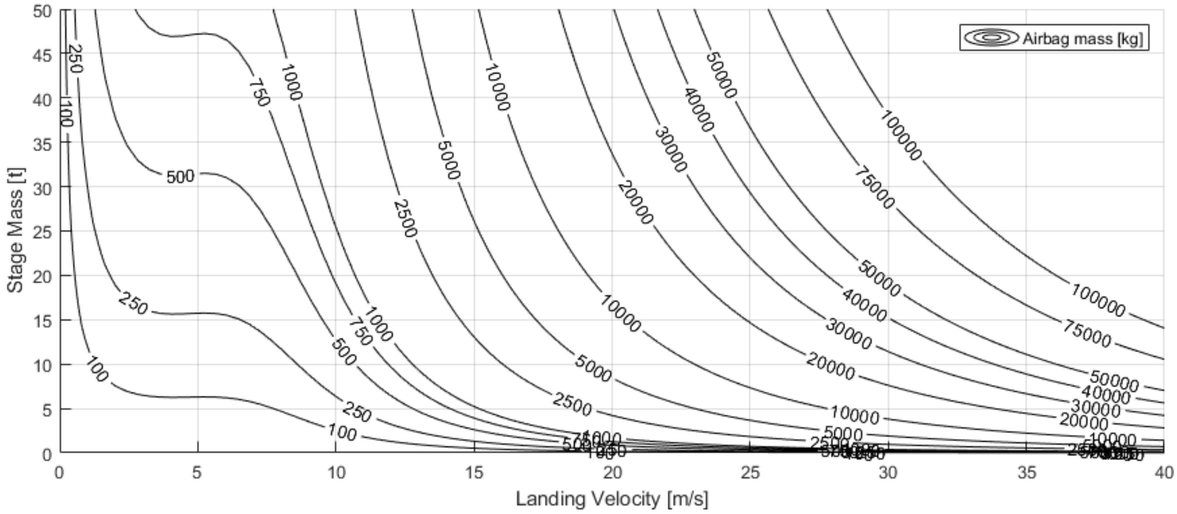

Figure 3.4: Airbag mass as a function of the stage mass and the landing velocity following the mass model from [52]

impact deceleration is not taken into account but judged to be around 8 g as this was the average [52]. Higher allowable g loading as was seen for the CL-289 (30 g - 40 g) would lead to lower airbag mass since it can become more compact[52, 114]. Other possible reasons for the large errors are the materials used either for the bag itself or the gas used to inflate. These could, especially on the smaller airbag systems, cause larger deviations percentage wise although the mass differences is manageable as for example for the CL-89.

3.2.3. Flotation Device

For a water landing, it is assumed that the stage is not buoyant on its own, so it will need the help of some flotation devices to keep afloat. These flotation devices are created in such a way that the displacement they cause is larger than the water displacement of the stage. The system is made up in such a way that it requires at least 4 flotation devices, this is done for the sake of stability. However, this is only the lower limit. When more volume is required the number of flotation devices are added with a constant radius of 0.84m.

The mass model for the system is a bottom-up model. For the flotation devices, it is assumed that Hypalon, which is also used for boat hulls, is used at the primary material. Also, it is assumed that the gas that is being used is CO_2 and is under a pressure of 2 bar. This is based on the model as was created by Pepermans [77]. For this model some small changes are made, first is that the amount of flotation devices is split into discrete flotation devices. First, the displacement volume needs to be known. This is done by assuming that the entire stage is underwater.

$$V_{displacement} = \frac{m_{stage}}{\rho_{water}} \tag{3.12}$$

The standard sphere being used for flotation is

$$V_{sphere} = \frac{4}{3}\pi 0.84^3 \tag{3.13}$$

This will lead to the number of flotation devices

$$n_{flotation} = \frac{V_{displacement}}{V_{sphere}} \tag{3.14}$$

This number is rounded up to the nearest integer. However, if the number is lower than four, the amount is set at four. This leads to the following system

$$V_{flotation} = \begin{cases} n_{flotation} V_{sphere}, & \text{if } n_{flotation} > 4 \\ n_{flotation} \frac{V_{displacement}}{4}, & \text{otherwise, } n_{flotation} = 4 \end{cases} \tag{3.15}$$

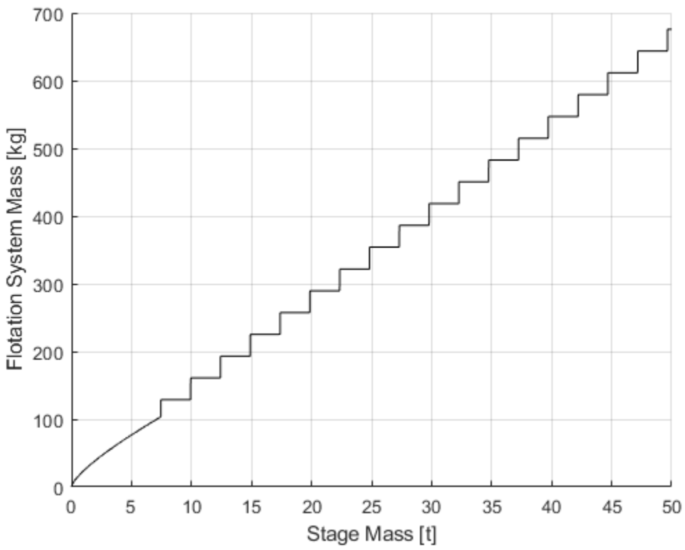

Figure 3.5: Flotation System mass as a function of the stage mass.

This distinction is important when calculating the total surface area of the bag for the bottom-up mass model.

$$m_{flotation} = n_{flotation}\left(S_{flotation}\rho_{hypalon}\right) * 2 + \frac{P_{flotation}V_{flotation}}{R_{specific}T} \tag{3.16}$$

The density of Hypalon is 1.3 kg/m^2 and the specific gas constant for CO_2 is 288.92 $J/(kg \cdot K)$. The resulting function of the flotation mass as a function of the stage mass can be found in Figure 3.5. For this model, no validation data could be found. Therefore an inaccuracy of 20% will be used for the sensitivity analysis. A validation data set would be preferred in order to give a better analysis of the mass required for the flotation system. As minimising the launcher mass is one of the critical parameters for most launcher designs.

3.3. Deceleration Systems

For deceleration systems, multiple mass models are needed. First, the model for the grid fins is given, followed by the parachutes and finally the HIAD.

3.3.1. Grid Fins

As the size of the grid fins is one of the optimisation variables, it would skew the results if the grid fins do not have a mass accompanying it. Therefore a separate mass model is used for the grid fins. However, this also has limited sources from which a simple model can be based on. As a first-order approximation, a study is used which designed the grid fin for minimum weight. They use a 1500mmx1500mmx150mm which eventually had a mass of 58kg[2]. To be able to use this, the mass of the fin is related to the frontal area of the fin. So the mass relation becomes:

$$m_{fin} = 26.028 S_{fin} \tag{3.17}$$

Finding any data to validate this model is difficult, as already mentioned. A possible source would be a NASA study which investigates a reusable launcher which also uses grid fins [104]. However, this study includes the grid fin mass into a fixed percentage for all systems which are required for landing; this mass mostly consists of the landing legs mass. Furthermore, they state that the grid fins are negligible when looking at the entire launcher. Another source would be military ordnance, where data could be found on the mass of grid fins used within the US Airforce[76]. These grid fins were, however, small compared to the one found in Ajayakumar[2] 0.01 m^2 compared to the 2 m^2. However, when applying these grid fins to the model, an average error of about 50% is obtained. The detailed results can be found in Table 3.6.

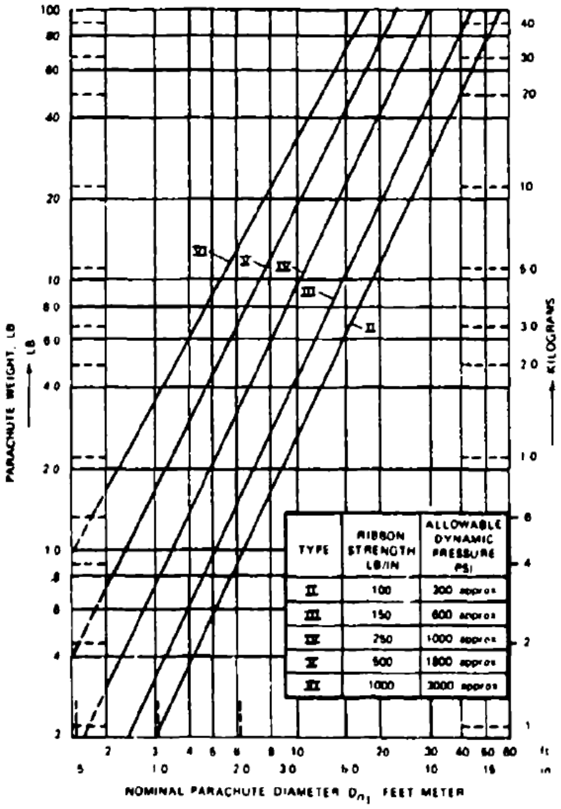

Figure 3.6: Mass model for a Hemisflo parachute[52]

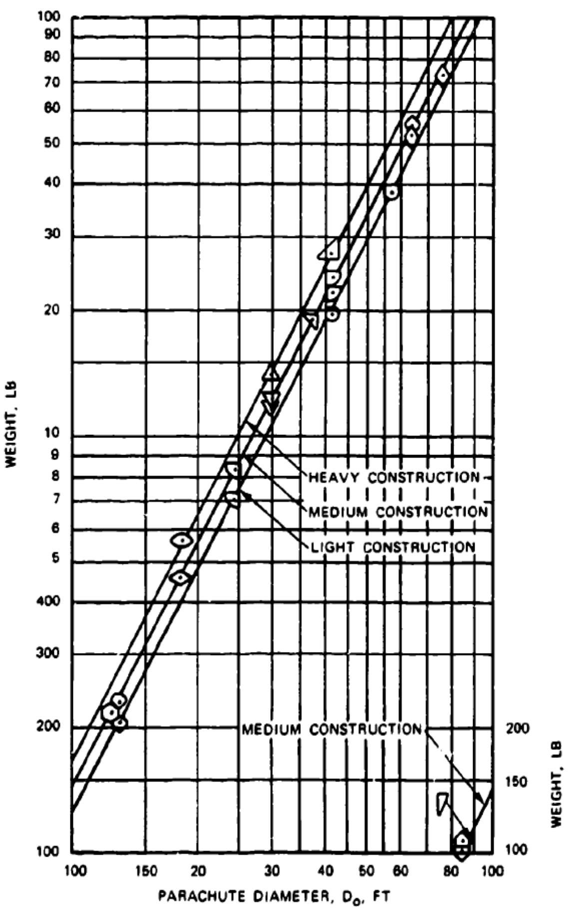

Figure 3.7: Mass model for a Ringsail parachute[52]

Table 3.6: Comparison of the mass for three grid fins

Study	Area [m^2]	Actual Mass [kg]	Model Mass [kg]	Difference [%]
Ajayakumar [2]	2.25	58.563	26.028	0
Orthner-1[76]	0.006452	0.3794	0.167922	55.74
Orthner-2 [76]	0.010323	0.504	0.268676	46.69

It should be noted that Ajayakumar had the objective to optimise the gird fins for minimum mass and Orthner is looking at the aerodynamics of grid fins. This could explain the difference between the masses for the two studies. Nonetheless, this error will be taken into account when investigating the cases in chapter 6.

3.3.2. Parachute Mass

In order to allow for variety in the final design a system mass model needs to be determined for only one parachute and not for an entire system. This model is supplied by Knacke[52]. As parachutes for the recovery of first stages two types are chosen these are the Hemisflo parachute which is designed for supersonic flight up to Mach 3 and a Ringsail parachute which can be used up to Mach 0.5. Here a mass model is given for different types of parachutes which can be seen in Figure 3.6 and Figure 3.7. For the Hemisflo ribbon parachute the II mass model will be used which is for parachutes up to ~2000 kPa which is about 6 times higher than the dynamic pressure limit used. For the Ringsail the light construction method is used as was done in [77]. However these only give the mass for a parachute mass and not the entire system including deployment system and attachment mass. This was estimated by [77] to be the same as the parachute mass, This is also used in this study. Therefore the mass of the different parachute systems becomes

$$m_{Hemisflow} = 2 * (0.01937 D_{parachute}^{2.1258}) \tag{3.18}$$

$$m_{Ringsail} = 2 * (0.0118 D_{parachute}^{2.0011}) \tag{3.19}$$

Where the resulting mass is in pounds and the diameter of the parachute has to be given in feet. Comparison of the model to actual parachutes can be found in Table 3.7.

Table 3.7: Comparison of the parachute models to actual data with the mean error and the standard deviation (STD) for both models.

Vehicle	Diameter [m]	Actual Mass [kg]	Model Mass [kg]	Difference [%]
Hemisflo Parachute				
Kistler K1 Drogue [42]	7.01	83.01	78.18	-5.8
CL-289 Drogue [114]	1.7	0.71	0.68	-3.8
CL-89 Drogue [114]	1.13	0.54	0.28	-47.9
Mean Error				-19.2
Error STD				20
Ringsail Parachute				
Mars Science Laboratory (MSL) Main Parachute [48]	30	150	104	-30.7
CL-289 Main [114]	5.99	2.22	2.08	-6.5
CL-89 [114]	9.45	5.03	5.16	2.8
Mean Error				-11.5
Error STD				14

Although the results from the model agree with the validation data there are two points that have a large error. These could be due to the choice of the model chosen for the light weight construction. Other than that general assumptions are made in the model with regard to the wiring connecting the canopy to the vehicle. These are by no means fixed although a lower limit is required to not have any interference from the body [52].

3.3.3. Hypersonic Inflatable Aerodynamic Decelerator Mass

For a Hypersonic Inflatable Aerodynamic Decelerator (HIAD) most research is done for Mars entry [43, 96]. This is also where the mass model is coming from. In Samareh the following mass estimation is given[96].

$$m_{HIAD} = \frac{\pi}{4} D_{HIAD}^2 \left(c_1 + c_2 D_{HIAD} + c_3 q + c_4 D_{HIAD}^2 + c_5 q D_{HIAD} + c_6 q^2\right) \tag{3.20}$$

The coefficients which can be found in Table 3.8

Coefficient	**Value**
c_1	0.19820998
c_2	0.01535624
c_3	-3.258e-3
c_4	-1.801e-4
c_5	5.40113e-6
c_6	2.86428e-9

Table 3.8: Coefficients for the HIAD mass model [96]

The accuracy of the model is estimated by using data from several sources. These can be found in Table 3.9. Here the diameter (D) and the dynamic pressure (q) of the HIADs are given as well as the actual mass and the mass given by the model.

Table 3.9: Validation data for the HIAD mass model

Study	D [m]	q [kPa]	Actual Mass	Model Mass [kg]	Error [%]
Ivanov MSL [48]	7.95	6.04	56.52	51.58	-8.7
Finchkof [43]	23	10.5	4360	4318.76	-0.9
Bose [22]	18	8	1620	1468.49	-9.4
Samareh Case 1 [97]	23	3	1368	1342.5	1.9
Mean error					-5.2
Error standard deviation					- 3.8

What can be seen in Table 3.9 is that the mass for the HIAD can be estimated to within 10%. The rounding of the input values could explain the remaining deviations. Since already rounding to the nearest 0.5 for both the diameter and dynamic pressure can already change the results significantly. Taking the Bose case as an example when rounding down (D=18.25,q=8.28) the error is -2.2%, and when rounding up (D=17.75,q=7.75), the error is -16.1%. Other than rounding of the inputs the material choice can also make a difference. This is not taken into account for the model. Another source of the deviation between the actual masses and the model mass is the design values for the dynamic pressure. As was mentioned in Ivanov, the design dynamic pressure has a safety factor of 4, meaning that the expected dynamic pressure is 1.51 kPa [48]. Although this would be a significant change to the results when a safety factor of four would be applied to all cases. A safety factor applied between the design dynamic pressure and the expected dynamic pressure would lead to an increase in the HIAD mass when the expected dynamic pressure is used for the validation of the model.

For the implementation of the model the dynamic pressure needs to be estimated beforehand. Otherwise, this would require an iterative process which, together with the ascent trajectory, increases the computation time significantly. From a small investigation, it was found that the maximum dynamic pressure is around 3-5 times the terminal dynamic pressure. To be on the conservative side the dynamic pressure is assumed to be ten times the terminal dynamic pressure. The terminal dynamic pressure is calculated when the drag force and gravity are equal.

3.4. Thrust Model

The thrust model is one of the most crucial systems, as this controls the ascent of the launcher and tells if the launcher is still capable of reaching orbit when attaching all of the systems needed to achieve reusability. The model is discussed first followed by the validation of the model. The model used allows for more flexibility to change the engine if required, both to actual engines as well as coming up with new engines. On top of this the model allows to put the engine into the optimisation loops if required.

3.4.1. Model Description

The liquid propulsion model is one where the ideal rocket theory from Thermal Rocket Propulsion is used [124]. To start with some data has to be known about the propellants used:

- Flame temperature - T_c
- Specific heat ratio - γ
- Propellant Molar Mass - M

For this research and validation of this model three propellant will be used. For each of these propellant the characteristics are given in Table 3.10

Table 3.10: The characteristics parameters used for this research

Propellant	T_c [K]	γ [-]	M [g/Mol]	OF ratio
LOX/LH2 [10]	2985	1.26	10.0	6
LOX/RP1 [11]	3670	1.24	23.3	2.56
UDMH/N2O4 [13]	3415	1.25	22.0	2.61

Also, the atmospheric pressure (P_a) is needed at the altitude at which the thrust needs to be calculated. The first thing that is calculated is the exit pressure. This is done using:

$$\frac{A_e}{A_t} = \frac{\Gamma}{\sqrt{\frac{2\gamma}{\gamma-1}\left(\frac{p_e}{p_c}\right)^{\left(\frac{2}{\gamma}\right)}\left(1-\left(\frac{p_e}{p_c}\right)^{\left(\frac{\gamma-1}{\gamma}\right)}\right)}} \tag{3.21}$$

Where A_e and A_t are the exit and throat area of the nozzle. Γ is the Vandenkerckhove function:

$$\Gamma = \sqrt{\gamma}\left(\frac{2}{\gamma+1}\right)^{\left(\frac{\gamma+1}{2(\gamma-1)}\right)} \tag{3.22}$$

Equation 3.21 has to be solved iteratively to get the exit pressure. In order to solve this, the pressure ratio is increased with steps of 10^{-5} in order to get the correct area ratio. After the exit pressure is known, the exhaust velocity can be calculated by using the specific gas constant $R = R_a/M$:

$$V_e = \sqrt{2\left(\frac{\gamma}{\gamma-1}\right)RT_c\left(1-\left(\frac{p_e}{p_c}\right)^{\left(\frac{\gamma-1}{\gamma}\right)}\right)} \tag{3.23}$$

Once the exhaust velocity is known, the mass flow can be calculated:

$$\dot{m}_{ideal} = \frac{\Gamma p_c A_t}{\sqrt{RT_c}} \tag{3.24}$$

After which the equivalent exhaust velocity can be calculated, which also includes the pressure thrust component.

$$V_{eq} = V_e + \left(\frac{(P_e - P_a)\,A_e}{m_{ideal}}\right) \tag{3.25}$$

After which the I_{sp} can be calculated:

$$I_{sp} = \frac{V_{eq}}{g_0} \tag{3.26}$$

After which the thrust can be calculated:

$$F_T = \dot{m}_{ideal} I_{sp} g_0 \tag{3.27}$$

Finally, for added accuracy, correction factors for the thrust and Isp are used, if known for an engine, at either sea-level or vacuum conditions. These correction factors and their accuracy are discussed in subsection 3.4.2. In order to be able to throttle the engine when needed, a coefficient is added to the mass flow equation which scales the mass flow accordingly.

3.4.2. Model Validation

For the validation of the model both the uncorrected as well as the corrected model will be looked at. For the thrust and specific impulse model, the mean errors and standard deviation for the ideal rocket theory model can be found in Table 3.11. A detailed validation of the uncorrected ideal rocket theory model can be found in Appendix B.

Table 3.11: Mean and standard deviation model error for the ideal rocket theory model

Model	**Mean Error [%]**	**Standard Deviation [%]**
Sea-level Thrust Model	13.10	15.49
Vacuum Thrust Model	10.35	13.10
Sea-level I_{sp} Model	3.00	3.53
Vacuum I_{sp} Model	2.50	3.19

The thrust model over estimates the thrust and specific impulse, this is due to the fact that the model is ideal rocket theory without any losses in the system. What can be seen is that the specific impulse error within 10% for all cases however the thrust force error is for three cases close to or over 20%. This can either be due to the following reasons:

- The propellant characteristics (O/F ratio, Flame Temperature) are different from the general values used in the model
- Nozzle geometry is different than reported in sources

On the first reason since propellant characteristics need to be generalised a detailed chemical analysis cannot be done for any engine. This means general values for the oxidiser to fuel ratio, isentropic coefficient, flame temperature and molar mass of the propellant have to be used. If there is a deviation from these values a difference should be observed in the specific impulse as well as the thrust force. For the engine geometry small difference in expansion ratios for the nozzle can give a difference in the resulting engine performance as an example if the expansion ratio is rounded to the nearest integer this could alter the result of the model.

In order to mitigate the errors in the ideal rocket theory model two approaches are used. First is the general correction, this applies a correction based on historical data for both the mass flow and the specific impulse. These correction factors are then applied to Equation 3.27 so it then becomes.

$$F_T = \xi_m \dot{m}_{ideal} \xi_{I_{sp}} I_{sp} g_0 \tag{3.28}$$

Where ξ_m and $\xi_{I_{sp}}$ are the correction factors. The correction factors based on validation data, given in Appendix B, are $\xi_m = 0.946562$ and $\xi_{I_{sp}} = 0.976429$. The validation of this correction can be seen in Table 3.13. The factors are established with the aid of data at vacuum conditions. This is done to rule out any additional error caused by the atmospheric model, since at vacuum condition $P_a = 0$.

The second approach is a correction for a specific case. It is based on the same equation as the previous model. The only difference is how the correction factors are determined. Where the previous model used all the data to give a correction factor, the second correction model uses either the sea-level or vacuum conditions for a specific engine to correct the model. This correction ensures that the values from the model are the same as the actual thrust and specific impulse at either sea-level or vacuum. The rest of the thrust curve is then still determined using ideal rocket theory. The validation of this model can be seen in Table 3.13 and Table 3.12 where the vacuum correction is applied for the engine where possible. In Table 3.13 the J-2, RL-10B2 and HM7B are not given for the second model since only vacuum properties are known for these engines. Although a vacuum correction could be applied to these engines this would result in no error as defined by the set-up of the model.

Table 3.12: Data used for the thrust model validation

Engine					Actual Data		
Name	D_e [m]	A_e/A_t [-]	P_c [bar]	Propellant	F_T [kN]	I_sp [s]	$\dot{m}$[kg/s]
Merlin 1D [12, 102, 121]	1.25	16	97	LOX/RP1	981	311	322
Rocketdyne F1 [7]	3.7	16	70	LOX/RP1	7770	304	2605
RS-68A [91]	2.44	21.5	108.9	LOX/LH2	3558	411	883
J-2 [8]	2.1	27.5	52.6	LOX/LH2	1033	421	250
RL-10B-2 [89]	2.21	280	44.12	LOX/LH2	110	466	24
RD-180 [14]	2x 1.575	36.87	267	LOX/RP1	4150	338	1252
Vulcain-2 [17]	2.09	58.2	117	LOX/LH2	1359	429	323
RS-25 [90]	2.4	69	206	LOX/LH2	2278	452	514
Viking 5C [16]	0.99	11	55	UDMH/N2O4	758	278	278
RD-253 [15]	1.5	26.2	147	UDMH/N2O4	1630	316	526
HM7B [40]	0.99	83.1	37	LOX/LH2	65	446	15

Table 3.13: Validation data for both model for calculating the performance at vacuum conditions

Engine	Actual Data			General Correction Model						Specific Correction Model					
				Thrust		I_{sp}		Mass Flow		Thrust		I_{sp}		Mass Flow	
	F_T [kN]	I_{sp} [s]	$\dot{m}$ [kg/s]	F_T [kN]	Diff [%]	I_{sp} [s]	Diff [%]	$\dot{m}$ [kg/s]	Diff [%]	F_T [kN]	Diff [%]	I_{sp} [s]	Diff [%]	$\dot{m}$ [kg/s]	Diff [%]
Merlin 1D	981	311	322	1220	24.32	307.88	-1.00	403.8	25.58	943	-3.86	311	0.14	309	-3.99
Rocketdyne F1	7770	304	2605	7711	-0.76	308	1.28	2553	-2.01	7790	0.26	303	-0.45	2624	0.71
RS-68A	3558	411	883	3903	9.67	424	3.18	938	6.30	3533	-0.72	408	-0.77	883	0.05
J-2	1033	421	250	1104	6.89	429	1.78	263	5.02						
RL-10B-2	110	466	24	107	-2.37	457	-1.78	24	-0.55						
RD-180	4150	338	1252	4805	15.77	320	-5.39	1532	22.37	4146	-0.11	337	-0.41	1255	0.30
Vulcain-2	1359	429	323	1184	-12.90	440	2.58	274	-15.10	1290	-5.05	426	-0.75	309	-4.33
RS-25	2278	452	514	2328	2.21	442	-2.13	537	4.45	2275	-0.15	448	-0.98	518	0.84
Viking 5C	758	278	278	636	-16.08	296	6.42	219	-21.14	765	0.93	280	0.67	279	0.27
RD-253	1630	316	526	1734	6.37	313	-0.94	597	13.44	1626	-0.27	315	-0.26	526	-0.01
HM7B	65	446	15	59	-8.5	445	-0.29	14	-8.24						

For the models the overall results can be found in Table 3.14.

Table 3.14: Validation Results for the two models used

Model Result	General Corrected Model		Specific Corrected Model	
	Mean Error [%]	STD [%]	Mean Error [%]	STD [%]
Vacuum Thrust	2.24	11.58	-1.12	2.14
Vacuum Specific Impulse	0.34	3.02	-0.35	0.54
Mass Flow	2.74	13.77	-0.77	-2.12

The results show significant improvement for both models compared to the initial model when comparing the thrust and specific impulse. The average errors are down from 10.35% and 2.5% for thrust and specific impulse respectively to 2.24% and 0.34% for the general correction and -1.12 and -0.35 for the specific correction. The results obtained for the general correction are comparable to Contant [31]. What is seen that the error for the model comes mostly from the mass flow calculations. These errors are probably due to the general values assumed for the flame temperature and the isotropic coefficient (γ). The outliers in Table 3.13 are the Merlin 1D, Vulcain-2, RD-180 and Viking 5C. For the Merlin 1D it is unclear why the difference is so large compared to the mean error with regard to the thrust but the specific impulse is relatively accurate. The issue might lie in the fact that the data is combined from three different sources whereas the others come from one source. For the Vulcain-2 it could be due to the different OF ratio. Where the Vulcain-2 had an OF ratio of 5.3 the general OF assumed is 6 [17]. For the RD-180 this engine is an dual combustion chamber dual nozzle engine, the model approaches this as two separate engines that are added together afterwards, this could be the reason for the differences as they might not be as separate as assumed. Although when the specific correction is applied the errors are mostly dealt with. Finally the Viking 5-C here again the OF ratio seems to be the parameter which is significantly different 1.7 for the Viking compared to 2.6 for the assumed value.

3.5. Drag Model

The drag model is split in two parts a general model which is applied for most of the cases and a special case for parachute inflation. This difference is made because during parachute inflation the force is significantly higher because the parachute over stretches thereby increasing the area over the steady state area.

3.5.1. General Drag Model

The drag model comes uses the standard equation as a basis[49]:

$$F_D = C_D q S \tag{3.29}$$

As the tool only deals in 3 degrees of freedom and the stage is treated as a lumped mass, the C_D only varies with the Mach number. For most of the drag components, the area remains constant, for example, the body of the system as well as the grid fins. However, for the parachute, the parachute inflation is modelled with increasing parachute area since that is where the highest forces are measured. The CD-Mach relation is a separate input value in the tool as discussed in chapter 5. For this research RASAero II is used to calculate the drag coefficient [92]. This is an open-source tool in which the geometry of the vehicle has to be given and it can calculate the drag coefficient between Mach 0 and Mach 25. A comparison between RASAero and windtunnel results can be seen in Figure 3.8. It is assumed that the angle of attack of the vehicle is 0 deg during the flight. This is an assumption that is used within the RASAero simulation package the results of this can be seen in Figure 3.9. Here 78% of the cases have all parameters within 10% of flight data and the altitude prediction has an average error of 3.35%[92]. The same assumption was made within ParSim, this resulted in an error of the trajectory to within 5% [78].

For the drag coefficient for the grid fins and HIAD are obtained from literature. These are again a function of the free-stream Mach number. The drag coefficient is given in Figure 3.10 [29, 125].

3.5.2. Parachute Inflation Model

For parachute inflation the equation for the drag is altered to look like[52]:

$$F_D = C_x X_1 C_D q S \tag{3.30}$$

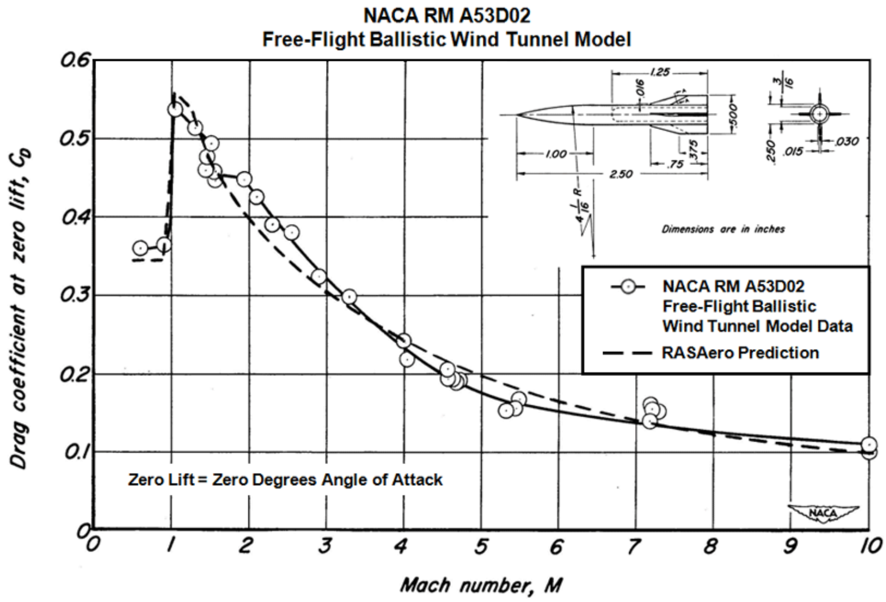

Figure 3.8: Comparison of RASAero and wind tunnel results for the NACA RM A53D02[92]

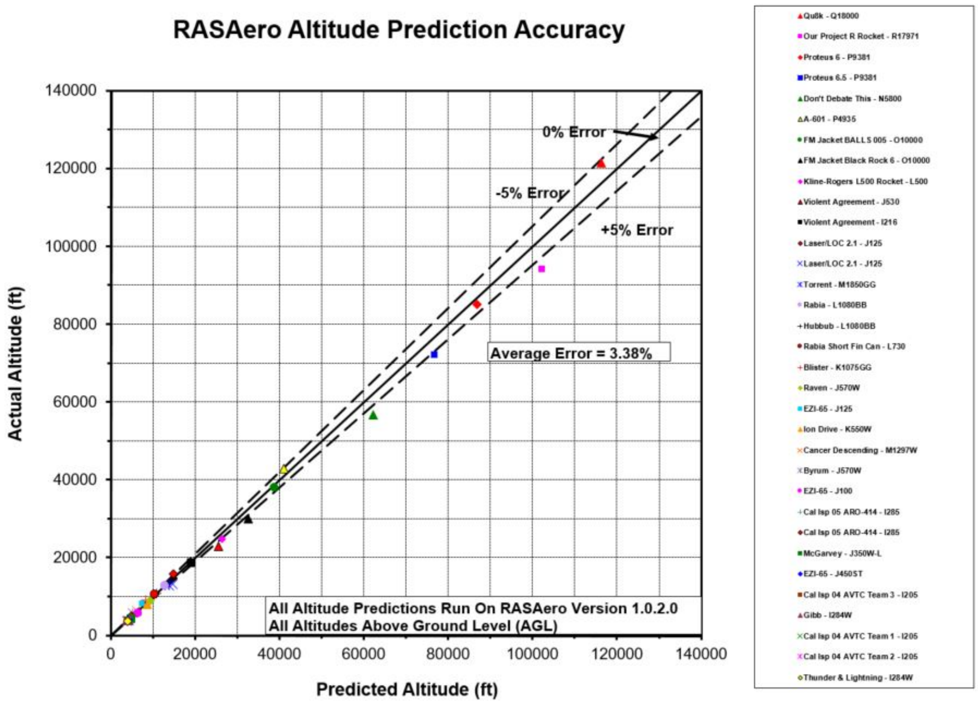

Figure 3.9: RASAero Altitude Prediction Accuracy[92]

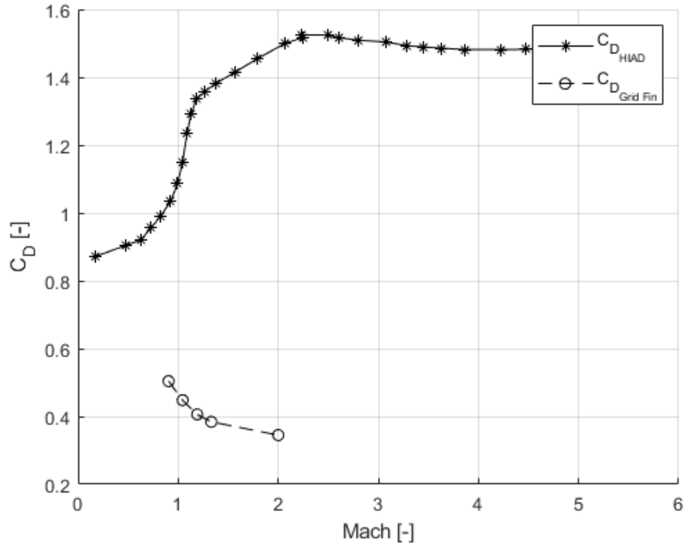

Figure 3.10: Drag coefficients of the HIAD and a Grid Fin [29, 125]

Where C_x is the opening force coefficient at infinite mass, X_1 is the opening force reduction factor and S is the construction area. The construction area can simply be seen as the entire surface of the parachute and not the cross-sectional area at the opening. In order to convert between diameter and production area the shape is assumed to be as a semi-sphere. The drag coefficient is determined using a "hybrid" system, the same which is used in ParSim[78]. Here the C_D at Mach 0 is used to scale the behaviour of the C_D at higher Mach numbers. These behaviours are obtained from Knacke and can be seen in Figure 3.11. How the model works is that the base C_D is used to scale the behaviour of the function given in Figure 3.11. What is also seen is that parachutes that operate below Mach 1 have a relative constant C_D. This model allows for quick changes or additions of parachutes without having to know the entire C_D behaviour but only the base value. For this research the following drag coefficients are used:

Table 3.15: The C_D values at Mach 0 for the different parachute as related to their constructed area[52]

Parachute	C_D
Ringsail	0.5
Hemisflow Ribbon	0.3

C_x is the factor which gives the opening force over the steady-sate force when there is no velocity decrease during the opening[52]. A graphical representation can be seen in Figure 3.12. C_x is constant for a specific parachute type for the Hemisflo ribbon parachute $C_X = 1.15$ and for the Ringsail parachute $C_x = 1.3$.

The variable X_1 is the reduction factor due to the possible velocity decay. This a function of a dimensionless ballistic parameter:

$$A = \frac{2m}{(C_D S)\rho g v_1 t_f} \tag{3.31}$$

Where m is the total mass of the system including decelerator in lbs, S is the parachute area in ft^2, g in ft/s^2, v_1 is the velocity at inflation start in ft/s, ρ is the air density $slugs/ft^3$ and t_f is the inflation time in s. The function can be seen in Figure 3.13. For the Hemisflo ribbon parachute and the Ringsail parachute the curve for n=1 has to be used. The plot is divided into two parts curve I and curve II these are not different models curve II is the same model only plotted on a different scale. These coefficients are applied from within the inflation time of the parachute and decay after the inflation time to the steady value where $C_k = C_x X_1 = 1$ where it becomes the general model. This can be compared to data from [78] where for two missions the shock loading factor C_k is known. The comparison can be found in Table 3.16.

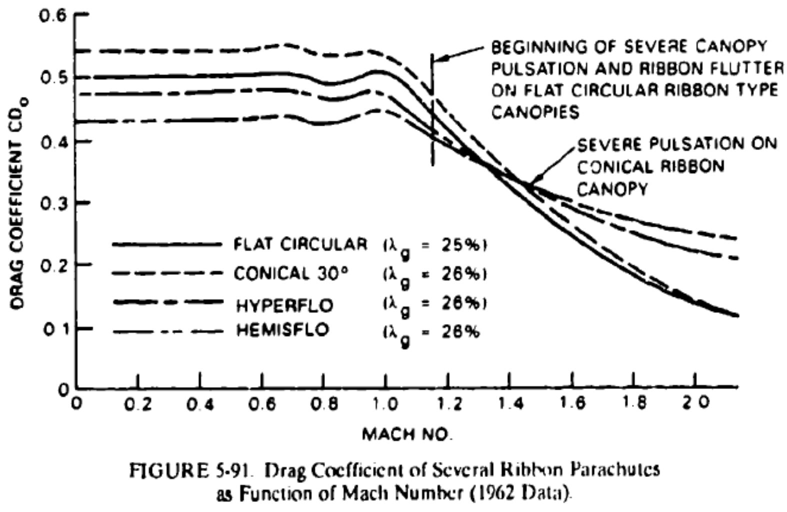

Figure 3.11: C_D behaviour for the Hemislo ribbon parachute [52].

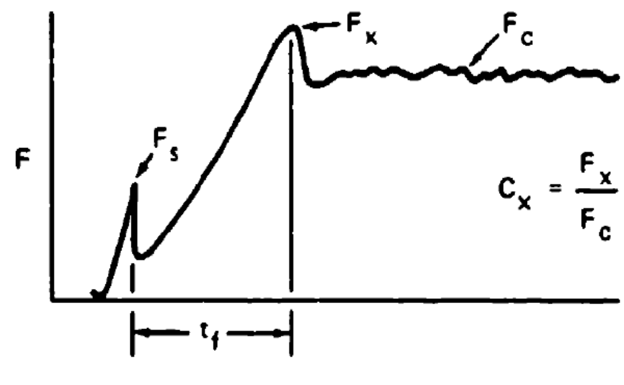

Figure 3.12: Parachute Force versus time for a infinite mass condition (wind-tunnel test)[52].

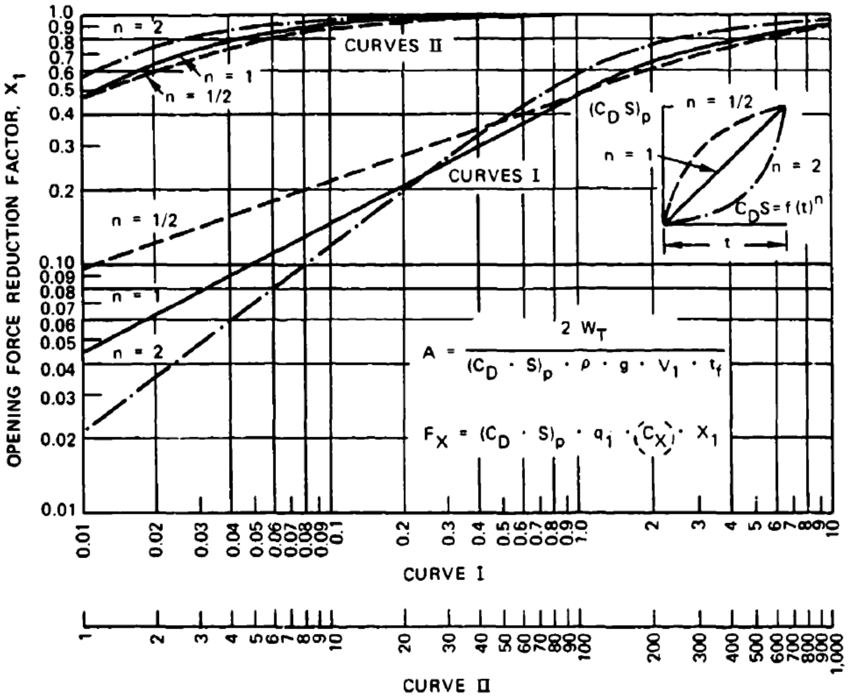

Figure 3.13: X_1 as a function of the dimensionless ballistic parameter[52].

Table 3.16: Comparison for shock loading factor C_k for two missions.

Mission	Model	Data	Error [%]	source
Supermax	2	1.91	4.7	[60, 78]
Aspire	1.22	1.28	-4.7	[50, 70, 78]

The final difference between the parachute inflation and the general drag model is that the area of the parachute is not a fixed value during inflation. The area is varied with the inflation time for a Hemisflo ribbon parachute which is calculated using[52]:

$$t_f = \frac{8D_0}{v_1^{0.9}} \tag{3.32}$$

with D_0 in feet and v in ft/s. The inflation time for Ringsail parachute is calculated using[52]:

$$t_f = \frac{4D_0}{v_1^{0.85}} \tag{3.33}$$

The area as a function of the inflation time is dependent on the type of parachute. For the Hemisflo ribbon parachute the area as a function of the inflation time is linear[52, 59]:

$$S(t) = S_{final}\frac{t}{t_f} \tag{3.34}$$

For the ringsail the function is a 6th power law[52, 59]:

$$S(t) = S_{final}\left(\frac{t}{t_f}\right)^6 \tag{3.35}$$

On top of this reefing is also introduced to the inflation. Reefing is used to limit the inflation loading by halting the inflation process at predetermined points. This is usually done by a wire around the parachute constraining the parachute from inflation further. Reefing is done for a parachute to "settle" in its current situation and already start decreasing its velocity so that when the parachute is at its full area the deceleration is significantly less than if no reefing would be introduced. For this study one reefing design is used consisting out of 2 reefing stages the area at which the inflation is halted as well as the time untill the inflation can continue can be found in Table 3.17.

Table 3.17: Details for the reefing stages used within the FRT tool

Reefing stage	A/A_{final} [%]	time [s]
1	9.82	6
2	39.27	6

This is representative of the reefing stages from the Ariane V booster and space shuttle solid rocket booster parachute systems [23, 113].

3.6. Aerothermal Heating

The aerothermal heating, although not as severe as coming from orbit, can still be quite high. To take this into account, a model is needed. However, there is no analytical model that describes the heating from re-entry. The heating model from re-entry is actually based on several different empirical models that are combined to get both an average and a range. To start with, the assumptions are discussed, followed by the model. After this is the validation of the model.

3.6.1. Assumptions

Since aerothermal heating is an important part, it is calculated during the descent, but it is also a difficult parameter to calculate accurately. This is due to the different shapes on the launcher and the different materials used. Therefore a couple of assumptions are made to be able to calculate the "general" temperature of the stage.

- Negligible conduction through the wall, based on a thin-walled structure assumption. This means there is no conduction between separate elements.
- Conduction through the air is negligible.
- System is treated as a lumped mass, all heat inputs and outputs work on the same mass.

3.6.2. Model Descriptions

Aerothermal heating during re-entry is a complicated variable to calculate therefore multiple models are used to calculate this value. Furthermore because these models are intended for orbital re-entry and not sub-orbital re-entry they are reaching the limit of their valid ranges for some of the models (>3km/s at the re-entry interface[24]). Therefore in order to compensate for any inconsistency between models at the end of the validated range multiple models are combined to give a single heat flux for re-entry. Only convective models will be discussed since according to [25] the radiative heat transfer is negligibly small if the velocity is lower than 10% of the escape velocity. This is backed up by figure 3.14 and the fact that Brandis does not have a radiative model below 9.5km/s[24].

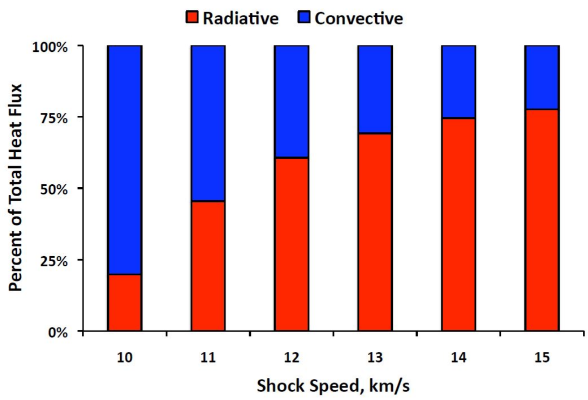

Figure 3.14: Division of radiative and convective heating for different entry velocities for a 1m nosecone radius[24].

The convective heat transfer rate during re-entry is expressed as[28].

$$q_s = \frac{C}{\sqrt{R_N}} \left(\frac{\rho_\infty}{\rho_0}\right)^n \left(\frac{\bar{u}}{\cos\varphi}\right)^m \tag{3.36}$$

With q_s as the heat flow in the stagnation point in $Btuft^{-2}s^{-1}$, R_N is the nose diameter ft, ρ_∞ is the free stream density in $slug/ft^3$, ρ_0 is the sea-level density, $\bar{u}$ is the ratio between the circumferential velocity component normal to the radius vector and the local orbital velocity in ft/s, φ flight-path angle relative to local horizontal direction positive for climbing flight, negative for descent. The values for the constants C and m, C=17600$Btuft^{-3/2}s^{-1}$ and m=3.15, are obtained from AVCO shock-tube experimental results[28]. In [28] it is assumed that the flow is laminar which corresponds to *n=0.5*.

In comparison to the previous model, the Sutton-Graves heat model[24] is relatively simple.

$$q_s = 18.8\sqrt{\frac{\rho_\infty}{R_N}} \left(\frac{V}{1000}\right)^3 \tag{3.37}$$

This relation is valid for enthalpies from 2.3 to 116.2 MJ/kg, pressures from 0.001 to 100 atmospheres and wall temperatures from 300 to 1111K. Unlike the previous two equations, in this equation all the variables have to be in SI units. The nose radius in m, ρ_∞ in km/m^3 and V the free-stream velocity in m/s

Brandis and Johnston [24] created a new model for the stagnation point heat flux.

$$q_s = 7.455 * 10^{-9} \rho^{0.4707} V^{3.089} R_N^{-0.52} \tag{3.38}$$

It should be noted that the models by Brandis and Sutton-Graves give their output in W/cm^2 Furthermore, there is a model made by Finke [44] that calculates the heat flux as follows;

$$q_s = \frac{865}{\sqrt{R_N}} \sqrt{\frac{\rho}{\rho_0}} \left(\frac{V}{10^4}\right)^{3.15} \tag{3.39}$$

Here every value has to be filled in in imperial units. Therefore R_N is in ft, ρ is in $slug/ft^3$ and V is in ft/s. The final method is by the FAA, which is given as[41].

$$q_s = 1.83 * 10^{-4} V^3 \sqrt{\frac{\rho}{R_N}} \tag{3.40}$$

Here everything has to be filled in in SI unit. q_s is in W/m^2, ρ in kg/m^3, R_N in m and V in m/s. What can be seen in all the models that they all depend on $\rho^{\sim 0.5} V^{\sim 3} R_N{}^{(\sim -0.5)}$. This means estimating the velocity and knowing the nosecone radius are most important when it comes to obtaining the heat flux.

These models are then averaged out, and a standard deviation is taken to calculate three temperatures. One is on the mean re-entry heating model, and the others are taken at plus and minus one standard deviation away. This is done since the re-entry heating is a difficult variable to calculate. Because even these five models have a significant difference between them. For a case of a 1m diameter sphere falling through the earth, the average heat loading of these models is $95kW/m^2$ but have a spread of 10%. As was seen during the literature study[95].

Besides the aerothermal heating during re-entry, which is the most important part of the heating model also other in- and outflow of heat is calculated. Once the vehicle is below Mach one it is assumed that the surface will not be heated anymore but instead be cooled by the air. This loss of heat is calculated by using convective cooling. This is calculated using [124]:

$$q_{conv} = h_\alpha (T_\infty - T_v) \tag{3.41}$$

Where q_{conv} is the convective heat flow in W/m^2, h_α is the convective heat transfer coefficient in W/m^2K, T_∞ is the free flow temperature and T_v is the temperature of the vehicle both temperature are in Kelvin. Note that the result is negative when the temperature of the vehicle is higher than the temperature of the free-flow meaning heat is leaving the system. The only parameter which isn't clear immediately is the heat transfer coefficient (h_α). This is calculated using:

$$h_\alpha = St \rho_\infty v C_p \tag{3.42}$$

Here St is the Stanton number, v is the velocity of the flow and C_p is the specific heat at constant pressure which is 1005 $J/(kgK)$ for air[49]. The Stanton number is calculated using[49, 124]:

$$St = \frac{c_f}{2} \text{ where } \begin{cases} c_f = \frac{1.328}{\sqrt{Re_c}} \text{ if } Re_c < 10^5 \\ c_f = \frac{0.074}{Re_c^{0.2}} \text{ if } Re_c > 10^5 \end{cases} \tag{3.43}$$

With Re_c being the Reynolds number over the entire length of the body. with the Reynolds number is calculated using[49]:

$$Re_c = \frac{\rho v x_{char}}{\mu} \text{ with } \mu = \mu_0 \left(\frac{T}{T_0}\right)^{3/2} \frac{T_0 + 110}{T + 110} \tag{3.44}$$

Where x_{char} is the characteristic length which in the case of the first stage is the length of the stage. Finally μ is the dynamic viscosity of air with $\mu_0 = 1.7894 \cdot 10^{-5}$ $kg/(m \cdot s)$ at an temperature (T_0) of 288.16 K [49].

These are however only heat fluxes and not the temperature. In order to calculate the temperature the following differential equation in used:

$$\frac{dT}{dt} = \frac{\Delta Q}{mC} \tag{3.45}$$

Where ΔQ is the total heat flow in W, m is the mass that is heated and C is the heat capacity in J/K. The heat balance ΔQ is the summation of the heat in and heat out. The overview of the heat in and out are given in Table 3.18. For these equations three parameters are important. First is the heat transfer area this can either be the entire surface area of the stage, which is assumed to be a cyclinder (A_{surf}). Or the area can be the frontal area (A_{front}). This is dependent where the heat flow occurs. For most the heat transfer area will be the surface area for the re-entry heating it will be the frontal area. The second and third parameters are the absorptivity (α) and emmisivity (ϵ) which are constants for the material used. For this reasearch aluminium is used which has an emmisivity of 0.09, an absorptivity of 0.14 [107, 108]. Finally the heat capacity of aluminium is 887 J/K.

Table 3.18: Overview of the various heat inputs and outputs considered

Heat	In/Out	Equation	note
Solar Heat	In	$Q_{solar} = \alpha 0.5 A_{surface} q_{sun}$	q_{sun} is the heat flux of the sun which is 1366 W/m^2 [120]
Sun heat reflected from the earth	In	$Q_{albedo} = \alpha 0.5 A_{surface} q_{sun}(1 - \alpha_{albedo})$	Heat from the reflective heat from the earth α_{albedo} is the albedo fo the earth which is 0.306 [73]
Re-entry Heat	In	$Q_{reentry} = q_{reentry} A_{front}$	Only above Mach 1
Convective Heating	Out	$Q_{conv} = h_\alpha (T_\infty - T_v) A_{surf}$	Only below Mach 1
Radiative Heat	In/Out	$Q_{radiative} = \epsilon A_{surf} \sigma (T_v^4 - T_\infty^4)$	σ is the Boltzmann constant. For this equation T_∞ is assumed to be zero when outside the atmosphere (>100km)

All these heat flows are summed together and are input into Equation 3.45 and then integrated over time to lead to a temperature. The mass in Equation 3.45 is a more difficult to determine as using the stage mass will lead to very low changes in temperature. The mass used for Equation 3.45 will be the mass primarily in the flow. This will be, for the entire vehicle and the second stage, the fairing. For the first stage this is the engine mass.

3.6.3. Validation

The validation of the temperature calculation is tricky since not a lot of missions fly with the temperature measurement as a primary objective. However, there was the SuperMax mission with this as one of the main objectives[60]. Table 3.19 gives the inputs which were used for the validation of the temperature calculation.

Table 3.19: SuperMax Inputs for the Heat model Validation

Parameter	**Input**
CD body	1.3
CD par	0.48
Ck	1.77
A_{par} [m^2]	1.28
H_{dep} [km]	19.1
T_{inf} [s]	0.022
Line length [m]	3
H0 [km]	163
V0 [km/s]	3
Gamma0 [deg]	85.37
D0 [mm]	290
M0 [kg]	13.76
Tip Radius [mm]	72.5
Heat Capacity [kJ/kgK]	0.5
Emissivity	0.6
Absorptivity	0.2
T0 [K]	289
L [m]	0.201
Shell Mass [kg]	13.7
Internal Heat [W]	0

The results from these inputs in ParSim V4, which uses the same heat model, are given in Table 3.19. Next to the results from the SuperMax mission as well as the error between the two.

Table 3.20: Results from ParSim as well as the results from the SuperMax Flight and the respective error [60]

Parameter	**SuperMax**	**ParSim**	**Error [%]**
Apogee [km]	679	680.2	0.18
Parachute Deployment			
Mach [-]	1.7	1.68	1.18
Inflation Load [kN]	12	13.39	11.58
Velocity [m/s]	495	494.29	0.14
Density [kg/m^3]	0.094	0.101	7.44
Temperature			
Time max T [s] after release	760	762	0.26
Temperature [K]	140	173	23.57
Heat flux [MW/m^2]	1.3	1.6	23.08
V at Heat flux max	2864	2909	1.57

What can be seen in Table 3.20 is that ParSim is very accurate when it comes to the trajectory. For the parachute loads, the biggest deviation comes not from the method of calculating the load but from the difference in the density which had a 7% error.

For the temperatures in SuperMax, the temperature was measured directly on the inside on the vehicle in the tip. Here a 23% error is observed for both the temperature and the heat flux. This is a significant deviation, but there are a couple of possible reasons for this:

- SuperMax did not have a steady angle of attack; it varied within 10 degrees. Therefore, the heat would decrease since the heat flux would be focused at a different point with a larger apparent tip radius, thereby decreasing the heat flux. This is because of the conical shape of the nose cone of SuperMax.

- As already seen the density at higher altitudes are different for SuperMax than the atmosphere used in FRT. With a higher air density, higher heat fluxes are calculated when the velocities are the same.

Regardless of the differences, the error for the temperatures and heat fluxes remain largely the same. This shows that the error in the temperature calculations comes mostly from the error in the re-entry heat flux.

3.7. Overview of the Models

In this chapter various models, figures and numbers have been mentioned. In Table 3.21 is an overview of the model discussed with their accuracy and where they originated from. The accuracy is given in the mean error μ and standard deviation σ where available. The effect of these inaccuracies are taken into account when performing the sensitivity analysis in chapter 6.

Table 3.21: Overview of the models discussed in chapter 3

Model	Origin	Accuracy [%]	note
Extra Tank Mass Model	Comparative model based on the design model by Zandbergen [124]	0.01 (± 6.1)	
Landing Legs Mass Model	Model based on historical data from various sources	0 (± 10)	Model was a percentage of the stage mass based on 10 data points.
Airbag Mass Model	Mass model from Knacke [52]	28.03 (± 43.76)	
Flotation Device Mass Model	Bottom-up Model created by Pepermans [77]	0 (± 20)	No validation data could be found
Grid Fin Mass Model	Model from article on design of mass optimised creation of grid fins [2]	34.1 (±24.4)	
Hemisflo Mass Model	Mass Model made by Knack [52]	-19.2 (±20)	
Ringsail Mass Model	Mass Model made by Knack [52]	-11.5 (±14)	
HIAD Mass Model	Parametric Mass model by [96]	-5.2 (±3.8)	
General Corrected Thrust Model	Ideal rocket theory with correction factors [124]	2.24 (± 11.58)	
Specific Corrected Thrust Model	Ideal rocket theory with correction factors [124]	-1.12 (± 2.14)	
Parachute Inflation Model	Inflation model based on variable parachute size and dynamic inflation coefficient [52, 78]	0 (± 4.7)	
Heat Model	Re-entry heating combined from 5 sources [24, 28, 41, 44]	0 (± 23)	Most of the error came from the re-entry heat calculation

4

Cost Models

To see whether 30% of the cost can be saved from reusing the first stage, a cost model is needed. This model does have to calculate the cost for the launcher as well as the cost for the different deceleration and landing elements described in chapter 3. Next to the cost of the launcher, the critical part is the refurbishment cost. Finally, the model will be validated using historical data.

4.1. TransCost Model

For the main cost model, the TransCost model from the Handbook of Cost engineering and Design is used[57]. This model aims to provide a cost estimation during the conceptual design phase. This means a limited amount of inputs are used to obtain the cost. The result is mainly dependent on the division of the masses of the system. Drenthe showed that this model is accurate for launcher with a payload mass larger than 700 kg[38]. Furthermore Trivailo gave an accuracy for TranCost to within 20 percent [109]. The model is divided into multiple parts, as can be seen in Figure 4.1. TransCost does not have any models for the recovery systems and reusable systems these are added separately. What is important to note here is that the cost is given in Man-Years. This is done to be relatively independent of the year and specific valuta[109]. For this research a Man-Year (MY) has a value, for the financial year 2018, of €301200 [57]. In each of the models, the general cost is calculated by:

$$C = a * M^b \tag{4.1}$$

Where a and b are dependent on historical data, and M is the mass to which this cost is related. For example, for the engine cost, M is the engine mass, and for the stage cost, the mass is the empty mass of the stage. The factors a, b and inputs M for the different models can be found in Table 4.1.

For the TransCost model, the following inputs are required per stage for a basic launcher with no boosters. These are the empty, propellant and engine mass per stage and the experience of the company. The last one is

Table 4.1: coefficients for various cost models from Transcost

Model	**a**	**b**	**M**
Development Cost			
pump fed liquid engine	277	0.48	Engine mass
solid engine	16.8	0.54	Engine Mass
stage development	98.5	0.555	stage empty mass
solid engine stage	22.4	0.54	stage empty mass
First Unit Production Cost			
RP1/LOX Engine Production	1.9	0.535	Engine Mass
LH2/LOX Engine Production	3.15	0.535	Engine Mass
RP1/LOX Tank Mass	1.84	0.59	Tank Mass
LH2/LOX Tank Mass	1.265	0.59	Tank Mass
Solid Engine & Stage	2.75	0.412	Stage Mass

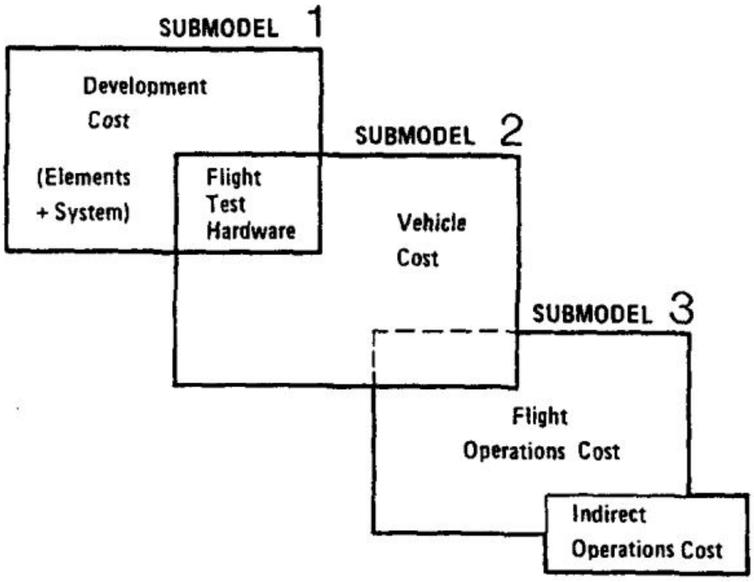

Figure 4.1: Overview of the TransCost Model[57]

a coefficient which changes dependent on the experience is designing and in producing the stage. These are subjective inputs for which some guidance is given; however, it is still open to interpretation. Finally, some inputs are needed for the engine characteristics, which are the type of engine, i.e. solid engine, liquid engine, and if it has a pump or is pressure fed. Finally, if the engine type is a liquid engine which propellant is used. This would be enough to calculate the cost for an expendable launcher with no boosters.

In order to compare the expendable launcher to the reusable one, the cost model is used first to calculate the cost of the expendable launcher. This is not done for, only the first unit, but for the number of launches that the reusable launcher is going to be reused for. The production cost is then averaged over the number of launches that are being investigated. With this, multiple key cost parameters are calculated. The cost per flight and the flight cost per kilogram payload are calculated. For the cost per kilogram for the expendable version two values can be given. One with the payload mass for the reusable case , and one with the maximum payload mass the launcher can put into orbit. There is a difference between the two since to make an expendable launcher reusable extra mass in the first stage comes at the cost of payload mass. The difference between the two payload masses is only of interest when comparing the flight cost per kilogram of payload, which can be done through the reuse introduced by ULA[83]. This Reuse Index is nothing more than the cost per kilogram of the reusable launcher divided by the cost per kilogram for the expendable launcher. This gives the cost that is saved by switching from expendable to reusable.

4.2. Reusability Cost Models

Since Transcost is missing models for deceleration systems, landing systems and refurbishment cost these models need to be added to the model.

4.2.1. Re-usability Hardware Cost Models

For the landing and deceleration systems most of the models are bottom up models with the exception of the landing legs these are folded into the main stage cost. The separate cost models are those for the Ringsail and Hemisflo ribbon parachute, the HIAD, flotation device and airbags. These cost models were developed by Lars Pepermans[77] and are also used here. Since validation data is lacking for most of these models they are considered rough order of magnitude models. The costs for these models will be made up out of two elements the material cost and the production cost. For the production cost the only parameter is the production hours which is given in Table 4.2.

Table 4.2: Production Hours for the different elements[77]

Element	Production Hours
Parachutes	95
HIAD	96
Airbag	72
Flotation	72

For the material production costs it is dependent on which materials are used in the relevant hardware.

HIAD Cost
A HIAD consists out of a layer of 40mm nextel 440, 47 plies of pyrogel 3350, a layer of 1mm kapton, and 10 plies of 5mm thick kevlar. This leads to the following equation for the cost of the system which is dependent on the frontal area of the HIAD (A_{HIAD}).

$$C_{HIAD} = 2 * \left(A_{HIAD}\rho_{Nextel}c_{nextel} + 47A_{HIAD}c_{pyrogel} + A_{HIAD}c_{Kapton} + 10A_{HIAD}c_{Kevlar}\right)] \quad (4.2)$$

The value for the parameters can be found in Table 4.3.

Table 4.3: Parameter values for the HIAD cost

Parameter	Value	Source
ρ_{Nextel}	0.5 kg/m^2	[36]
c_{nextel}	116 USD/kg	[77]
$c_{pyrogel}$	4.89 USD/ft^2	[27]
c_{kapton}	5.678 USD/ft^2	[30]
c_{Kevlar}	20 USD/m^2	[77]

Parachute Cost
For the parachute cost models are similar in form only the materials that are being used are different.

$$C_{parachute} = 1.1\left(A_{canopy}c_{canopy} + n_{suspension}L_{suspension}c_{suspension} + L_{riser}c_{riser}\right) \quad (4.3)$$

The canopy costs are directly related to the area given by the optimisation process. The cost for the suspension lines and the riser are dependent on the length of either of those parts, the total length is determined by a ration which is found in Knacke[52]. For this research a simple rule will be used which is of the total length of wiring 80% is suspension length and 20% is riser length, this is done to make sure the suspension lines aren't too short. For the suspension lines it is assumed that there is one suspension line every 50cm for the entire circumference. Using this only the cost for either a unit of length of an area needs to be known, these can be found in Table 4.4.

Table 4.4: Costs for the parachute material [77]

Parameter	Ringsail	Hemisflo
c_{canopy}	18 USD/m^2	20 USD/m^2
$c_{suspension}$	1 USD/m	2USD/m
c_{riser}	5USD/m	10 USD/m

Airbag Cost
For the airbag cost it is assumed that the bag is made out of vectran of which the cost is 4500 Yen/kg which is about €37.05 per kilogram[54]. This can be used on the airbag mass obtained in subsection 3.2.2.

Flotation System Cost
For the flotation system, the mass model was already a bottom-up model, so the mass of the flotation spheres is already known. The only need is for the cost per kg of mass, and the material cost is known. The cost is €99.6 per kg [26].

4.2.2. Retrieval Cost

For retrieval, there are two options; one is a boat or drone ship. For simplicity, these will be the same cost. The other option for retrieval is Mid-Air capture and retrieval (MAR).

For ship retrieval, there are two major costs. One is the ship cost, and the other is for the manpower needed. For the ship operations, it is assumed that 20 people are needed for the time of the operation plus the cost for the ship. It is assumed that the average velocity of the ship is 13.5 knots (25km/hr), and it has to travel to and from the target location. On top of that, the time is extended by 20% as an extra buffer. This comes down to:

$$C_{ship} = \frac{1.2 t_{travel} 20}{T_{MYrH}} + \frac{760000}{LpA \cdot C_{MY}} \tag{4.4}$$

The first part is the man-hour cost for the retrieval where t_{travel} is the travel time from the launch site to the final landing location and back in hrs, T_{MYrH} is the number of working hours in a year, which is is based on 52 weeks five days a week and 8 hours in a day. The second part is the ship cost itself which is €760000 per year [99]. This is divided over the number of launches that are performed in a year (LpA). This is converted into a Man-Year(MY) format

For the Mid-Air retrieval, the same set-up is used as for the ship retrieval. However, there are a couple of differences. Instead of 20 people, it is assumed only to have 3, and the speed of the helicopter is increased from 13.5 knots to 140 knots (259 km/hr).

$$C_{MAR} = \frac{1.2 t_{travel} 3}{T_{MYrH}} + \frac{775000}{LpA \cdot C_{MY}} \tag{4.5}$$

The cost of the helicopter itself was set at €775000 per year [99]. The prices for the vehicle was determined by M. Snijders on the advice from (former) employees of Airbus Helicopters, Zwijnenburg Shipbuilding and Damen Shipyards [99]. An overview of the retrieval cost can be found in Figure 4.2. It shows that in general

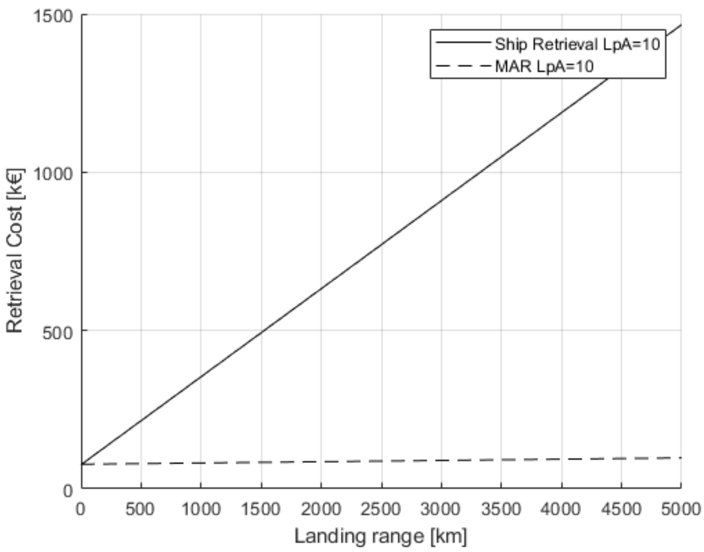

Figure 4.2: Retrieval cost as a function of the landing distance for 10 launches per year.

MAR is cheaper for retrieval than the ship. However it does add stricter requirements on the system with regard to mass and a maximum velocity during capture. When altering the amount of launches per year the graph only moves up or down the gradient stays the same as is expected.

4.2.3. Refurbishment Cost

Refurbishment cost is everything that has to be done between the moment the stage is retrieved, and the launcher is ready to be launched. This does not include the fuel and operations that are needed on the launch site; these fall under operational costs. Refurbishment is an important parameter in the economics of reusable launch vehicles. However, this is also one of the least known parameters in reusable launch vehicles[103]. Most refurbishment costs are expressed in a fraction of the production cost of the part that is refurbished, but these fractions vary widely between 3%-50% of the production cost [46, 57]. However, besides this, there is also the fact that refurbishment increases with the number of reuses that are performed. Since historical experience has shown that refurbishment and repair cost increase with the age of the vehicle [119]. In [119], it is suggested that a "learning curve" is applied that increases the refurbishment cost by 105% to 115% to account for that increase. For this study, 115% is used

Combining all this the following refurbishment model will be used:

$$C_{refurbishment} = C_{production}\left(0.25n^{\left(\frac{ln(1.15)}{ln(2)}\right)}\right) \tag{4.6}$$

This would mean that there is a 25% initial refurbishment cost. This refurbishment cost will then be averaged over the number of reuses. So the average refurbishment will be determined only by the maximum amount of reuses. The average refurbishment cost as a function of the number of reuses can be found in Figure 4.3.

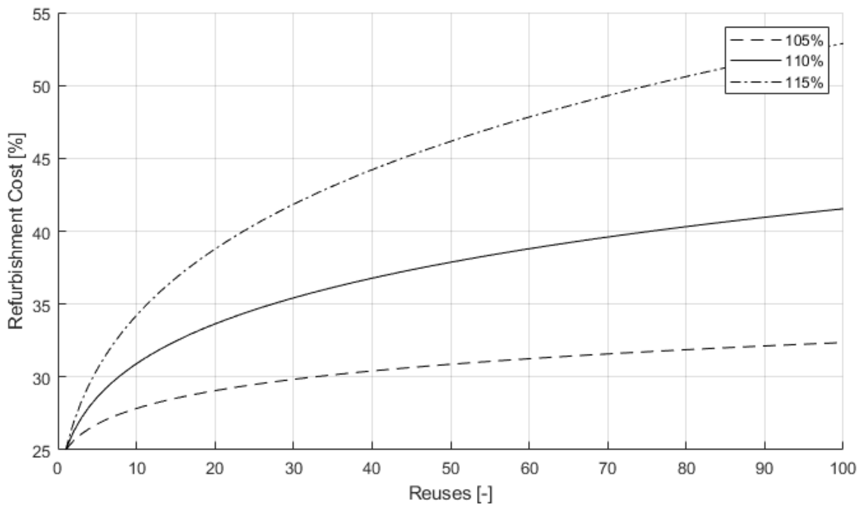

Figure 4.3: Refurbishment cost fraction as a function of the number of reuses

4.3. Verification & Validation

The validation of the cost model is a difficult thing to do. Because the cost which are publicly available are commercial prices. These prices are dependent on the actual costs per flight, but also the development cost and the time in which the company wants get that cost back. For the validation here it is assumed that the development cost is returned within 100 launches. On top of this there will be an 8% profit margin [38]. Finally it is assumed that no governmental subsidies apply which could lower the cost. These assumptions for the return of the development cost and the profit margin are general values. In reality all these values are dependent on the specific financial situation of a company/institution and here the subsidy from any governmental institution does make a difference. Furthermore for these assumptions it is assumed that the company is making a profit with every launch. However, a company could set a fixed rate which initially loses money for the first flights and the more flight the more profit the company will make.

Table 4.5: Validation data for the cost model used in the tool comparing flight costs from historical data and the cost model.

Launcher	Empty Mass [kg]	Error [%]	Real Price [M$]	Cost Model [M$]	Note	Sources
Atlas V 501	23301	-37.04	109	68.62		[110]
Atlas V 551	43636	-44.17	153	85.42		[110]
Ariane V ECA	85240	-21.99	137	106.88		[47]
Delta II 7920-9	19500	-6.41	51	47.73		[1]
Falcon 9FT (expendable)	31500	28.64	61.2	78.73		[101]
Falcon 9 FT (reusable)	31500	-11.97	50	44.01	10 reuses	
		-20.03		39.99	100 reuses	[101]
Mitsubishi HII-A	37000	-9.33	90	105.78		[74]
Proton-M	45100	90.41	65	123.76	Model for RP1/LOX propellant is used	[74]

What can be seen in Table 4.5 is that costs are indeed challenging to estimate at a conceptual level. The average error in the validation may be only -3.5%, the standard deviation is, however, 41%. This shows a considerable spread of the costs. Clear outliers are the Proton-M, but also both the Atlas cases and the Ariane 5. These deviation are, however, do not have to contradict to the 20% accuracy previously mentioned. The reason for this is again the commercial price. In Table 4.5 assumptions are made to the profit margin and development recuperation time. These are not part of the TransCost model but additions or fractions of the production and development cost. Furthermore these values for profit margin and recuperation time can be significantly different dependent of the specific company.
The only reusable data point in the validation is the Falcon 9, which shows an overestimation on the expendable case but an underestimation on the reusable case. Knowing this accuracy is essential, but the impact is somewhat lessened when comparing expendable and reusable launcher which is based on the same vehicle.

As for the the specific cost models validation data is hard to obtain. So they will be compared to each other in order to check if the models are correctly implemented. The cost of the various deceleration systems is given in Figure 4.4 and Figure 4.5. These models were created by using the Falcon 9 launcher as a baseline launcher. This was needed since some of the models depend on some estimates that include parameters of the vehicle such as for the HIAD.

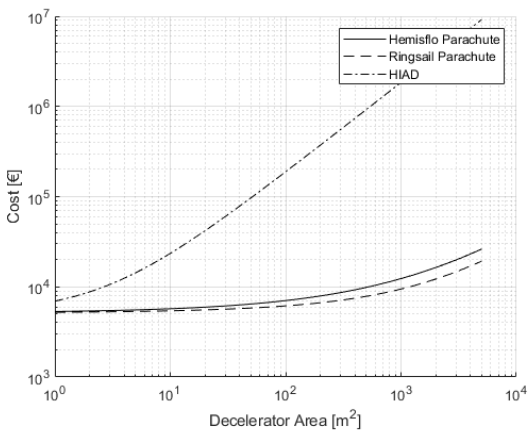

Figure 4.4: Deceleration System cost as a function of the area

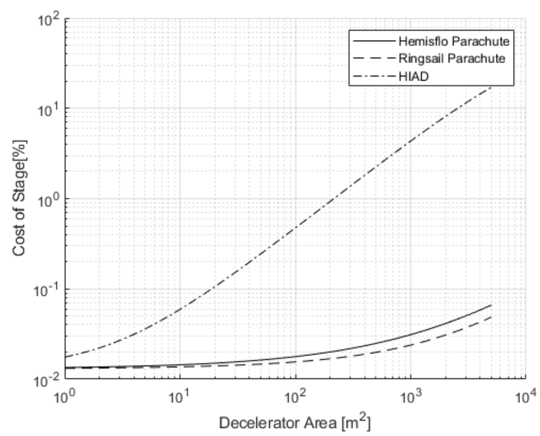

Figure 4.5: percentage of deceleration cost to the total vehicle cost as a function of decelerator area

What can be immediately seen in Figure 4.4 is that the HIAD costs significantly more than the parachutes.

This makes sense since it is heavier when comparing them with the same area parachute. Furthermore more costly materials are used in the construction, which can be seen in the steeper gradient. The parachute costs are comparable. However, the Hemisflo parachute is more expensive. Again, it follows from the more expensive materials which are used compared to the Ringsail parachute. For the Hemisflo, mostly aramids are used with a cost of 20 USD/m^2 compared to the 18 USD/m^2 for the canopy and the lines for the ringsail are 50% of the cost.

When looking at Figure 4.5 it can be seen that the cost of the deceleration system is for all cases below 1% of the unit cost, except for HIADs over 200 m^2. However these HIAD sizes have such a significant mass that it becomes almost unpractical to use them.

From these results it can be said that the models have been implemented correctly however about the validity little can be said. Therefore an accuracy of ±50% is used on cost models for which no validation could be performed. Although 50% may seem significant, for the launcher cost model it was already seen that the costs can vary significantly. As the total recovery cost will be in the order of 1M€. At worst the 50% accuracy will change the overall price for the cheapest launcher in Table 4.5 by 1%.

5

First Stage Recovery Tool (FRT)

In order to determine what method of reusing the first stage is more economically viable a tool needs to be created. This is the First Stage Recovery Tool(FRT) this tool will perform all the calculation required. As a basis of the tool, the general equations of motion and foundation from the ParSim tool are used. ParSim is a tool developed by Delft Aerospace Rocket Engineering(DARE) for calculating the force coming from the parachute when deploying in mid-air. In order to do this, it calculates the entire trajectory. In [78] it was shown that the trajectory is accurate up to 5% for the parachute forces. Furthermore, it is accurate up to 1% for the altitude and velocity over time. FRT is made in such a way that users are able to include and exclude the relevant options. The tool is also modular that if a better model for cost or for masses becomes available, this can be implemented without changing the architecture of the tool.

5.1. Background

Initially, the choice was made to create this tool within the TUDat environment the same as Contant did [31]. However, this proved not to be possible to perform the tasks within the time frame required. The reasoning for using the TUDat framework was to not create the entire structure from zero. So a replacement for the TUDat framework was needed that had most if not all of the same essential functions already validated. The ParSim tool developed by Delft Aerospace Rocket Engineering was already validated and used in two articles [78, 79]. So it was decided to use ParSim as a base and continue to develop the tool from there instead of using TUDat.

The general dynamics model is taken from ParSim. ParSim comes in two versions both are made in MATLAB, one is a 2D version, and one is a 3D version. It is the latter one which is used for this research. It is a 3 Degree of Freedom integrator which has already been used and validated [78, 79]. It has an error when calculating the trajectory of lower than 2% for altitude, velocity and time of flight. For the calculation of the parachute force it has an error of 5%.

5.2. General Trajectory

The axis-systems in the model is as defined in [69] with a slight modification. Since the perturbations of the rest of the planets and moons are ignored in this research, the inertial reference system is the same as the body-fixed reference system at t=0. This is done to simplify the computation. The rest of the axis-systems are still the same, as can be seen in Figure 5.1.

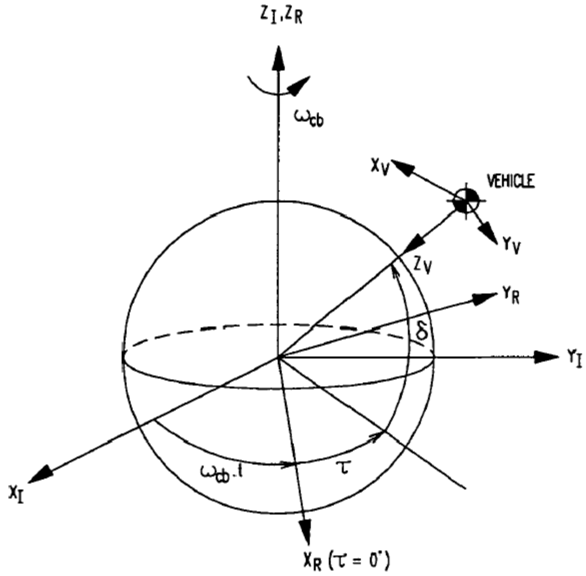

Figure 5.1: Definition of the inertial and local horizon frame[112]

ParSim is a 3DOF (Degree of Freedom) model that assumes a constants angle of attack during the flight. For the gravity model, the central gravity field is used, which is only dependent on the distance from the centre of the earth. The option to use spherical harmonics with ParSim/MATLAB exists; however, this increases the computation time significantly. The atmosphere model is the 1976 COESA (Committee on Extension to the Standard Atmosphere). The model has a range between 0 and 84852 m and is extrapolated above and below it. The extrapolation is linear for temperature and logarithmically for the pressure.
Next to the model, ParSim also has some assumptions. First is that no lift is generated by any vehicle or body. Next is that the drag from any body is always in line with the velocity. This is a consequence of the angle of attack assumption and the lack of lift. Finally, the drag is assumed to be variable with the Mach number.

Integration of the equations of motion and all other differential equations are done using the standard set of MATLAB integrators. These are ODE45, ODE113 and ODE15s. ODE45 is based on an explicit Runge-Kutta (4,5) formula. This is the standard solver used for most situations[64]. The other two ODE113 and ODE15s are used in specific cases to improve computation time. ODE113 is a variable step variable order Adams-Bashforth-Moulton PECE solver. It is more efficient than ODE45 with stringent tolerances [62]. This is used for integrating orbital trajectories or when high accuracy is required. Finally, ODE15s is an implicit solver which is used if ODE45 either fails or is very inefficient[63]. These can be used for sudden abrupt changes. The primary example is parachute inflation, where for smaller parachute the inflation time is less than a second.

Since ParSim was never imagined to also include the ascent of the launcher a thrust model and ascent trajectory calculation have to be included. These models as well as non-parachute deceleration models will have to be included to simulate the descent of any stage. These deceleration models were discussed in chapter 3.

5.3. Inputs & Outputs

FRT aims to produce the required results with a minimal set of inputs. In this section the required inputs are given as well as a general overview of the outputs.

5.3.1. Inputs

FRT uses existing launcher and coverts them into reusable launchers. This requires the tool to be able to run on a limited amount of information since any detailed information might be hard to acquire. This could be either due to that these inputs are commercially important as for the actual flight cost of the launcher or could be used to redesign the system by for example releasing a detailed mass breakdown. The inputs that are required start with the mission to be flown and the initial conditions:

- Payload mass
- Target orbit
  - Apogee altitude
  - Perigee altitude
  - inclination or launch heading
- Initial location
  - latitude & longitude
  - altitude
  - velocity
  - orientation (azimuth and heading)

Since FRT is aimed to alter existing vehicles in order to make them reusable after the mission the vehicle has to be defined

- Sizing and mass for the individual stages & boosters
  - Empty mass
  - Propellant mass
  - Engine mass
  - Stage diameter
  - Stage length
  - Nose tip radius (for re-entry heating)
- Engine specifications
  - Nozzle exit and throat diameter
  - chamber pressure
  - thrust limit
  - real-life correction factors for either sea-level or vacuum conditions(optional)
- Drag coefficient as a function of Mach number
- Mass to be used for heat calculations

After this the inputs for the reusable part of the tool have to be given. These include which deceleration options to use, which landing method, some information on the production of the launcher and the general constraints. The information on the production is high-level information, these are the amount of launchers previously produced, the challenge of modifying the system and the amount of launches which are performed per year. These are only required to give a realistic value for the costs. If none are given the tool will still compare the results. Finally the last inputs are the constraints on the return flight these are the maximum deceleration, temperature and dynamic pressure.

5.3.2. Outputs

The outputs of the tool are given in four categories. These are:

- Mass overview of the final vehicle
- Overview of the trajectory flown
- Cost overview of the vehicle
- Sensitivity of the final result

These are spread over multiple graphs, and also a custom graph can be created. A complete list of all 34 outputs is given in Appendix A. For the outputs there is a difference between what is shown and what is stored, as the latter is a subset of the former. All the data can be saved in a .mat file which can be opened with any MATLAB program. The results that are shown within the tool are on the vehicle and critical points during the trajectory. An example of the key trajectory numbers can be seen in Figure 5.2. Besides key points during the trajectory also the ground track of the trajectory as well as other graphs of the trajectory are given an illustration of these output figures can be seen in Figure 5.3 and Figure 5.4, these serve only as an example and not as a result of a relevant case.

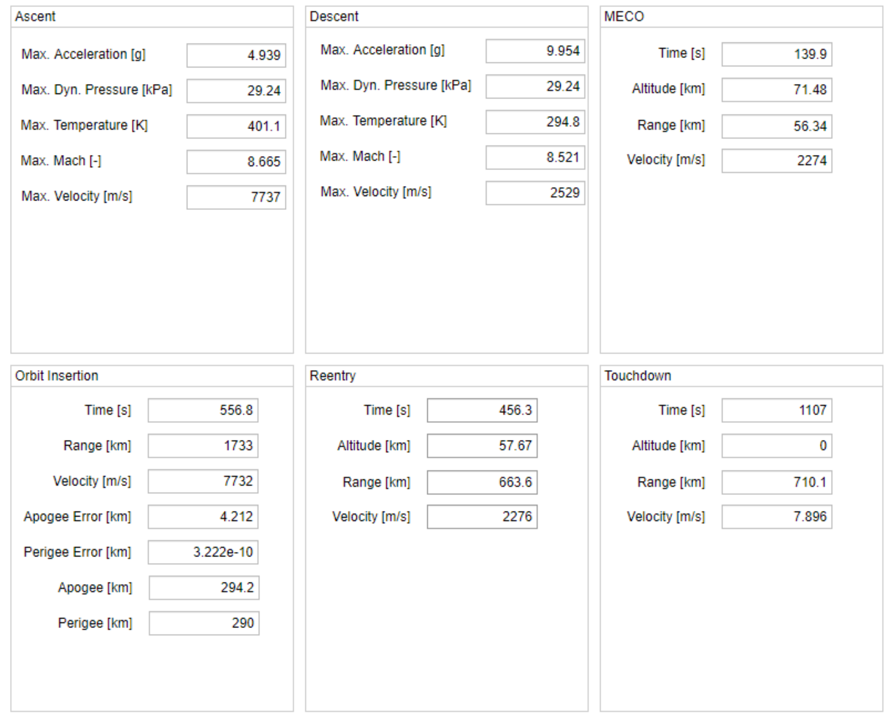

Figure 5.2: Results of the critical point of the trajectory

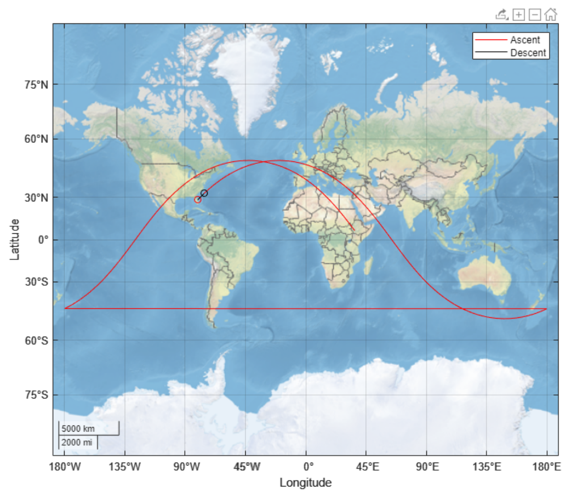

Figure 5.3: A typical ground track as given by FRT

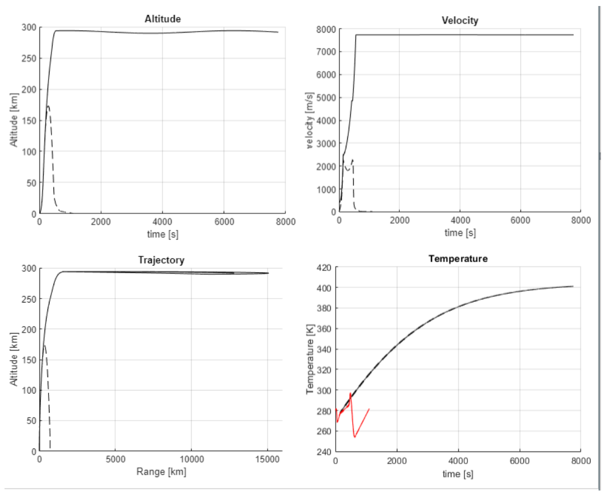

Figure 5.4: Typical results for a LEO case within FRT

5.4. Main Optimisation Loop

The main optimisation loop determines the cost for the different configurations for the reusable launcher. First the chosen optimisation algorithm is discussed. This is followed by the main function and the flow of computational operations. Finally the excluded combinations are discussed.

5.4.1. Surrogate Optimisation Algorithm

For the main optimisation function the surrogate optimisation algorithm from MATLAB is used. A surrogate optimisation is an algorithm that creates a simpler function based on the results of the first randomly chosen point and searches near the best point. After which it starts randomly searching in the neighbourhood of the best value. It starts the search with a large range and than narrows the range centred on the best point. It continues to do this until minimal distance is reached. It can than reset and start all over until the maximum amount of function evaluations is reached. A graphic representation of the surrogate algorithm can be found in Figure 5.5.

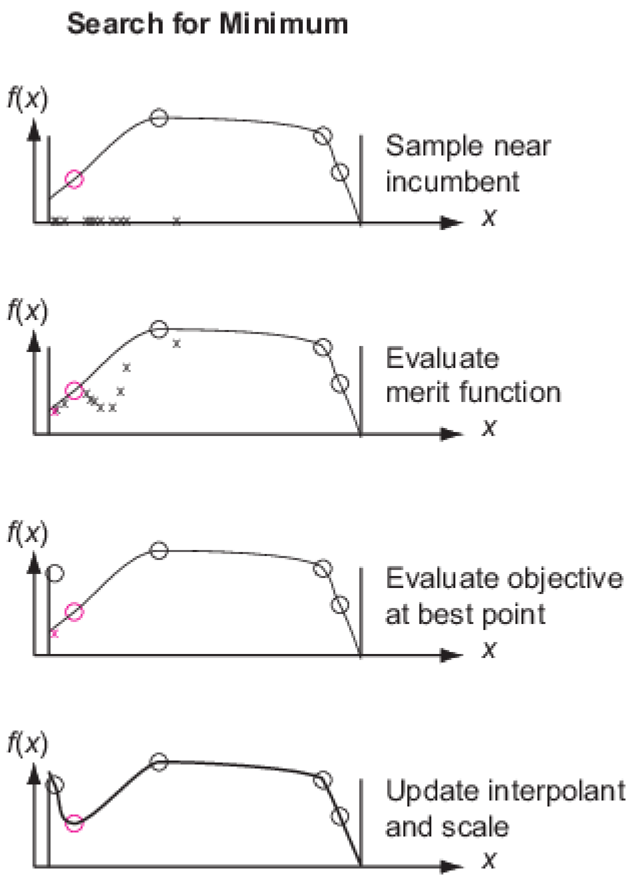

Figure 5.5: Graphical representation of a surrogate optimisation algorithm[66]

The idea to use surrogate optimisation came from the computation time needed for the genetic optimisation algorithm. Although the genetic optimisation algorithm functioned as expected, it did so very slowly. Therefore a faster alternative was desired but not apparent at the start. Since it was known that the genetic optimisation was the only discrete optimisation algorithm MATLAB possesses. After searching through the global optimisation toolbox alternatives were considered among which were the pattern search and particle swarm optimisation. They showed an improvement in speed for this problem, but none were capable of discrete optimisation. This led to the consideration of performing the discrete optimisation separate from the design optimisation. This would mean that the design would be optimised for each of the discrete options separately. This was luckily not required since with the introduction of MATLAB 2019b the discrete surrogate optimisation was added which as stated is to be used for computationally expensive objective functions. Although surrogate optimisation algorithms are relatively new, they already have been used within the TU Delft but mostly for continuous problems [58, 123]. Furthermore, the surrogate optimisation within MATLAB itself is relatively new being only introduced in 2018 and discrete surrogate optimisation only being introduced in MATLAB version 2019b [65]. This shows that using discrete surrogate optimisation is very new at least within the MATLAB toolboxes.

The benefits of a surrogate optimisation over a genetic optimisation algorithm is that the surrogate optimisation is created for optimisations for which the objective function is computationally expensive to evaluate. Which is beneficial in this case since it is possible and likely that the algorithm needs to perform an ascent optimisation during the evaluation of the main optimisation function. This can take quite a while, and therefore it is more efficient if the amount of function evaluations can be limited. However, the downside of the surrogate optimisation is that it does not necessarily finds the global minimum value. It finds a point in the vicinity of the global optimum but not necessarily the global optimum, where a genetic optimisation does. A comparison between the genetic optimisation and surrogate optimisation algorithms for the FRT tool can be seen in Table 5.1. As a little more information the optimisation was done on a case which was already run. Meaning that there was already a case specific file for the ascent trajectories in order to decrease the amount of new ascent trajectory optimisations required. Also both algorithms are run using parallel computation to cut-back on the computation time even further.

Table 5.1: Comparison of the optimisation algorithm for two FRT Cases

	Falcon 9 LEO Propulsive			**Falcon 9 GTO Non-Propulsive**		
	Sur Opt	Gen Opt	Diff [%]	Sur Opt	Gen Opt	Diff [%]
Functions Evaluations	750	4950	-84.8	1100	5200	-78.9
Time spent	20min	2hr 3min	-83.7	55min	26hr 15min	-96.5
Minimal function evaluation	5.536e+07	5.523e+07	+0.23	3.263e+07	3.248e+07	+0.46
Minimal Cost per flight [M€]	52.99	52.86	+0.25	32.63	32.48	+0.46
Minimal function point						
Entry Speed [m/s]	3.14e+03	3.59e+03				
Re-Entry Throttle Setting	58.9	86.2				
Landing Throttle Setting [%]	82.1	47.9				
Type 1 []				Super Par	HIAD	
Altitude 1 [m]				8.257e+03	4.25e+04	
Area 1 [m^2]				54.15	33.9	
Type 2 []				Sub Par	Sub Par	
Altitude 2 [m]				5.20e+02	1.07e+03	
Area 2 [m^2]				5.10e+03	5.75e+03	
Landing System	Legs	Legs		Airbags	Airbags	
1st Stage Propellant reserve [%]	0.8	1.6				
1st Stage Propellant Mass [kg]	3.710e+05	3.58e+05		3.610e+05	2.33e+05	
2nd Stage Propellant Mass [kg]	9.273e+04	1.02e+05		8.194e+04	1.08e+05	
Grid Fin Area [m^2]	2.52	0.13				

Table 5.1 shows the surrogate optimisation can give a result in about 20% of the time. The surrogate optimisation also finds the minimum value to within 1% of the value found by the genetic optimisation algorithm. The minimal point for both cases are relatively similar after some investigation. These results were obtained using a laptop with an Intel i7 2.20 GHz with 32GB of RAM. Although the RAM is not of great importance since the RAM used is no more than 4GB.

For the LEO case which was a propulsive landing case, the entry speed for both cases is higher than the entry speed that is obtained during a free-fall trajectory therefore this does not influence the result. Both entry and landing throttle settings are not similar however they both comply with the acceleration limit. They do not influence the cost of the final launcher, only the acceleration constraint. The only variable which differs is the propellant reserve between the two cases and the grid fin area. The grid fins however have a limited influence on the trajectory and are mostly used for control in this case. The example shown is for a propulsive landing case. Where propulsive landing cases have mostly continuous variables, with the propellant reserve and entry velocity.

A different comparison is made for the Falcon 9 GTO case. This was done for a complete stage non-propulsive recovery. Going from 7 to 11 variables has an impact on the number of function evaluations that have to be performed—going up by 5% compared to the propulsive case for the genetic algorithm. The massive increase in time for the genetic optimisation is partly due to the significant amount of ascent optimisations that needed to be performed. It should be noted that both started from the same point. When comparing the optimal points, there are some differences. The first deceleration system is different for the two optimisation algorithm, although the two minimal function values are similar. This shows that the cost for the different systems is low, compared to the cost of the launcher, which is to be expected. It also shows that multiple combinations lead to a similar cost. The second deceleration system is similar both in size and when the parachute is deployed.

Non-propulsive landing cases have more variables and more discrete variables. Going from 7 variables to 11, for non-propulsive cases the amount of function evaluations for the surrogate optimisation is increased from 750 to at least 900 plus 50 for every deceleration options that is selected. This is expended by another 150 evaluations if boosters are used leading to a maximum 1250 evaluations.

This is a comparison of purely the optimisation algorithm within the scope of the tool. It should be noted that for completely new cases, which is not the one run for Table 5.1, both will take significantly longer. This is due to the fact that new coefficients need to be found for the ascent trajectory, this will be further discussed in section 5.5. This does tie into the main optimisation loop for a genetic algorithm which takes a look at the complete field this means running more ascent trajectory optimisation than for a surrogate optimisation. Since a surrogate optimisation looks near the minimal value, this means less ascent trajectory optimisations have to be performed. This is important since these cost the most computation time.

Although the surrogate optimisation is the preferred and the standard option to optimise the main loop it is possible to use a genetic algorithm if needed. As shown in Table 5.1 the genetic algorithm is better but it does take more time to complete. The genetic optimisation used, is the standard genetic optimisation included in the global optimisation toolbox from Matlab. Although not completely the same, it works similar to the algorithm use by Pepermans [77].

5.4.2. Main optimisation function

The main optimisation function is the key function of the tool as this achieves the overall goal to find the cheapest solution to reuse a launcher. This function is also complex since it has to bring all the models together that make up the rest of the tool as well as perform the trajectory analysis.

Optimisation variables

There are two sets of variables which are optimised to reach the optimal solution. These two sets are the general set and a specific set. The variables for the general set are:

- 1^{st} stage propellant mass
- 2^{nd} stage propellant mass
- Engine Separation (yes/no)
- Landing System
- Amount of Boosters

The second set is the specific parameters these differ between propulsive landing and non-propulsive landing. For the propulsive landing the following parameters are added to the list of optimisation variables:

- Propellant fraction reserved for all descent operations
- Grid Fin Area (if selected)
- Velocity at Re-entry
- First Stage Throttle setting for Re-entry burn
- First Stage Throttle setting for Landing burn

For the non-propulsive landing the following parameters are used to optimise the reusable launcher:

- Deceleration System 1 (DS1) Type
- DS1 Area
- DS1 Deployment Altitude
- Deceleration System 2 (DS2) Type
- DS2 Area
- DS2 Deployment Altitude

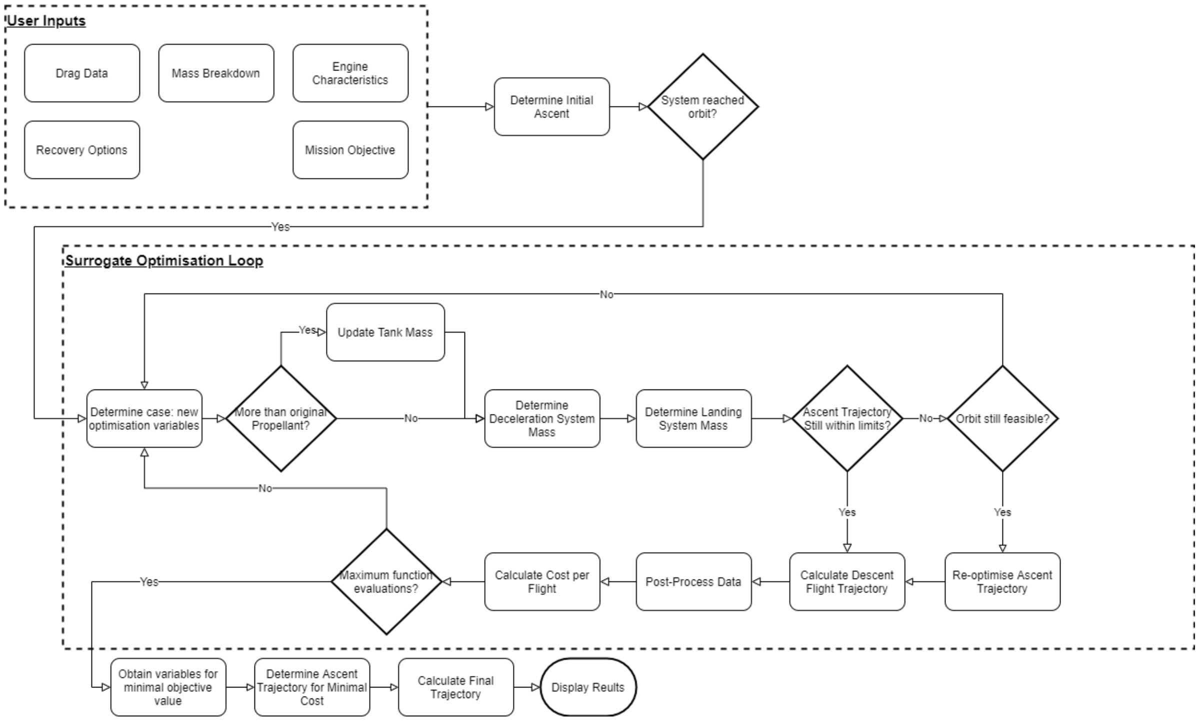

Figure 5.6: Flowchart of the main optimisation loop used in the first Stage recovery tool

Objective function overview
The main optimisation function optimises for the minimal cost per flight. An overview of the main optimisation loop can be found in Figure 5.6. To not spend time on infeasible cases these are removed based on ΔV required for orbit. This is obtained through a check if the case can still reach orbit and if the thrust to weight ratio at launch is larger than 1.01. If both of these are not higher than the limit it will give a fixed high number for the function and will continue with the next case.

Constraints
If all goes well and the case is feasible the function has to comply with a number of requirements. These are split into general constraints which apply to all cases and some specific constraints which are specific for some but not all cases. The following general constraints are set:

- The maximum acceleration/deceleration during the flight
- The maximum temperature during the flight
- The maximum dynamic pressure during the flight

For the propulsive landing one specific constraint is applied. Since the starting altitude for the landing burn is estimated analytically, a difference between the actual optimal starting altitude and the estimated one can occur. This can lead to the stage still having a velocity higher than 0 m/s at landing. The estimation is done to cut-back on computation time. Though the optimisation only takes ~10s when applied to the main optimisation loop this has to be performed 750 times. In order to mitigate this error it is checked if there is still propellant to decrease the velocity from the landing velocity to zero. More detail on the approximation and the error is given in section 5.6

For non-propulsive landing there is one constraint which applies to all cases that use Mid-Air Retrieval this is the velocity during capture. Since trying to catch a the vehicle in mid-air and absorbing that momentum can not be ignored. Therefore for this research a limit is set at an absolute velocity of 15m/s. Also constraints are set for the parachute systems which are used. These are the dynamic pressure and the mach number at deployment. The dynamic pressure is the minimal dynamic pressure which is needed to inflate the parachute. If the dynamic pressure is lower than this limit the parachute does not inflate properly and might entangle.

The limiting mach number is maximum mach number that can occur during deployment, this is a limit set for a parachute type[52]. Finally a small alteration of the temperature constraint is applied if a HIAD is used as the first deceleration system. Since a HIAD also doubles as a heat shield it can take a higher temperature than the rest of the vehicle.

All these elements are incorporated into the main objective function. This is done to cut-back on the computation time required and not to have the same thing calculated twice as is normal with MATLAB optimisation functions. Therefore if a constraint is breached, it is technically still counted in the objective function. However, to make the solutions outside the constraints "unappealing" the concept of error coefficients are introduced. These are nothing more than a coefficient that if one of the constraints are met but get a non-one values if they do not meet the constraint. This can be done in two ways. First is giving it a fixed value, this is done if the launcher does not reach orbit. The other option is to give it a value relative to the error. Furthermore, these coefficients were found to work better if they have the same magnitude during the development of the tool. This helps the surrogate optimisation algorithm to determine a function which shows a gradient even if the point is outside the constraints. As an example, the coefficient for the maximum deceleration (a_{max}) constraint is set as such:

$$c_{accel} = \begin{cases} 1 \text{ if } a_{max} \leq a_{lim} \\ a_{max} \text{ if } a_{max} > a_{lim} \end{cases} \tag{5.1}$$

The rest of the constraints are given in the same manner and scaled to be somewhere between 10-1000. This means if no value can be found within the constraints, the algorithm will still give a solution. Since technically according to the algorithm, there are not constraints only jumps in the function when a constraint is breached.
This method does pose an issue with objective functions that have their minimum around zero. As with zero values, almost no error coefficient can make the solution worse than values that fall within the constraints. The solution here is to either fix to objective function or add a fixed error. This does make it harder to find the optimal value for algorithms that use a gradient or looks at the function values themselves to determine the next step. This is, however, not used within the main optimisation function.

Initial Population
For the MATLAB surrogate optimisation algorithm, there is an option to include a custom initial population; this option is used for FRT. The initial population is still just randomly selected only here the biggest constraints are already applied. This means the initial population already gives a decent overview of the objective function. This is needed since if left alone, the chances of getting more than 2-3 points that fall within these constraints are low. The initial population is randomly chosen using a uniform distribution having with all points having an equal chance of being chosen. After this is done it passes through the initial constraints which are:

- The excluded combinations from subsection 5.4.3
- The launcher has enough ΔV to get into orbit, this is discussed further in subsection 5.5.3
- the Thrust to weight Ratio at launch is larger than 1.01

For the non-propulsive cases, the ranges are adjusted to ranges that fit more with the type of decelerator, as parachutes are usually larger than HIADs or grid fins. Therefore the ranges in Table 5.2 are used.

Table 5.2: The ranges for the areas of the non-propulsive deceleration systems in m^2 for the initial population

Deceleration System	Lower Limit	Upper Limit
Parachutes	0.5	1000
HIAD	0.5	200
Grid Fins	0.5	100

These ranges only apply to the initial population. As will be seen in chapter 6 for the parachute areas sizes will be found which are almost always larger than the upper limit of the initial population.

5.4.3. Combinations

Although a lot of elements are included in FRT there are some combinations which due to some circumstances are not possible.

- Because a HIAD system should be alligned in the center of the stage and will take up most of the area of the launcher. It is decided that two HIADs are not a possibility within the same deceleration system.
- For a propulsive landing the stage needs to be oriented with the engine pointed towards the ground. This would mean that any airbag system would be present at/near the very hot nozzle during the landing burn. This means airbags and a propulsive landing are excluded for fear of catching fire and/or bursting the bag.
- Mid Air retrieval is only available below a mass of 10000 kg. This limit was chosen as the maximum carrying capability of a helicopter is about 16000kg[122]. However this is a static loading, so in order to capture a mass the limit is decreased to 10000kg. This limit only comes into effect for the cases in chapter 6 if the entire stage is recovered or significant mass is added to engine only recovery.
- For Mid Air retrieval a parachute is needed as the final deceleration system.
- Going for a non-propulsive landing means giving up a certain amount of knowledge about where the stage will land. This means landing on a drone ship similar to what is being done for the Falcon 9 is out of the question. This, since most launch sites are next to or near the ocean, means that landing legs will not be an option for non-propulsive cases.

5.5. Ascent Trajectory

The ascent trajectory is key for the descent trajectory as this determines where and how fast the first stage starts the descent. In order to achieve this the launcher needs to be able to get into the required orbits using a control law that will define the trajectory. To get the correct control law the trajectory needs to be optimised for the minimal orbital error.

5.5.1. Overview

To determine the most optimal first stage recovery system, the initial point of the return flight should be known. This in contrary to the upper stage, cannot be viewed separately from the operations of the entire launchers. Since the orbit in which the first stage is released is one which intersects with the earth. Therefore the ascent of the launcher should also be taken into account. If weight is added to the vehicle to make it reusable the point of separation will differ either in altitude of velocity or both. The ascent of the launcher is broken up into a couple of parts the first stage burn is done as one continuous burn. However because of a limit on the maximum dynamic pressure it can reach, there is a throttling capability until 15km. This throttling start only when the reduced setting produces a thrust to weight ratio that is higher than one. Once the launcher is above 15km the launcher goes back to 100% thrust until main engine cut-off (MECO). After MECO there is a coasting phase which represents separation as well as creating distance between the first and second stage. After which the second stage ignites to raise the apogee of the current "orbit" to the Perigee of the target orbit. After the first second stage cut-off (SECO) there is a second coasting period to reach the point when the second stage engine is ignited for a second time to reach the final orbit. If needed deviations from this scheme can are performed. Most significant is the first burn of the second stage, after separation. This burn can be skiped if the apogee is already at the right altitude. This mostly occurs during launcher with boosters, low payload masses and a low perigee altitude. An example of a general ascent trajectory can be found in Figure 5.7.

5.5.2. Control Law

In order to get the launcher into an orbit a control law has to be devised to get the ascent trajectory with the smallest error in the final orbit. For the ascent trajectory a control law is used, which is a fourth-degree polynomial as was suggested by van Kesteren[112]:

$$\theta(t) = a_0 + a_1 t + a_2 t^2 + a_3 t^3 + a_4 t^4 \tag{5.2}$$

In initial testing a fifth order control law was considered however the fifth power was almost never used so it was discarded. The angle is expressed with respect to the local horizontal plane. In order to allow for more flexibility the pitch program is separated into three parts:

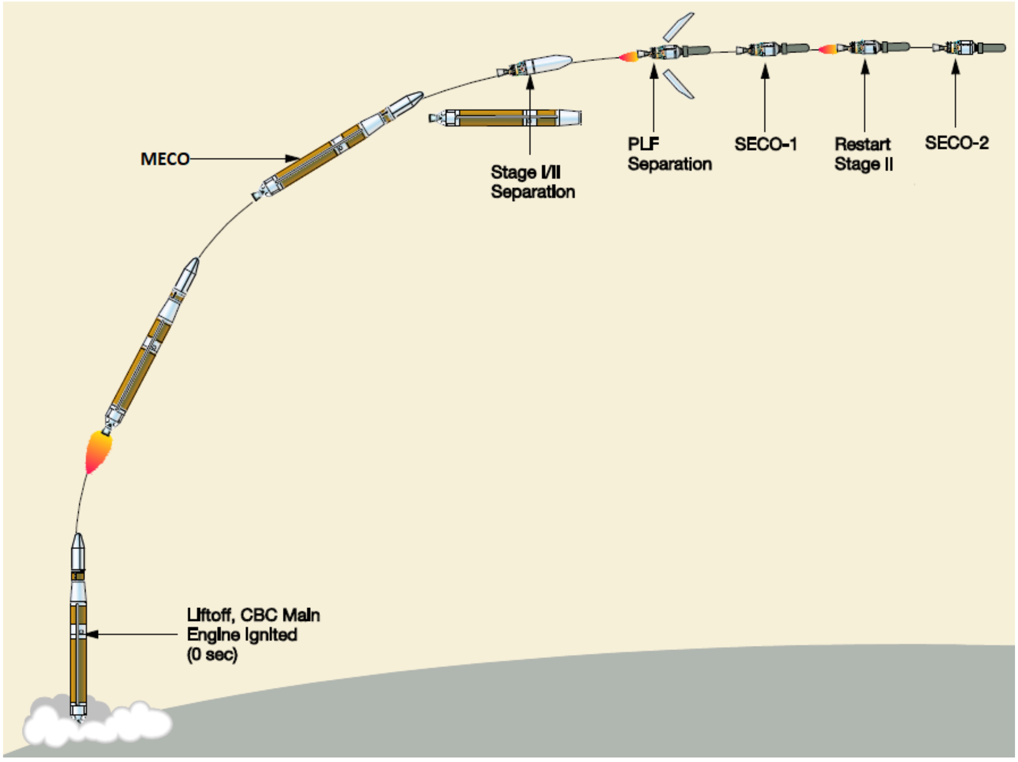

Figure 5.7: Example of the different phases in the ascent trajectory of the Delta IV launcher [3].

1. First Stage Ascent until MECO
2. Second Stage until first SECO
3. Final Orbit Insertion

For the first stage, the full fourth-order is used; however, for the second stage, only a second-degree polynomial is used. This is done to cut back on the number of parameters that need to be optimised. Furthermore it was also seen just as for the fifth order attempt of the first stage control law that the remaining parameters were for the most part not used. For the first stage control law, the pitch program at t=0 is known this is equal to the initial flight path angle which for most orbital launchers is 90 deg. The final orbit insertion is done by aligning the thrust with the velocity vector. The initial angle and the throttle setting for the first stage are used to minimise the error in the final orbit for a final pitch program. To furthermore simplify the ascent is modelled in a single plane. Which means no inclinations can be achieved, which are lower than the latitude of the launching location. As an example, no pure equatorial orbit can be achieved from any location other than a launching location on the equator.

5.5.3. Optimisation Algorithm

The optimisation function is the sum of the error of the perigee altitude and apogee altitude. The only constraint in the optimisation is the maximum dynamic pressure during the ascent. The optimisation function is a simplified one where the constraints are included in the primary function. This is done to lower the amount of function evaluation which have to be performed. This poses a risk; however that it converges on an infeasible point is no feasible point exist. The final trajectory has to fall within the error limit which is 2.5% of the sum of the apogee and perigee altitudes with respect of the surface of the earth.

$$f = Error_{PE} + Error_{AP} \text{ Limit: } f < 0.025((r_{AP} - r_{earth}) + (r_{PE} - r_{earth})) \tag{5.3}$$

In order to not optimise the ascent with every descent trajectory, a system has been thought off to minimise the number of ascent trajectories which have to be optimised. This is done by including a database and an exclusion system. The exclusion system is based on the highest ideal ΔV that could not reach the target orbit.

To begin, the limit is set as the orbital velocity needed at perigee and 25% of the velocity needed to get to the target perigee:

$$\Delta V_{lim} = \sqrt{\mu\left(\frac{2}{r_{pe}} - \frac{1}{a}\right)} + 0.25\sqrt{2g_0\left(r_{pe} - R_E\right)} \tag{5.4}$$

Where r_{pe} is the perigee altitude with respect to the centre of the earth, and a is the semi-major axis. After this a base version of the launcher is launched into orbit, from this the ΔV losses are obtained due to both gravity and drag. These are calculated as part of the differential equations where all of the variables used vary with time:

$$\Delta V_{losses,Drag} = \frac{F_{Drag}}{m} t \tag{5.5}$$

$$\Delta V_{losses,Gravity} = a_g sin\left(\varphi\right) t \tag{5.6}$$

These losses are then added to final the orbital velocity to achieve the first minimum ΔV for the ascent. It does this for four points for 95%, 97.5%, 99%, 100% of the initial propellant of the first stage. Following this a logarithmic function is drawn through these four point to give an initial guess of the limiting ΔV. If afterwards a higher value is found this is then set as the new limit. The exclusion is not a single value but is a function of the fraction of the original propellant mass and the used propellant mass. A separate list is used when boosters are used, within the tool it is merely separated by multiplying the propellant fraction by $10^{N_{boosters}}$.

Besides the exclusion system, a system is used that saves that coefficient of the control law and the thrust level for the throttling phase of the first stage. This database is made in three levels. First is the coefficients that were used last. If that does not fall within the limit, it uses the set of trajectories that have succeeded within the case. The database for the case is newly created upon every launcher case. If no feasible solution is found here, it searches one level higher. This is the entire database of all the ascent trajectories that have been found during any previous case. Here the case-based database is a subset of the entire database. Once no solution was found in all these databases, the actual optimisation starts. First, a gradient optimisation is started the initial point of which is the database set which is closest to the final orbit. The gradient optimisation only searches for a local optimum.

If a local optimum is found, it is again checked against the limit. If the trajectory still does not reach the required limit, the global optimisation is started, which is the particle swarm optimisation. The particle swarm is chosen for its accuracy in combination with the computation time. After an optimum is found from the optimisation, it is checked against the database to see if it is a unique solution. An overview of the optimisation can be seen in Figure 5.8. A particle swarm optimisation algorithm creates a swarm completely at random throughout the search space that was defined. It starts by calculating the optimisation function value at the point. After which it gives the point a quasi-random direction and velocity through the space to reach the second point. The quasi in quasi-random comes from the fact that the direction and the velocity are influenced by the nearest best neighbour of a individual point. This is done in order to converge to a global minimum. Because the next iteration in the optimisation is not based on the gradient of the optimisation function, a particle swarm optimisation function as well as a genetic optimisation function does not have to be continuous. Which in the case of the ascent trajectory means bad ascent trajectories can be rooted out quickly by letting the function pas certain "gates" and giving it a fixed high value if that "gate"cannot be passed. The benefit of a particle swarm over a genetic algorithm are that no new generation has to be generated which saves in overhead calculations that need to be done. However a particle swarm does require that the variables that need to be optimised are continuous, so no integer optimisation can be done using a particle swarm.

The objective function has, however, some weaknesses in orbits with large eccentricities since the total error can occur at either end of the orbit. Where a 200km error at the apogee of 30000km is unfortunate but within limits the same error on a 200km perigee is disastrous, while also still within limits. In order to be able to control the trajectory in case of non-circular orbits two constraints are set for maximum allowable the perigee error and apogee error individually as well. These limits are set at 5% for both the maximum error of the target apogee altitude and perigee altitude. This is done because the optimisation function is a combined function, so that the driving factor near the limit is the total error and not the constraint.

Furthermore in order to speed up the optimisation process discrete points during the ascent are used to check the progress. In these point it is checked if the ascent trajectory either already intersected with the ground or went above 120% of the perigee altitude and the maximum allowable error. This is done during either the first stage engine burn or the first burn of the second stage. This makes sure that no time is wasted on ascent

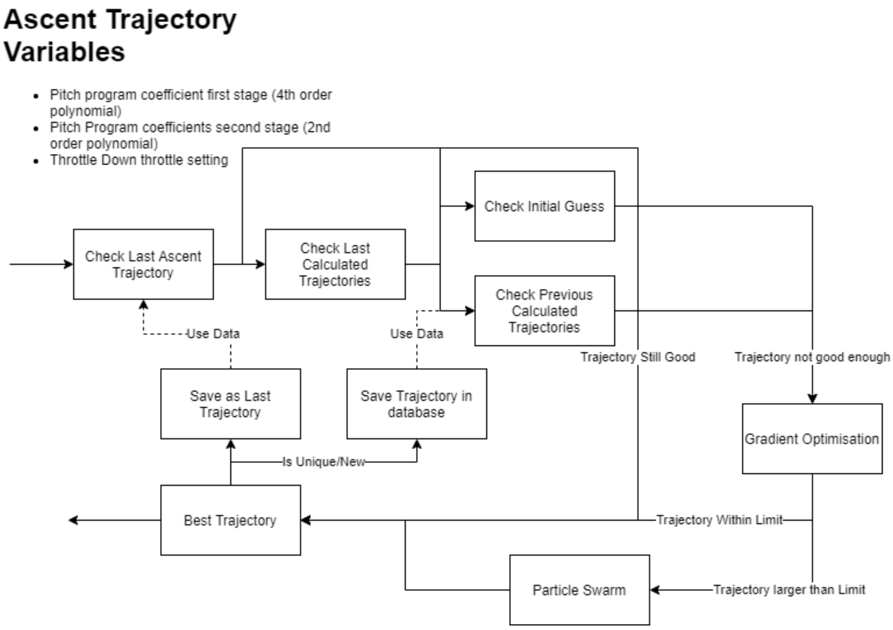

Figure 5.8: Flowchart of the Ascent optimisation algorithm

trajectories which are not able to reach the required orbit.
Finally one extra constraint is used during the ascent and this is the maximum dynamic pressure during the ascent. This is done to limit the drag losses during ascent which leads to a better performance, as well as limiting the drag loads on the vehicle during ascent.

5.6. Landing Burn Altitude

The descent is split into two parts, one for propulsive landing and one for the non-propulsive landing. This is done for one reason and that is the need for a landing burn for the propulsive landing case. This besides being the critical element for a successful propulsive landing also takes some time to calculate accurately. This is done by using yet another optimisation loop. However in order to not have to optimise the landing during every iteration, during the main optimisation loop the landing burn is approximated by using an analytical equation. This equation is based on the final velocity achieved when not performing a landing burn. This is used to calculate how much ΔV is required.

$$H_{burn} = sin(\varphi_{burn})\left(\left(I_{sp} g_0 \frac{M_1}{\dot{m}} ln\left(\frac{M_1}{M_0}\right) + t_{burn}\right) + \frac{1}{2} g_0 t_{burn}^2\right) \tag{5.7}$$

The flight path angle φ_{burn} is an average angle of the flight path angle when not performing a flight path angle and 90 degrees. M_1 is the final mass of the first stage and M_0 is the mass right before starting the landing burn. Finally t_{burn} is the time the burn will take. This is calculated by using the mass difference between M_1 and M_0 and then dividing is by the mass flow $\dot{m}$. This is, however, not accurate enough since it omits the drag forces and the average angle also is not correct since the flight path angle does not vary linearly during the landing burn. Therefore, there will most likely still be a velocity at the end of the flight. This velocity is accepted by the main optimisation loop if there is still enough ΔV available at the end to counteract this. This brings down the computation time from about 10s for the complete optimisation to less than a second, for determining the landing burn altitude. To give an overview the estimated and optimal values for the standard sensitivity analysis sweep is given in Table 5.3.

Table 5.3: Estimated and optimal start of the landing burn altitude for the Falcon 9 LEO mission standard sensitivity sweep

Estimated Value [m]	Optimal Value [m]
372.69	365.39
379.34	371.51
376.22	368.40
377.45	370.37
375.56	368.40
376.30	368.91
339.81	335.37
413.25	402.76

What can be seen is that the estimated values are always a bit higher this is due to the drag losses not being taken into account.

After the altitude is approximated during the main optimisation loop during the final calculations the landing burn is determined by using a particle swarm optimisation algorithm. This was used over a simple gradient based optimiser since the tolerances in the integrator could cause small deviation from a smooth function causing it to find a false optimum. Furthermore the optimisation is split into two parts. First an optimisation is done within 4km of the approximated value. If this does not lead to an optimum value the range is extended to include the entire range from re-entry interface (55km) to ground level.

5.7. Maximum Payload Calculations

Although the tool was created to determine the optimal first stage design for a reusable launcher. It is also capable of handling other operations. In order to make things simpler and to remember simple details the tool is capable of saving and reading different cases. Also for simplicity it is capable of reading results. This it does using the latest version of the tool. This means when changing out certain models the results also change with them.

Using the tool also the maximum payload capacity can be calculated if required. A small overview of the cases run using the inputs from subsection 6.2.1 and subsection 6.3.1 can be found in Table 5.4

Table 5.4: The expendable payload for various cases calculated from the tool as well as the theoretical maximum payload[86, 87]

Vehicle	**Orbit**	**Source [kg]**	**Model [kg]**
Falcon 9 Block 5	185km x 28.5deg (LEO)	22800	24380
Falcon 9 Block 5	185km x 35788km (GTO)x 28.4deg	8300	8765
Delta IV	401km x 51.6deg	8510	9066

This shows two things. The first is that the system for calculating the ascent trajectory of the tool can get a vehicle into orbit with its given maximum payload. Second is that the maximum payload that is being calculated by the tool has an average error of 6.35% of the given theoretical maximum payload. It has to be noted that all the calculated payloads are higher than the maximum payloads given by the launch provider. This can be expected since the FRT calculates the ultimate maximum and not the maximum operational payload. The difference between the two is that FRT only has one flight condition where the launch provider needs to take into account different cases for different winds and temperatures during launch.
Although the limit can be found using this method, this requires the tool to go to the limit of the vehicle which requires a significant amount of re-optimising the ascent trajectory which consumes a lot of time. So it would be advised to not do this for every optimisation and case that is being run, but do it once for a particular mission and vehicle and save the value. Also, if possible, it would be advised to use known values when fast computation time is required.

5.8. Boosters

Within FRT, there is the possibility to use boosters. These can be either liquid or solid. For the liquid boosters, the thrust is modelled the same way as for the core stages using the thrust model from section 3.4. Although they use the same logic, the cross-feeding propellant is not supported. The solid boosters works differently than the liquid engines, since here the internal geometry determines how much thrust is produced[124]. It is challenging to create a general solid booster model that works in all cases. The choice is made to work backwards, and therefore the model requires the thrust curve and the specific impulse at sea-level as inputs. From this, it calculates the thrust, mass flow and specific impulse during the flight according to the equation found in section 3.4.

5.9. Sensitivity Analysis

Besides the optimisation of the design, the sensitivity of it is also determined using the tool. For these two sensitivity analysis options are used. Both these sensitivity analyses use a single file in which the ranges for each parameter is defined. This is done such that changes from new data can be incorporated quickly and independently from the tool.

The two sensitivity analysis options are the "standard" sensitivity analysis in which one parameter per turn is changed by the amount given in the database. Here the extremes of the database are used. The second option is the Monte Carlo Analysis. With this, all parameters are changed to show the interaction between the changes. For this analysis, the parameters are also changed randomly. This can be done using a multitude of probability density functions. For this research, a uniform distribution is chosen. This distribution is chosen because it gives equal chances to every value within the sensitivity range. These two methods are used by Contant and Pepermans, although Contant focuses only on the standard analysis and Pepermans only on the Monte Carlo Analysis. The Monte Carlo can give a better overview of the sensitivity of the solution as it can result in more extreme cases when everything is varied. The Monte Carlo analysis is also faster when a large amount of parameters/variables are varied. Since it does not have to vary one variable at a time but combines all the changes into one case. However, the standard analysis can give an overview of what the most influential parameters are.
For the implementation of the sensitivity analysis itself, a switch is created that can only act within the sensitivity analysis in order to prevent modification during regular optimisation tasks. Once this switch is activated, it can either give the extreme of the value in the file for the standard option. Alternatively, it can give a random number in between the two extremes in the file for the Monte Carlo Analysis.

5.10. Tool Availability

This tool is made in MATLAB 2019b using a multitude of toolboxes among which the most important are the global optimisation and local optimisation toolboxes as well as the aerospace toolbox. This tool is available for anybody who wishes to use it. A manual for the tool is available to be used as reference material and is also available upon request.

6
Cases

Now that the tool and the models have been explained the time has come to apply the tool to the research question. In order to answer the question, a couple of cases are used in order to give a comprehensive answer. The first case is a Falcon 9 like launcher launched to a 290 km circular orbit. This is done with the heaviest payload mass the Falcon 9 has launched into orbit while still recovering the first stage, which is 15600 kg. The second case is done using the same launcher, the Falcon 9 launcher, but the difference with the first case is that the target orbit is a GTO orbit of 32827 km x 218 km. This case is done with a payload of 6500kg. After this, a second launcher is investigated, one which is not designed with reusability in mind. This is a launcher like the Delta IV-M. Since this launcher was not designed with reusability in mind, this should give an insight if this makes a difference in the result. Finally a comparison is made between the best solutions from all missions investigated.

6.1. Overview & Set-up

In order to run the different cases, first, the boundaries and the missions need to be defined for both the normal run as well as for the sensitivity analysis. The different cases are divided into two parts. First is the normal run that determines what the optimal solution is. Second is the sensitivity analysis which determines how robust the solution is by varying various parameters.

6.1.1. Boundaries

For all the cases, the constraints and boundaries are applied.

1. Maximum deceleration during the descent is 10g [31, 98]
2. The maximum temperature allowed for the engine is 500K
3. The maximum dynamic pressure during the descent is 200kPa [31, 98]
4. The maximum dynamic pressure during the ascent is 30kPa for the Falcon 9 and 70kPa for the Delta IV [3, 98]

The limits for dynamic pressure during ascent are not hard limits mentioned but are the maximum found during the ascent of the Falcon 9 for their simulation and from the Delta IV user manual[3]. These values will also be used in this research. The dynamic pressure during ascent are mostly aimed to reduce the drag losses. Furthermore, for the Falcon 9 cases, the cost calculation for the expendable launcher is done without taking the landing legs into account. This is done to compare the fully expendable launcher and not a reusable launcher that is not reused. Finally, for the Delta IV case, the maximum amount of boosters is set at four, for the Falcon 9 case no boosters are allowed.

6.1.2. Missions

The two missions that are used are based the Starlink mission and the SES-10 mission that were flown with the Falcon 9. The Starlink mission is a circular LEO mission, and the SES-10 mission is a highly elliptical GTO mission. For both missions, the starting location is Kennedy Space Center (KSC) with a starting latitude and longitude 28.4 deg and -80.61 deg respectively. An overview of the two missions can be found in Table 6.1. The Falcon 9 GTO mission used is also comparable to the one used by Contant [31]. For the Falcon 9 mission,

Table 6.1: Overview of the missions analysed

Parameter	**LEO**	**GTO**
Apogee Altitude [km]	290	32827
Perigee Altitude [km]	290	218
Inclination [deg]	53	28.4
Falcon 9		
Payload mass [kg]	15600	6500
Delta IV+		
Payload mass [kg]	9000	4500

the payload mass is reduced from the theoretical limit. This is done because this is the maximum payload demonstrated by SpaceX[87]. For the Delta IV+ the payload mass is kept the same as the theoretical maximum for the expendable version this was done since for the Delta IV boosters can be used to extend the payload carrying capability. For each mission, the results for three cases are calculated:

Table 6.2: Case Description for the different missions

Case #	**Description**
Case 1	Using the engine to land the complete stage
Case 2	Separating the engine from the stage and landing the engine safely
Case 3	Returning the complete stage but only using non-propulsive means

6.1.3. Sensitivity Analysis

In the previous chapters multiple models have been discussed, none of these models were perfect and consequently they had an error when compared to their validation data. In order to investigate the effect of these errors a sensitivity analysis is performed. Here either the models or some of the inputs are varied in order to check how the solution changes, either in trajectory or in cost.

For the sensitivity analysis there are two modes that can be used. One is that standard sensitivity analysis which varies one variable up or down at a time to give a result. This is then repeated for the total amount of variables that are being investigated. The other option is a Monte Carlo analysis where random variations for all variables are taken. This is done to see the connection between the variables. For both options the limits of the variations need to be given. In Table 6.3 the models/parameters that are being varied and what the limits are. An overview of the variations are given in Table 6.3.

The only value which has not been discussed previously is the variation of the initial empty mass. This variation is not due to any model that was previously mentioned. This variation is there because of the initial conditions. These values are obtained from sources which are usually not the direct producer of the launcher. Therefore the certainty of these values can be taken into question. Therefore the empty mass is varied as this is one of the most important parameters as it not only influences the trajectory by the difference in mass. It is also used as an input for several mass and cost models. For the cases, they will be compared for the constraints, so the acceleration, dynamics pressure and temperature limits and finally the cost per flight and the Reuse-Index. This is done to show how the variations are within the design space given. The cases will not be re-optimised to get their optimal design; only the current design will be re-flown with the shifted parameters. This comparison will be made using a Monte Carlo analysis where the variations are randomly chosen between the bounds given in Table 6.3. For the Monte Carlo Analysis, 50 points are used as the set where variations are applied.

6.2. Falcon 9

For the Falcon 9, first the inputs for the vehicle are given followed by the cases for the LEO and GTO missions. Followed by a conclusion based on the results found for this vehicle.

Table 6.3: Variations of the various models/inputs for the sensitivity analysis

System	Category	Bounds	(Sub)Section
Parachute Models	Mass	$-2.5\%, 25\%$	subsection 3.3.2
	Cost	$\pm 50\%$	section 4.3
HIAD Models	Mass	$0\%, 10\%$	subsection 3.3.3
	Cost	$\pm 50\%$	section 4.3
Airbag Models	Mass	$-30\%, 30\%$	subsection 3.2.2
	Cost	$\pm 50\%$	section 4.3
Flotation Device Models	Mass	$\pm 20\%$	subsection 3.2.3
	Cost	$\pm 50\%$	section 4.3
Landing Legs	Mass	$\pm 10\%$	subsection 3.2.1
Refurbishment	Cost	$-10\%, +30\%$	subsection 4.2.3
Added Tank Mass	Mass	$-10\%, +8\%$	subsection 3.1.2
Thrust Model	Trajectory	$-1\%, +5\%$	subsection 3.4.2
Grid Fins	Mass	$\pm 50\%$	subsection 3.3.1
C_D Total Launcher	Trajectory	$\pm 10\%$	section 3.5
C_D First Stage	Trajectory	$\pm 10\%$	section 3.5
Empty Mass	Initial Condition	$\pm 10\%$	subsection 6.1.3

6.2.1. Vehicle

The inputs used for the Falcon 9 launcher can be found in Table 6.4 and Table 6.5. Where in Table 6.4 the masses and general geometry of the launcher is given and in Table 6.5 the inputs for the engines. The values for the vehicle are obtained from Space Launch Report. These are taken from one source to keep consistent values. These values are compared to other sources among which is FlightClub which is a simulation tool that also has roughly the same inputs[71]. There are some deviation for the empty and propellant masses for the first stage. For the engines, although they are in essence the same engine for the first and the second stage with a different nozzle design getting a complete set of the required inputs from one source is difficult. Therefore at least three sources are needed. Here the risk is run that the data is given for different versions of a slightly changed engine. These deviation stem from the lack of official publications from SpaceX

6.2.2. LEO Mission

To start with the Falcon 9 launcher on a LEO mission. The resulting vehicles were found for the three different cases. In order to compare the resulting launcher given in Table 6.6, more investigation has to be done with regard to the flights of the different cases and the eventual masses and costs of the cases. The expendable launcher in Table 6.7 is the expendable launcher from which the reusable launcher is created. The propellant masses are the maximum propellant mass without extending the tank and is not an optimised version of the expendable case. This expendable launcher serves as a reference case only and the values are the ones given in Table 6.4. In Table 6.7 it can be seen that case 2 is the lightest when it comes to the final empty mass of the first stage. This is mostly due to the fact that to decelerate only the engine section, which is about 4500 kg, less material is needed with regards to the deceleration system. It is greatly helped by the use of Mid-Air Retrieval(MAR) for which a landing and flotation system are not needed. With regard to the propellant loading it is interesting to see that for the propulsive landing almost all the available propellant mass is being used. When propellant is lower than the capability of the initial propellant mass, 411000 kg for the Falcon 9, the tank is not shrunk and remains at the original mass. Therefore the empty mass can either increase or remain the same.

Although the FRT is capable of extending the tank, for some extra propellant mass if needed, case 1 is on the limit of the initial propellant mass. For the other two cases they do use most of the second stage propellant but the first stage propellant levels are both lower with 85% and 89% for cases 2 and 3 respectively. Finally a large difference in HIAD mass can be found whereas the areas differ less significantly. This difference is due to both the difference in area and the difference in dynamic pressure which is about 1.5 times for the complete stage compared to the engine only recovery.

For the return flight, the critical values were calculated, which can be seen in Table 6.8. In Table 6.8 it can

Table 6.4: Vehicle Masses and Dimensions for the expendable Falcon 9 FT launcher[87]

Parameter	Falcon 9
First Stage	
Initial Empty Mass [kg]	24720
Initial Propellant Mass [kg]	411000
Engine Mass [kg]	4230
Diameter [m]	3.66
Length [m]	40.9
Nosetip Radius [m]	1.5
Second Stage	
Empty Mass [kg]	5700
Initial Propellant Mass [kg]	111500
Engine Mass [kg]	470
Diameter [m]	3.66
Length	16
Nosetip Radius [m]	1.5

Table 6.5: Engine Inputs for the Falcon 9 [12, 102, 121]

Parameter	Falcon 9
First Stage Engine	
Propellant []	RP1/LOX
Exit Area [m^2]	1.227
Throat Area [m^2]	0.0767
Chamber Pressure [MPa]	9.7
Amount of Engines [#]	9
Lower Thrust Limit [%]	11 [a]
Model Correction	Sea-level
Sea Level Thrust [kN]	7686
Sea Level I_{sp} [s]	282
Second Stage Engine	
Propellant []	RP1/LOX
Exit Area [m^2]	12.66
Throat Area [m^2]	0.0767
Chamber Pressure [MPa]	9.7
Amount of Engines [#]	1
Lower Thrust Limit [%]	50
Model Correction	Vacuum
Vacuum Thrust [kN]	934
Vacuum I_{sp}	348

[a] This is the total thrust limit not for only one engine

be seen when trying to recover the first stage for the LEO mission the deceleration limit is the critical parameter, as it is close to the limit for all cases, the dynamic pressure is less of an issue when not using a propulsive landing. For a propulsive landing, it becomes more critical. However, it not as close to the limit as the deceleration is. For the propellant left, it is interesting to see that for the propulsive landing, the second stage keeps a lot of propellant is unused at the end. This is probably to limit the separation velocity, thereby limiting the re-entry speed and controlling the deceleration. The same applies to the remaining first stage propellant. So the extra propellant is there to limit the separation velocity and thereby limiting the deceleration upon re-entry. It should be noted, this remaining propellant in the second stage could be replaced by extra payload mass if required. This does not mean, however, that this would be the maximum payload capacity for this case.

An overview of the different costs can be found in Figures 6.1, 6.2, 6.3 and 6.4 What can be seen in Figure 6.1 is the average production cost of the entire launcher for the different cases. The entire launcher is given instead of the only the first stage because when increasing the amount of reuses more second stages have to be build. This, because of the learning curve, decreases the production cost of the second stage and possibly what parts have to be rebuild for the first stage. This is important if there is an asymmetric production. For example the Delta IV uses sometimes two and sometimes four solid boosters. This leads to 62 core stages being produced and 68 boosters. On top of this the cost of the second stage also influences the Reuse-index shown in Figure 6.4. A breakdown of the initial production cost can be seen in Table 6.9. In Figure 6.1, the launcher that uses propulsive landing is the most expensive launcher to produce initially of the four calculated. This is mostly due to the landing legs. After that is Case 3, this follows from the same logic. As a system needs to be built to recover the entire stage with approximately 3000kg being added in the form of airbags, parachutes and a HIAD. These are also larger than for Case 2; therefore, this is the cheapest launcher to produce initially of the reusable cases. However, the cheapest launcher to produce initially is the expendable case. This makes sense as this launcher has no extra features. The difference in slope for the costs is due to the extra experience from building new first stages drives the production cost of them down. When looking at the impact of the number of launches it can be seen that all reusable launchers have a lower average unit cost, which is due to part of the stage or the whole stage being reused. In Figure 6.1 Case 3, has approximately the same cost as Case 1 therefore they are very similar in unit cost. Case 1 is slightly more expensive though in average production cost. What can be seen is that the Assembly Integration and Test Cost (AIT) is significant

Table 6.6: Optimisation Variables for the three cases for the Falcon 9 LEO mission

Variable	**Case 1**	**Case 2**	**Case 3**
1^{st} stage Propellant mass	395155	350668	366097
2^{nd} stage Propellant mass	110732	103365	100544
Landing System	Landing Legs	MAR	Airbags
Deceleration System	Entry Velocity: 1857 m/s Re-entry burn Thrust level: 34.9 % Propellant for Descent: 2.2 % Landing Thrust Level: 53.5% Grid Fin Area: 0 [m^2]	Type: HIAD Area: 39 m^2 Deployment Altitude :NA Type: Ringsail Parachute Area [m^2]: 1756 m^2 Deployment Altitude : 2.0 km	Type:HIAD Area: 62 m^2 Altitude:NA Type: Ringsail Parachute Area: 6692 m^2 Altitude: 4.3 km

Table 6.7: Vehicle Masses overview for the three cases for the Falcon 9 LEO mission

Parameter	**Expendable Launcher**	**Reusable Launcher**		
		Case 1	Case 2	Case 3
First Stage				
Final Empty Mass [kg]	24720	27192	24910	28622
Structural mass [kg]	24720	24720	24720	24720
Landing system [kg]	NA	2472	0	2601
Grid Fins [kg]		0		
Hemiflow Ribbon Parachute System [kg]				
Ringsail Parachute System [kg]			129	494
HIAD System [kg]			61	807
Propellant Mass [kg]	411000	395155	350668	366097
Descent Propellant Fraction [%]	0	2.2	0	0
Second Stage				
Payload Mass [kg]	15600			
Empty Mass [kg]	5700			
Propellant Mass [kg]	111500	110732	103365	100544

being at least 35% of the initial production cost.

The operational costs can be seen in Figure 6.2. For the operational cost, it can be seen that the expendable launcher is the cheapest because the least amount of effort is needed. For the other three, the costs are mostly dependent on the refurbishment cost. The refurbishment cost, as explained in subsection 4.2.3 is a percentage of the production cost of what is reused. Therefore it follows that case 1 has the highest refurbishment cost, followed by case 3 and case 2. Case 2, where only the engine is recovered, needs the least amount of refurbishing than the cases where the entire stage is recovered.

Now looking at the total picture which is the cost per flight and the Reuse-Index (RI), Figures 6.3 and 6.4 respectively. Here it is quite obvious at first glance that the reusable cases are cheaper per flight than the expendable launcher. This holds for cases 1 and 3. Cases 1 and 3 are the cheapest per flight, followed by Case 2. Two groups of lines can be found in Figure 6.4. First, is the grouped generally below the expendable line, (RI=1), and one group above. The group below is the cost-saving with regard to the expendable when both are flying the same payload mass. Since the Reuse-Index is calculated for a cost per flight per kilogram payload, it makes sense that the reusable launchers are cheaper than the expendable when comparing them at the same payload mass. Since in this case you can compare the costs per flight (Figure 6.3).
However, when comparing the reusable cases to the theoretical maximum payload flown in the expendable

Table 6.8: Re-turn Flight Parameters for the three cases for the Falcon 9 LEO mission

Parameter	Case 1	Case 2	Case 3
Start Landing Burn Altitude [m]	368	NA	NA
Maximum deceleration [g]	9.8	7.3	9.7
Maximum dynamic pressure [kPa]	132.8	20.5	32
First Stage Propellant Left [kg]	468	0	0
Second Stage Propellant Left [kg]	1614	2292	1263

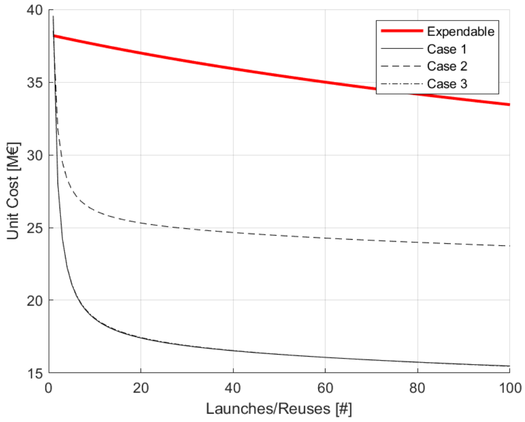

Figure 6.1: Unit cost for the complete launcher as a function of the number of launches

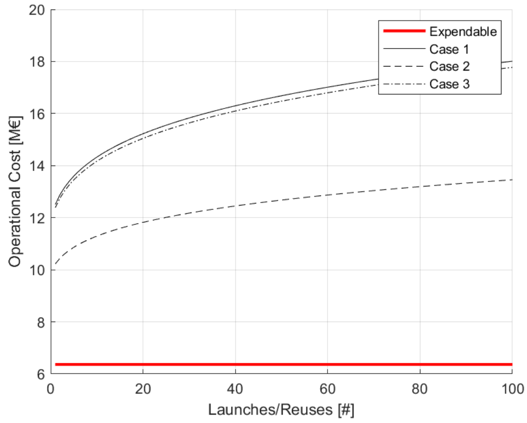

Figure 6.2: Operational cost as a function of the number of launches

configuration, the story is significantly different. Here all the reusable launchers are more expensive in cost per flight per kilogram payload than the expendable launcher. This means that for the Falcon 9 if the payload of the reusable launcher cannot be increased the launcher is not cost-effective. In order to break-even, the reusable launcher would at least need a payload capacity of 18t for recovering the complete stage and 20t for recovering the engine only. However, this is only to make the reusable launcher as expensive/cheap as the expendable launcher. As a final note for the Falcon 9 LEO case, it should be noted that more reuses of the launcher will not improve the result as it can be seen that the RI is increasing after about 10-15 launches. This number is effected mostly by the learning curve on both the decrease in production cost and the increase in refurbishment cost.

From the RI given in Figure 6.4, it is seen that recovering the entire stage using non-propulsive means (Case 3), is the cheapest option for this mission. In Figure 6.5 the altitude can be seen as a function of time, for both stages of the launcher. What can be seen is that the final orbit is not entirely circular. The final orbit is 299x290 km. The ground track of the flight path can be seen in Figure 6.6. The final range of the first stage is 754 km. Although this range is used to calculate the retrieval cost, it can be seen that for this case it might be better to sail from a location further up the coast in order to reduce the travel time and transport it back on land to the launch site using other means. This does not hold only for Case 3, but all cases have a similar ground track.

For the critical parameters during flight, the deceleration and the dynamic pressure, they can be seen in Figure 6.7 and Figure 6.8. Here it can be seen that the maximum acceleration for the ascent is about 5 g and the maximum deceleration is near the constraint set of 10 g. This is the deceleration due to re-entry, which can be distinguished by the smooth curve going into the peak. The smaller peak around 550 seconds is the deceleration due to deployment of the parachute. Looking carefully, one can notice that the stage briefly accelerates before the parachute peak. This is because the HIAD is discarded. This is done to reduce the mass at landing leading to a smaller parachute being required.
The same behaviour can be seen in the dynamic pressure where it is a smooth curve going into the dynamic pressure peak around 450s. The sharp drop around 550s is again the parachute deployment. Two peaks can be seen for the dynamic pressure during ascent (t<300). This is because of the throttling of the engine during

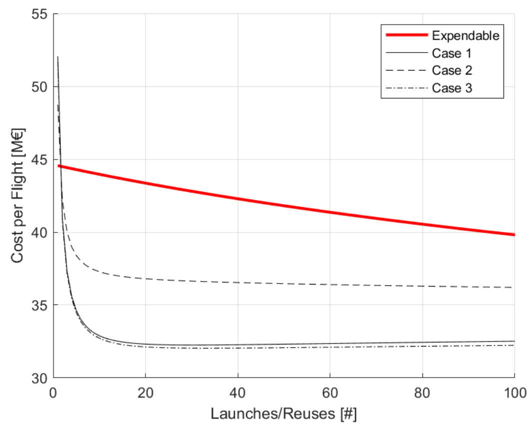

Figure 6.3: Cost per flight as a function of the number of launches for the Falcon 9 LEO mission

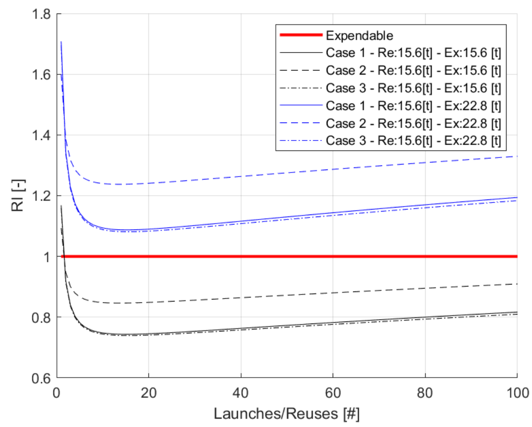

Figure 6.4: Reuse index as a function of the number of launches for the Flacon 9 LEO mission

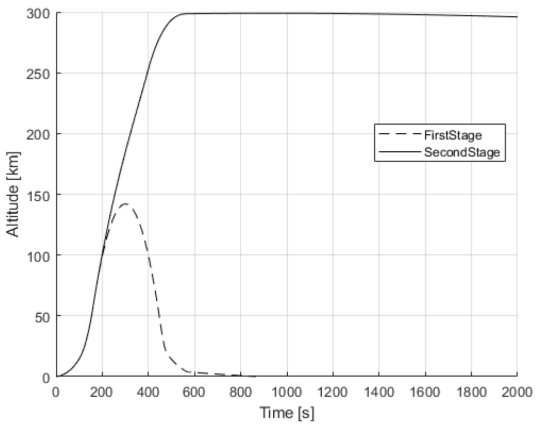

Figure 6.5: The altitude over time for the first and second stages for Case 3

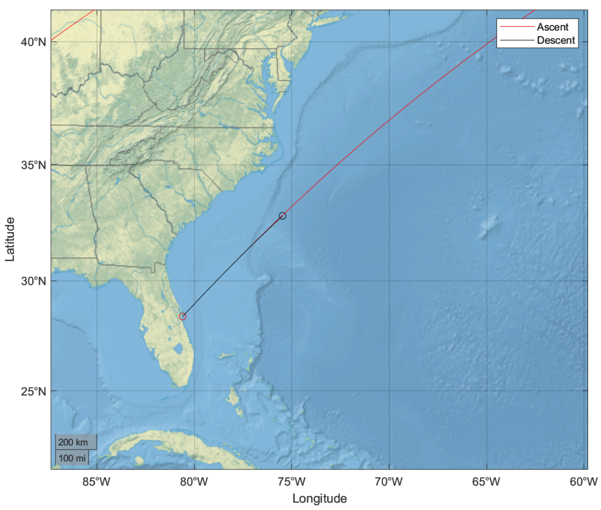

Figure 6.6: Ground track for Case 3

Table 6.9: Initial production cost breakdown for the Falcon 9 LEO mission in M€

Part	Expendable	Case 1	Case 2	Case 3
1st stage tank	11.6	11.6	11.6	11.6
1st stage engine	5.92			
1st stage additional reusability cost	NA	0.8	0.1	0.2
2nd stage tank	5.6			
2nd stage enigne	1.3			
AIT Cost	13.8	14.2	14.0	14.5

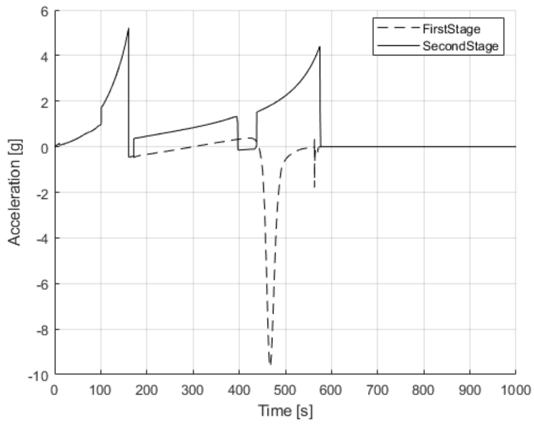

Figure 6.7: The acceleration over time for the first and second stages for Case 3

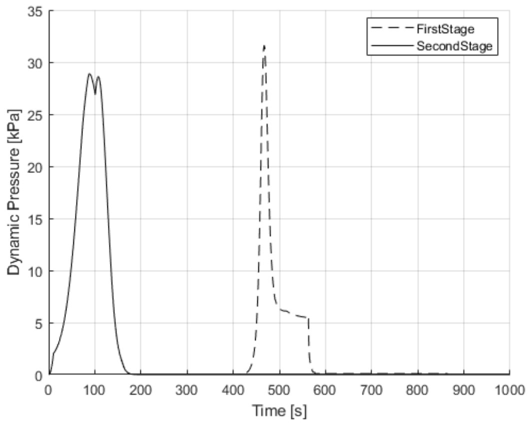

Figure 6.8: The dynamic pressure over time for the first and second stages for Case 3

ascent in order to keep the dynamic pressure, and thereby the drag losses, to a minimum.

Sensitivity Analysis

The sensitivity of the cases is also worth looking at to see how robust the solutions are, especially since the deceleration constraint is leading. Also, the dynamic pressure for case 1 is getting near the limit. The sensitivity is given in a boxplot format. In this format a box is created in which define the 25th and 75th percentile of all cases with the median being a line within the box. Outside the box two whiskers are given which extend to the most extreme points which are not considered outliers. The outliers are displayed separately. This method if displaying results is specially useful for the Monte Carlo analysis where a good overview can be given of how big the spread is of the results. In Figures, 6.9 and 6.10 the sensitivity of the maximum deceleration and maximum dynamic pressure can be seen which are encountered during the descent. What can be seen is for the deceleration,all cases have a median below the 10g limit, with cases 2 and 3 having all cases below 10g. It can also be seen that the maximum deceleration falls within at maximum a 2 g range. The smallest range is for case 3 where it falls in a 1 g range. For case 1, more than 25% of the cases have a maximum deceleration higher than 10 g, with one outliers as high as 19 g.

For the maximum dynamic pressure, Figure 6.10, cases 2 and 3 are way below the set 200 kPa limit and do not vary significantly. However, the propulsive landing, case 1, varies between 110 and 160 kPa with a median around 135 kPa.

The biggest contributors to the variations seen in Figures 6.9 and 6.10 are the variation in empty mass and the variation in the drag coefficient. Where the variation in empty mass can cause both the deceleration and dynamic pressure vary by at most 8.5% and 11.7% respectively. What is interesting is that the variation is opposite. So for example, if only the empty mass goes down by 10%, the deceleration goes up by 8.4%, but the maximum dynamic pressure goes down by 8.6%. An overview of the standard sensitivity analysis can be found in Appendix C.

Finally, the sensitivity of the cost in the form of the Reuse-index. What immediately is noticeable in Figure 6.11 is that the range for case 1 is significantly larger than for case 3. The refurbishment costs for case 1 are higher than for the other two. Therefore if the refurbishment costs are varied it has a larger impact on

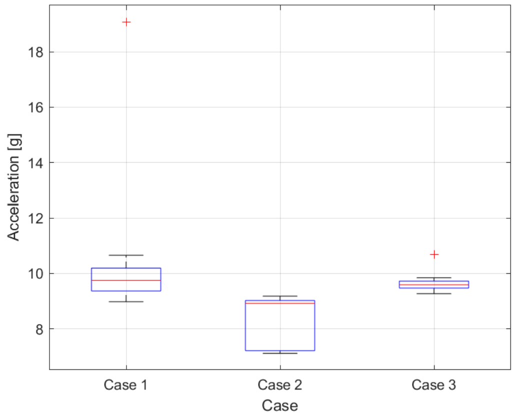

Figure 6.9: Sensitivity of the maximum deceleration during the descent for the Falcon 9 LEO mission

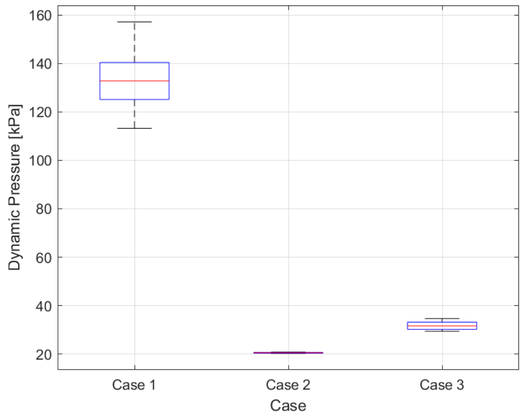

Figure 6.10: Sensitivity of the maximum dynamic pressure during the descent for the Falcon 9 LEO mission

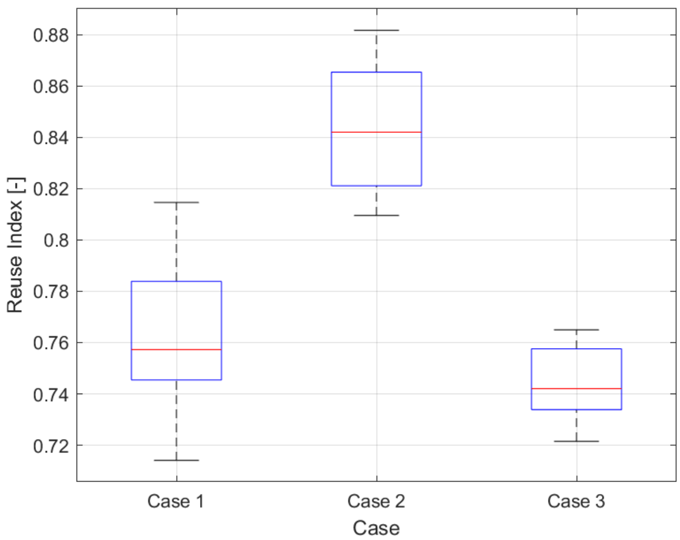

Figure 6.11: Sensitivity of the Reuse-index for the Falcon 9 LEO mission

case 1 than on the other two. Also, case 3, the complete stage non-propulsive case, is less sensitive with regard to the reuse-index than the other two cases with all cases between a RI of 0.77 and 0.72. Lowest RI value is achieved for case 1, which is 0.717, this is due to a combination of decreasing the landing leg and initial empty masses as well as reducing the refurbishment costs. Finally all cases have an RI below on meaning that even with all variations all cases are cheaper than the expendable launcher.

6.2.3. GTO Mission

For the GTO mission the resulting optimised variables can be found in Table 6.10. These results are comparable to the ones for the LEO mission. For case 1, the propulsive landing case is comparable to the LEO mission with about 3% of propellant being used for the descent. For the non-propulsive cases, the results are also similar with both using a HIAD and Ringsail parachute. Furthermore, the propellant loading for all cases are comparable to each other and the LEO mission. The comparison of vehicle masses for the different cases for the GTO mission can be found in Table 6.11. In Table 6.11 it can be seen that the empty mass for case 3 is the highest, followed by case 1. Again as with the LEO mission the expendable is the lightest first stage with regard to the empty mass. What it interesting to see is the difference between the non-propulsive cases. As a comparison the deceleration and landing system added that are are 25.5 %, 1.1 % and 11.4 % of landing mass for cases 1, 2 and 3 respectively. This does not say anything directly but shows that propulsive landing case is much less efficient with its mass than the non-propulsive cases.

Table 6.10: Optimisation Variables for the Falcon 9 GTO mission

Variable	**Case 1**	**Case 2**	**Case 3**
1^{st} stage Propellant mass	342472	362526	338452
2^{nd} stage Propellant mass	110230	100190	94525
Landing System	Landing Legs	MAR	Airbags
Deceleration System	Entry Velocity: 2427 m/s Re-entry Burn Thrust Level: 52.0 % Propellant for Descent: 2.72 % Landing Thrust Level: 53.9% Grid Fin Area: 0 m^2	Type: HIAD Area: 10.58 m^2 Deployment Altitude :NA km	Type: HIAD Area: 34.9 m^2 Altitude: NA km
		Type: Ringsail Parachute Area: 3726 m^2 Deployment Altitude : 2.20 km	Type: Ringsail Parachute Area: 8384 m^2 Altitude: 4.0 km

Table 6.11: Falcon 9 masses overview for the Falcon 9 GTO mission

Parameter	**Expendable Launcher**	**Reusable Launcher**		
		Case 1	Case 2	Case 3
First Stage				
Final Empty Mass [kg]	24720	27192	25005	27902
Structural mass	24720	24720	24720	24720
Landing system [kg]	NA	2472	0	1822
Hemisflo Ribbon Parachute System [kg]				
Ringsail Parachute System [kg]			275	619
HIAD System [kg]			10	741
Propellant Mass [kg]	411000	342472	362526	338452
Propellant Reserve [%]	0	2.7	0	0
Second Stage				
Payload Mass [kg]	6500			
Empty Mass [kg]	5700			
Propellant Mass [kg]	111500	110230	100190	94525

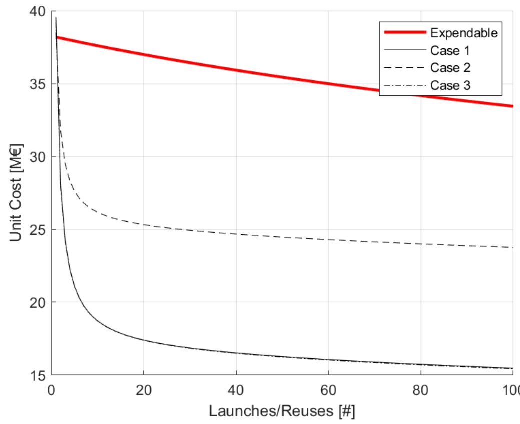

Figure 6.12: Unit cost as a function of the amount of launches for the Falcon 9 GTO mission

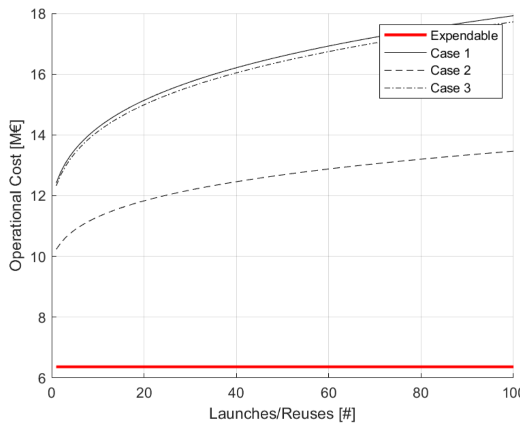

Figure 6.13: Operational cost as a function of the amount of launches
for the Falcon 9 GTO mission

Where in the LEO case the deceleration was close to 10g for all cases here only case 1 comes close to the

Table 6.12: Re-turn Flight Parameters for the three cases fort he Falcon 9 GTO mission

Parameter	**Case 1**	**Case 2**	**Case 3**
Start Landing Burn Altitude [m]	429	NA	NA
Maximum deceleration [g]	9.0	5.9	6.4
Maximum dynamic pressure [kPa]	119.4	50.2	58.1
First Stage Propellant Left [kg]	5226	0	0
Second Stage Propellant Left [kg]	63	1014	552

limit. The reason for the lower deceleration limits is due to the fact the for the GTO mission the apogee of the first stage is much lower. Where in the LEO mission the apogee was at around 150-200km for the GTO case is apogee does not go above 100km for all cases. So when the HIAD is deployed after the rotation of the stage, it already starts to decelerate the stage earlier than for the LEO case. Furthermore the specific ascent trajectory flown also makes a difference. Since the perigee is at 200km this means the stage has to go horizontal still within the atmosphere thereby having more drag losses.
Again for the unit cost and the operational costs, Figures 6.12 and 6.13 the same trend is seen as for the LEO mission cases. Case 3 is the cheapest for the average production cost followed closely by case 1 using propulsive landing. For the operational cost the expendable is again the cheapest of all cases calculated and case 2 using only engine recovery is the cheapest in operational cost of the reusable launchers. A breakdown of the initial production cost can be seen in Table 6.13. For the cost per flight and the Reuse-Index the same

Table 6.13: Initial production cost breakdown for the Falcon 9 reusable launcher for the GTO mission in M€

Part	**Expendable**	**Case 1**	**Case 2**	**Case 3**
1^{st} stage tank	11.6	11.6	11.6	11.6
1^{st} stage engine	5.9			
1^{st} stage additional reusability cost	NA	0.8	0.1	0.2
2^{nd} stage tank	5.6			
2^{nd} stage enigne	1.3			
Assembly Cost	13.8	14.2	13.9	14.1

behaviour is observed as for the LEO mission. Case 3 using non-propulsive recovery methods and recovering the complete stage is the cheapest per flight with a flight cost of 31.82 M€ per flight, Figure 6.14. For the Reuse-Index again two groups are created. One which compares the the price per kilogram payload with both using the reusable payload of 6500. The other group is comparing the price per kilogram payload with the reusable launchers using the 6500 kg, which demonstrated maximum payload for GTO missions for a

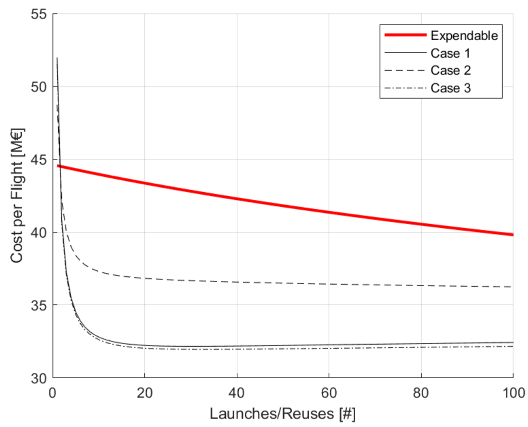

Figure 6.14: Cost per flight as a function of the amount of launches for the Falcon 9 GTO mission

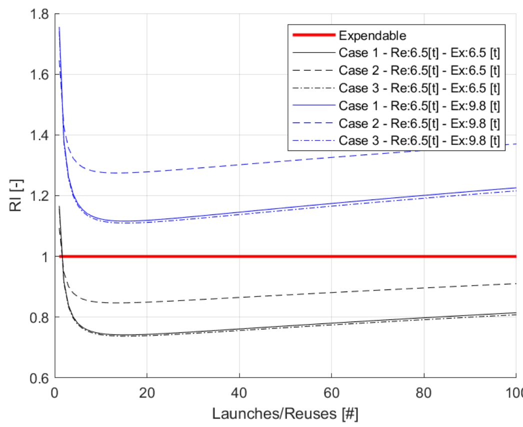

Figure 6.15: Reuse index as a function of the amount of launches for the Falcon 9 GTO mission

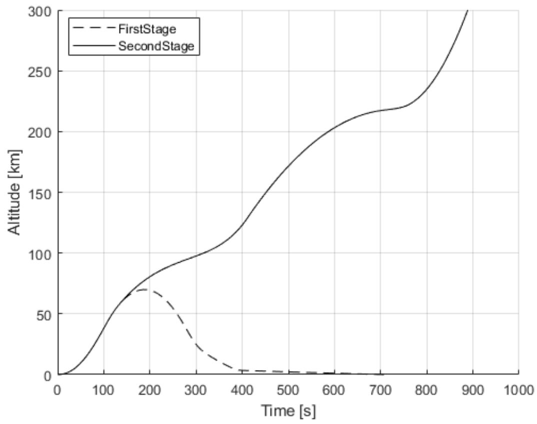

Figure 6.16: The altitude over time for the first and second stages for Case 3

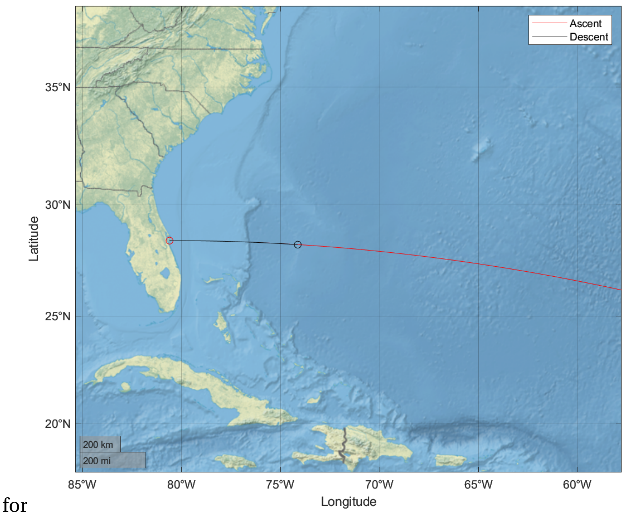

Figure 6.17: Ground track for Case 3

reusable launcher and the theoretical expendable payload which is 9800kg. The comparison can be seen in Figure 6.15. The RI for cases 1 and 3 are the lowest with 0.744 and 0.735 respectively, when comparing the same payload masses. However again if the reusable launchers are compared to the theoretical maximum payload for the expendable launchers all reusable launchers are more expensive per kilogram payload than the expendable launcher.

The cheapest solution for the GTO mission is again Case 3, which, using non-propulsive means, lands the entire stage with the help of airbags. For the altitude plot it is difficult to capture both stages in one plot completely since the apogee reaches 33000 km. So the focus has been given to the first stage in Figure 6.16. The final error in the orbit is 1.6 km for the perigee and almost 0 km for the apogee altitude. For the ground track, in Figure 6.17, the flight path starts with a heading of 90 degrees, as is usual for a GTO orbit. The touchdown distance for the first stage is 719 km away from the launch site. The acceleration, in Figure 6.18, the maximum deceleration occurs during the deployment of the Ringsail parachute with a maximum deceleration of 6.4 g. What is noticeable is that the maximum acceleration during the final burn of the second stage is 8.3 g. the smooth curve for the first stage around 300 seconds is the deceleration due to the drag caused by re-entry, This is slightly higher than the deceleration caused by the parachute inflation loading which is 6.3 g.

For the dynamic pressure of the first stage the re-entry is around 300 s, when the largest peak of 100 kPa occurs. Following this the first parachute is deployed around 350 s. The reason for the small increase in dy-

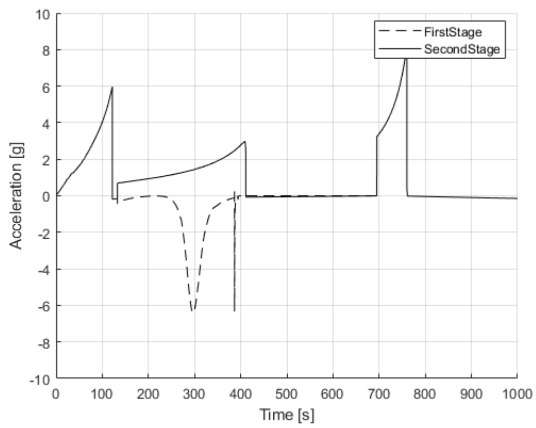

Figure 6.18: The acceleration over time for the first and second stages for Case 3

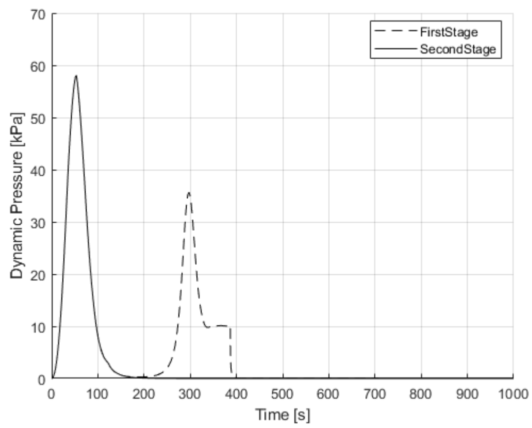

Figure 6.19: The dynamic pressure over time for the first and second stages for Case 3

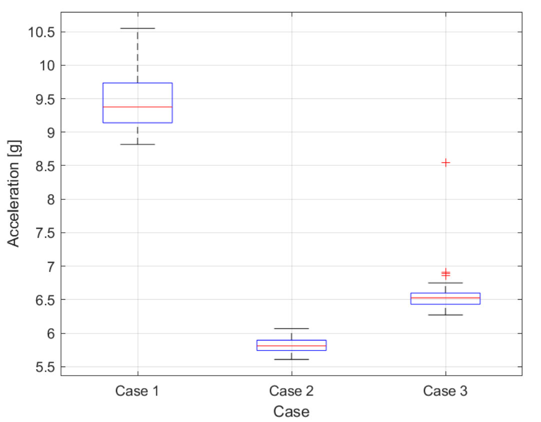

Figure 6.20: Sensitivity of the maximum deceleration during the descent for the Falcon 9 GTO mission

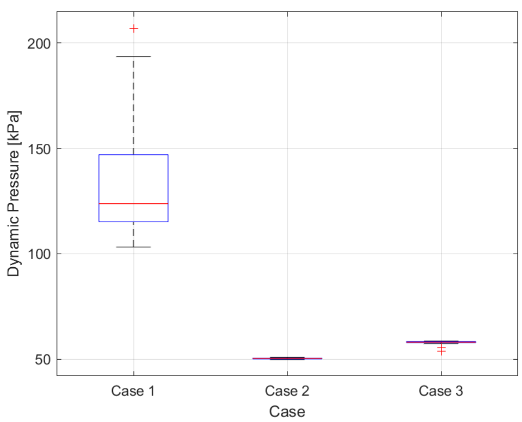

Figure 6.21: Sensitivity of the maximum deceleration during the descent for the Falcon 9 GTO mission

namic pressure between re-entry and Hemisflo parachute deployment is because the velocity is levelling of but the density is increasing.

Sensitivity Analysis

Unlike the LEO mission the GTO mission is not as close to the limits, but the sensitivity is still interesting. From the sensitivity maximum deceleration, in Figure 6.20, it can be seen that most of the cases are below the 10 g limit, with the exception of the top 25% of case 1. This is similar to the LEO mission where also case 1 has 25% of its cases above 10 g. For the dynamic pressure it is interesting to see that the dynamic pressure for case 1 is higher than for the LEO mission. For the GTO mission the dynamic pressure is between 110 and 190 kPa. This is a significant range which is probably because for the Falcon 9 GTO case the chosen re-entry velocity is higher than the velocity during re-entry, which mean the stage performs a ballistic entry. For the cost sensitivity, Figure 6.22, again the engine only case is more expensive and but this time the median is 2% lower. Also the maximum cost is about 4% lower. For the propulsive and non-propulsive complete stage cases, cases 1 and 3, the difference in median is more pronounced than for the LEO mission, 0.03 difference for the GTO mission as compared to 0.01 for the LEO mission.

6.2.4. Conclusion

For the Falcon 9 it can be seen that for both missions the complete stage recovery is the cheapest and specifically the case using non-propulsive means (case 3). This solution is also the most robust when looking at the Monte Carlo analysis. However where all cases were cheaper than the expendable case, none resulted in a

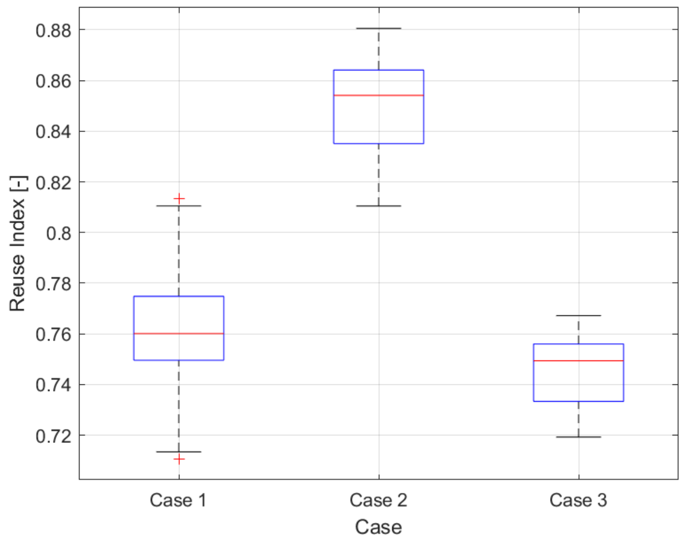

Figure 6.22: Sensitivity of the Reuse-index for the Falcon 9 GTO mission

reduction of 30% of the cost. The largest saving was a 28% cost reduction on the total launch cost. All cases at 10 reuses are cheaper than the expendable launcher. Also none of the solutions had a RI higher than one, also during the sensitivity analysis, meaning that all solution were cheaper than the expendable launcher. When comparing them to the maximum expendable payload mass all cases are more expensive per kilogram of payload. This comes with a caveat though since for the GTO mission it was seen that the maximum performance of the Falcon 9 was not needed. Therefore the Falcon 9 should be able to carry more payload into the GTO orbit. This should bring it closer to the LEO mission where more was required from the launcher to achieve the results.

For using non-propulsive landing using a HIAD/Ringsail seems to be favourite combination as the HIAD flattens the deceleration peak making it easier to stay within the 10 g limit. This option is used by all non-propulsive cases. Also grid fins which are an option to be used for all cases are not used, not even for the propulsive landing, in order to decelerate the system a little bit. So from this it can be concluded that for the Falcon 9 the grid fins are only for attitude control and not really for deceleration.

Comparing the results here to the actual Falcon 9, the results are comparable. At least when talking the about the propulsive landing option. This is nearly the cheapest option and the difference between this and the complete stage recovery using non-propulsive manner is less than 1 M€.

6.3. Delta IV+

For the Delta IV+ case, first the inputs for the vehicle are given followed by the cases for the LEO and GTO missions. Followed by a small conclusion based on the results found for this vehicle.

6.3.1. Vehicle

The next vehicle which will be looked at is a modified version of the Delta IV. The modification is part of the upper stage, because FRT is made for a two part second stage burn, as discussed in subsection 5.5.1, the optimisation architecture is made around this as well. However the original Delta IV has so little thrust that the exclusion system discussed in section 5.5 has some issues because the sensitivity required cannot be met. This means the variable used to distinguish the limiting ΔV reaches the limit where it is no longer the dominant factor. FRT is able to handle this and the launcher is capable of reaching the required orbit. As the original Delta IV was used to calculate the maximum payload mass in Table 5.4. However, this causes the issue that with the exclusion system implemented it can give miss-leading results as it might exclude options that should not have been excluded. However when this system is not used the computation time increases immensely. This could be fixed given more time, however for this vehicle it was decided to add one engine to the second stage to omit this issue. This should be possible since the Centaur upper stage uses the same diameter and engine and for this upper stage there is a single engine and dual engine version[18, 19]. For these two version the empty mass does not change by more than just the mass of the engine, this will be applied to the Delta IV second stage as well. This means one engine mass is added to the empty mass of the Delta IV, but the propellant mass for the second stage remains the same, this vehicle will be called the Delta IV+ for the remainder of the research. The overview of the masses and engine characteristics can be found in Table 6.14 and Table 6.15. For the Delta IV engines the inputs are much more clear than the Falcon 9. Here the

Table 6.14: Vehicle Masses and Dimensions for the Delta IV and Delta IV+ [3, 20, 86]

Parameter	**Delta IV**	**Delta IV+**
First Stage		
Initial Empty Mass [kg]	26390	
Initial Propellant Mass [kg]	204000	
Engine Mass [kg]	6686	
Diameter [m]	5.1	
Length [m]	36.6	
Nosetip Radius [m]	2.5	
Second Stage		
Empty Mass [kg]	2780	3081
Initial Propellant Mass [kg]	21317	
Engine Mass [kg]	301	602
Diameter [m]	4	
Length [m]	12.2	
Nosetip Radius [m]	2	
Boosters		
Empty Mass [kg]	3786	
Propellant Mass [kg]	29700	
Diameter	1.524	
Length[m]	13.16	
Minimal Boosters [#]	0	
Maximum Boosters [#]	4	

Table 6.15: Engine Inputs for the Delta IV and Delta IV+ [5, 89, 91]

Parameter	**Delta IV**	**Delta IV+**
First Stage Engine		
Propellant []	LH2/LOX	
Exit Area [m^2]	4.67	
Throat Area [m^2]	0.2172	
Chamber Pressure [MPa]	10.9	
Amount of Engines [#]	1	
Lower Thrust Limit [%]	45	
Model Correction	Sea-level	
Sea Level Thrust [kN]	3136	
Sea Level I_{sp}	362	
Second Stage Engine		
Propellant []	LH2/LOX	
Exit Area [m^2]	3.618	
Throat Area [m^2]	0.0129	
Chamber Pressure [MPa]	4.4	
Amount of Engines [#]	1	2
Lower Thrust Limit [%]	50	
Model Correction	Vacuum	
Vacuum Thrust [kN]	220	
Vacuum I_{sp}	465.5	

producer of the engine, Aerojet Rocketdyne, has the data needed on their website. For the inputs of the Delta IV itself the same issues persist were one source is used when all the data required is there. For the booster the GEM-60 sea-level thrust curve can be found in Figure 6.23 and a sea-level specific impulse of 273.9 s is used[20].

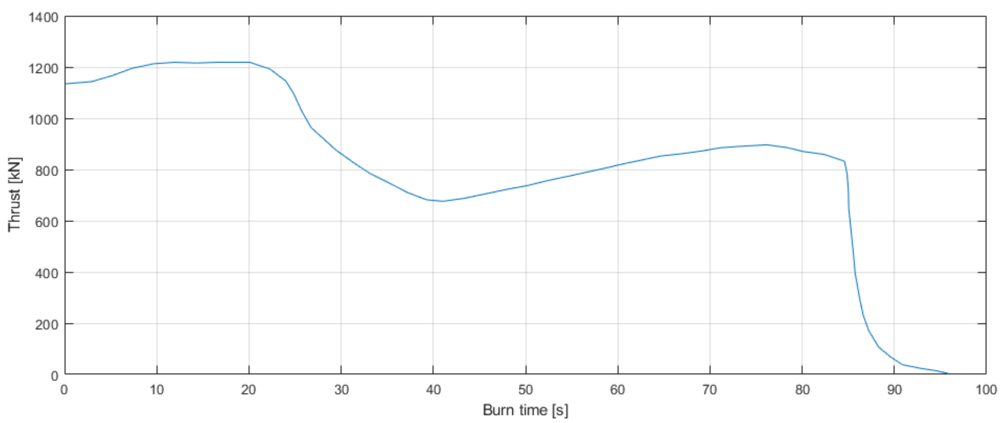

Figure 6.23: Sea-level thrust curve of the GEM-60 solid rocket booster [20]

6.3.2. LEO Mission

Starting with a mission in low earth orbit. The tool is used to optimise the Delta IV+. Where the version of the Falcon 9, which was used in the previous section was designed as a reusable vehicle. It could be assumed that all reusable options would lead to satisfying result. However since the Delta IV was designed as a purely expendable launcher here the same assumption can not be made. So it is entirely possible that some cases do not lead to a result within the constraints. The optimisation solutions for the Delta IV+ LEO mission can be found in Table 6.16.

In Table 6.16 it can be seen that both case 1 and case 3 needs boosters in order to fulfil the mission, while

Table 6.16: Optimised variables for the three cases

Variable	**Case 1**	**Case 2**	**Case 3**
1^{st} stage Propellant mass [kg]	189372	195077	358890
2^{nd} stage Propellant mass [kg]	20479	16458	15121
Landing System	Landing Legs	Airbags	Airbags
Boosters [#]	2	0	2
Deceleration System	Entry Velocity: 2247 m/s Re-entry burn Thrust level: 64 % Propellant for Descent: 9.6 % Landing Thrust Level: 59% Grid Fin Area: 1.1 m^2	Type: HIAD Area: 20.1 m^2 Deployment Altitude :NA	Type: HIAD Area: 312 m^2 Altitude: NA km
		Type: Ringsail Parachute Area [m^2]: 6869 m^2 Deployment Altitude : 1.1 km	Type: Ringsail Parachute Area: 9268 m^2 Altitude: 4.0 km

case 2 does not. Case 3 needs 155 t of propellant extra. For the Delta IV+ a HIAD is used in order to limit the maximum deceleration. Also the re-entry velocity is, for the propulsive landing case, close to the velocity found for all Falcon 9 cases. For the propulsive landing, grid fins are used, whereas in the Falcon 9 case grid fins were absent. The sizes of the Ringsail parachutes are approximately 6900 m^2 and 9300 m^2,l this corresponds to a diameter of 66 m and 77 m. Although this is larger than the main parachutes of the Space Shuttle and Ariane 5 solid rocket boosters this is not outside the range as the parachutes can be split into multiple parachute into a cluster. This does changes some values as the drag will probably be reduced according to Knacke [52]. On top of this the mass of the parachute system will probably also increase as gradient of the parachute model is steepest near zero. This means three parachute of 20 m^2 will have a larger mass than one single parachute of 60 m^2.

The various masses for the Delta IV+ can be found in Table 6.17. Here a snowball effect can be found for case 3 where because of the extra propellant mass the corresponding deceleration systems need to be larger and therefore heavier resulting in an airbag and flotation system that is 4.7t. For the remainder the masses are relatively similar for the other two cases.

For the return flight again the deceleration is the critical parameter with all at the limit of 10 g. However looking at the maximum dynamic pressure these are lower or comparable to the Falcon 9 LEO mission specifically for the propulsive landing where the dynamic pressure is only 79 kPa, where the Falcon 9 propulsive landing all had more than 100 kPa. Finally almost all the propellant is used for all cases except for the second stage propellant for case 3. For the cost comparison of the Delta IV+ LEO mission for which the comparison of the unit cost and the operational cost can be found in Figures 6.24 and 6.25.

For the unit cost, Figure 6.24, it can be seen that the cases are much closer together than for the Falcon 9. At ten reuses case 1, is the cheapest followed by case 3 and case 2 is the most expensive to produce on average over the ten reuses with a difference between all cases of less than €400,000 for cases 2 and 3. Also, case 3 becomes increasingly cheaper with an increasing amount of reuses more so than case 1, the propulsive

Table 6.17: Delta IV+ LEO mission vehicle masses overview

Parameter	Expendable Launcher	Reusable Launcher		
		Case 1	Case 2	Case 3
First Stage				
Final Empty Mass [kg]	26390	29150	27207	44345
Structural mass	26390	26390	26390	35685
Landing system [kg]	NA	2650	250	4674
Grid Fins [kg]		110		
Hemisflo Ribbon Parachute System [kg]				
Ringsail Parachute System [kg]			507	684
HIAD System [kg]			60	3302
Propellant Mass [kg]	204000	189372	195077	358890
Propellant Reserve [%]	0	9.6	0	0
Second Stage				
Payload Mass [kg]	9000			
Empty Mass [kg]	3081			
Propellant Mass [kg]	21317	20479	16458	15122
Boosters				
Total Empty Mass [kg]	NA	7571	0	7571
Total Propellant Mass [kg]	NA	59394	0	59394

Table 6.18: Re-turn Flight Parameters

Parameter	Case 1	Case 2	Case 3
Start Landing Burn Altitude [m]	1027	NA	NA
Maximum deceleration [g]	9.9	10.0	10.0
Maximum dynamic pressure [kPa]	79.1	27.6	15.6
First Stage Propellant Left [kg]	551	0	0
Second Stage Propellant Left [kg]	163	461	2840

landing case. The reason that case 2 is now suddenly around the same level as the other two when comparing unit costs is due to the addition of the boosters. Since they are not reused, they have to be built every time.A breakdown of the initial production cost can be seen in Table 6.19. However, when comparing the operational

Table 6.19: Initial production cost breakdown for the Delta IV+ reusable launcher for the LEO mission in M€

Part	Expendable	Case 1	Case 2	Case 3
1st stage tank	20.9	20.9	20.9	28.59
1st stage engine	11.8			
1st stage additional reusability cost	NA	1.9	0.1	0.7
2nd stage tank	6.2			
2nd stage engine	3.6			
Assembly Cost	23.8	27.4	24.8	31.1
Boosters	NA	4.5	NA	4.5

costs, Figure 6.25, the results are more distinct from each other. Case 2, recovering only the engine, has the least operational cost. Again as stated before, this is because there is just less to refurbish since most of the stage is rebuild each time. From this, it is also logical that case 3, is the most expensive to refurbish since about 9000 kg of extra tank mass also has to be refurbished.

Finally the cost per flight and the reuse index can be seen in Figure 6.26 and Figure 6.27. It is clear that the savings are less than for the Falcon 9. Where the Falcon 9 had a minimal RI of 0.71, here the Delta IV+ does not come below a RI of 0.8. However, in the case of the Delta IV+, the order of the cheapest and most expensive is reversed. Where for the Falcon 9 case 3, recovering the complete stage using non-propulsive

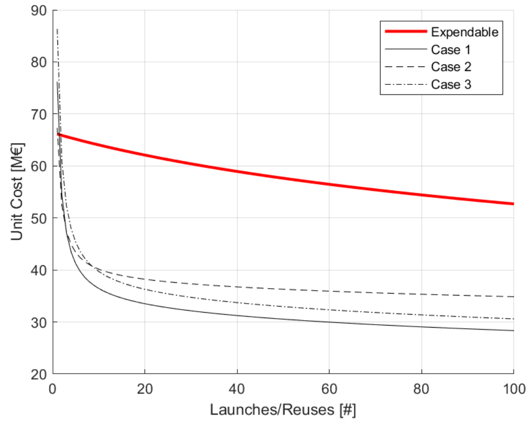

Figure 6.24: Unit cost as a function of the amount of launches for the Delta IV+ LEO mission

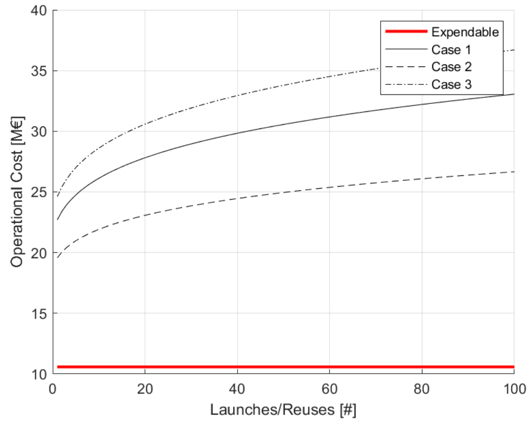

Figure 6.25: Operational cost as a function of the amount of launches for the Delta IV+ LEO mission

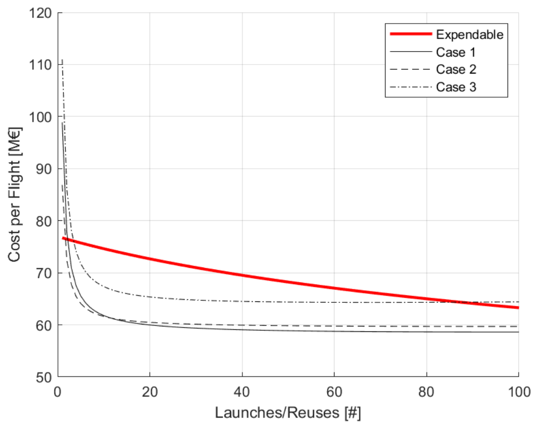

Figure 6.26: Cost per flight as a function of the number of launches for the Delta IV+ LEO mission

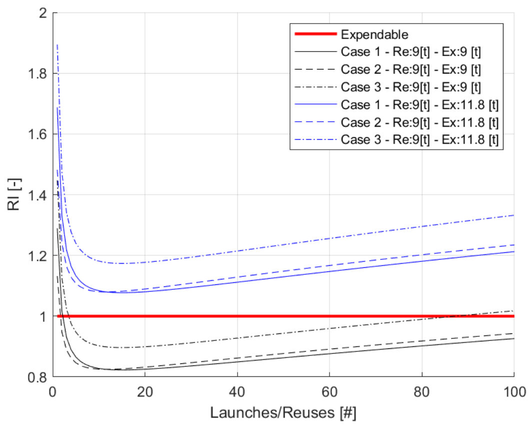

Figure 6.27: Reuse index as a function of the number of launches for the Delta IV+ LEO mission

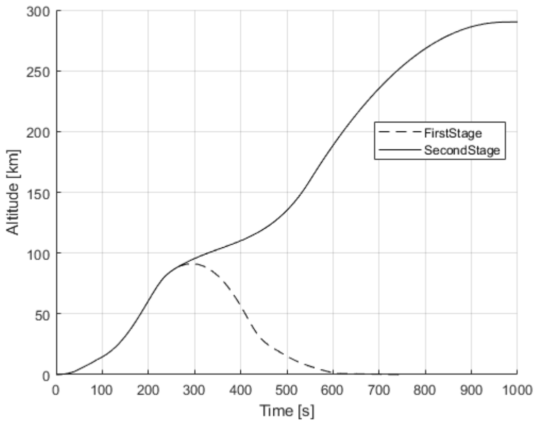

Figure 6.28: The altitude over time for the first and second stages for Case 2

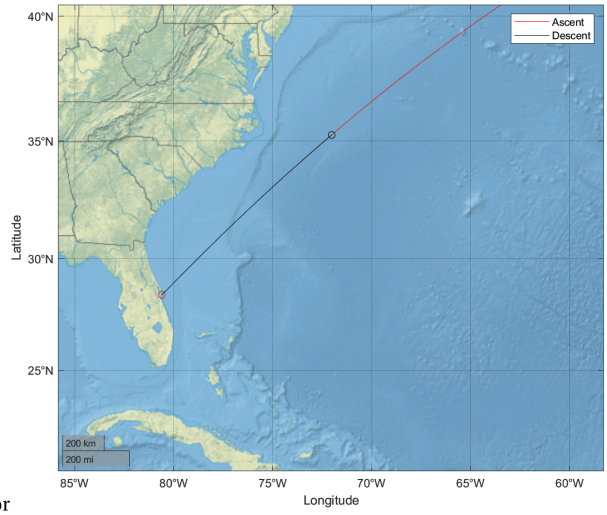

Figure 6.29: Ground track for Case 2

means, is the cheapest for the Delta IV+ it is the most expensive. The cheapest is the engine only recovery, case 2, which cost M€ 61.6.
When comparing the RI, Figure 6.27, it can be seen that the propulsive landing and the engine only recover, cases 1 and 2, are the cheapest and have a RI of 0.828 and 0.826 respectively. This is however close to the cross over point where case 1 becomes cheaper, which is at 12 reuses. Also because of the increasing refurbishment cost for more reuses case 3, becomes more expensive than the expendable case even when comparing the same payload mass at 88 reuses.

Case 2 is the cheapest option, by a small margin. For this case the altitude over time as well as the ground track can be found in Figure 6.28 and Figure 6.29. What can be seen in Figure 6.28 is that orbit insertion of the second stage happens after the first stage has already landed. This shows that the second stage needs quite some time to get from the separation velocity to orbital velocity. The final orbit reached is 290.5x290 km for the second stage. The ground track this is not really remarkable however it does show that for this mission, 50 deg inclination, a hybrid retrieval system as was suggested in the Falcon 9 LEO case could be a possibility. Where the boat only tows the stage to the nearest port and the stage is transported back to the launch site on land for the remainder. The final touchdown distance for the engine section is 1120 km downrange from the launch site.

For the descent that the maximum deceleration for the first stage is 10 g as already mentioned in Table 6.18. From Figure 6.30 it can be seen that this deceleration occurs during re-entry. The interesting is that the maximum dynamic pressure for re-entry is not nearly near the 200 kPa limit, it reaches a maximum of 28 kPa which can be seen in Figure 6.31. This shows that although the location of the dynamic pressure and deceleration peaks for re-entry occur around the same time the magnitude of the dynamic pressure peak is not dependent on the maximum deceleration.

Sensitivity Analysis
To underscore the fact that the deceleration limit is the key parameter for the Delta IV+, which can be seen in Figure 6.32, is that the median for two of the three cases is above 10 g. For case 1 the median is at 9.9 g. More than half of the cases have their maximum deceleration at more than 10 g. Both cases 2 and 3 have 25% of the cases above 13 g. Case 3 even has more than 75% of the cases above 10 g. This shows that managing the deceleration for the Delta IV+ for this mission is key since it does not take much for the deceleration to be over 10 g. The reason for this is probably because of the high re-entry speeds which are 3749 m/s, 4363 m/s and 5125 m/s for cases 1,2 and 3 respectively. This coupled with a stage that has a 5m diameter means that when the stage hits the atmosphere it decelerates rapidly. Since the stage doesn't not leave the atmosphere completely for this case under nominal conditions, 100km being the cut-off, it should be sensitive to small increases in velocity. This means the apogee of the first stage will come outside the atmosphere which does not have any drag to slow it down.

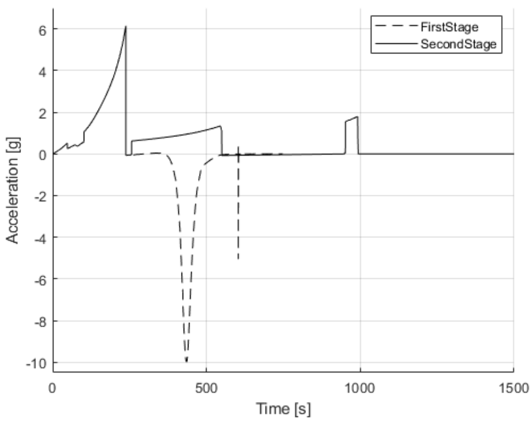

Figure 6.30: The acceleration over time for the first and second stages for Case 2

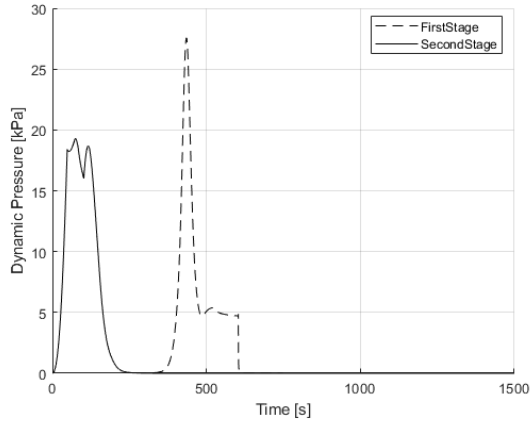

Figure 6.31: The dynamic pressure over time for the first and second stages for Case 2

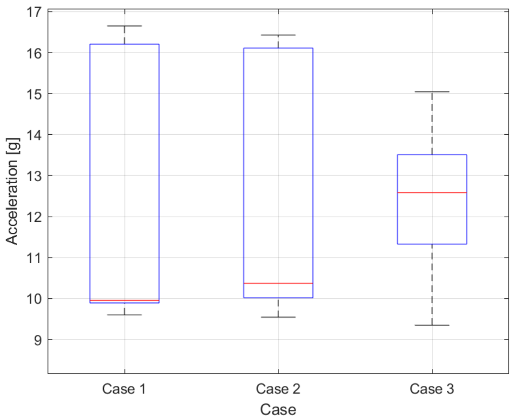

Figure 6.32: Sensitivity of the maximum deceleration during the descent for the Delta IV+ LEO mission

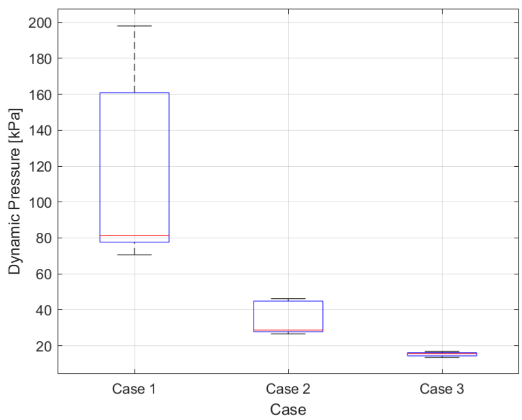

Figure 6.33: Sensitivity of the maximum deceleration during the descent for the Delta IV+ LEO mission

For the sensitivity of the maximum dynamic pressure Figure 6.33 the medians for all three cases are below 100 kPa. However for case 1, propulsive landing, 25% of the cases are between 160-200 kPa, which means that for case 1 the dynamic pressure comes near the limit in the sensitivity analysis. The ranges for cases 2 and 3, as can be seen in Figure 6.33, are very narrow so the Delta IV+ is not sensitive to changes in dynamic pressure when using a HIAD for LEO missions.

What is also interesting, for the Delta IV+, the sensitivity of the landing velocity of the stage, which can be seen in Figure 6.34. The sensitivity for cases 2 and 3 are not particularly interesting; these are not varying significantly. However for case 1, the results are very significant, this shows the median of the landing velocity is not at near-zero anymore but at 5 m/s and the highest value is around 18 m/s. This shows that case 1 is susceptible to changes in the landing velocity, with small changes already could lead to the system not being able to land safely. This is partly due to the small leftover propellant in the first stage which was found in Table 6.18.

Finally, the sensitivity to the cost can be found in Figure 6.35, here cases 1 and 2 have about the same lower limit at an RI of 0.79. However, case 1 has a bigger range than case 2, furthermore, the median for case 2 is lower than for case 1. This all leads to the fact that although they are close when calculating the RI when taking the sensitivity into account case 2, recovering only the engine is not only slightly cheaper but is also less sensitive than case 1. What should also be noted is that all cases are again below an RI of one. Even case 3 where 155t of extra propellant and 9000 kg of extra tank mass was added is below and RI of 1.

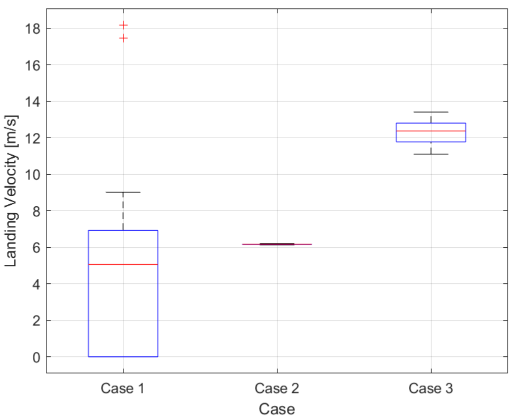

Figure 6.34: Sensitivity of the landing velocity for the Delta IV+ mission

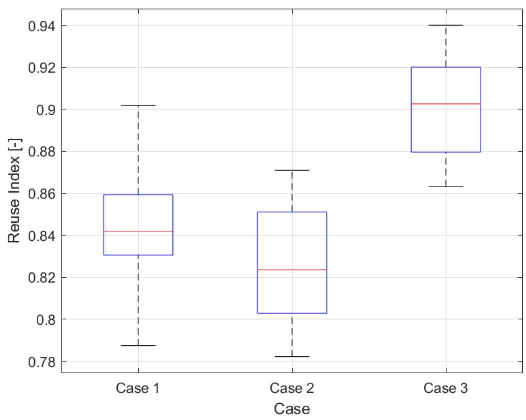

Figure 6.35: Sensitivity of the Reuse-index for the Delta IV+ LEO mission

6.3.3. GTO Mission

The final mission is the Delta IV+ on a GTO mission. The results of the optimisation process is given in Table 6.20. It can be seen that cases 2 and 3 are relatively comparable to the Delta IV+ LEO mission, although

Table 6.20: Optimised variables for the three cases for the Delta IV+ GTO mission

Variable	**Case 1**	**Case 2**	**Case 3**
1^{st} stage Propellant mass [kg]	203940	181882	366479
2^{nd} stage Propellant mass [kg]	20529	20203	20402
Landing System	Landing Legs	Airbags	Airbags
Boosters [#]	4	0	2
Deceleration System	Entry Velocity: 4083 m/s Re-entry burn Thrust level: 54.7 % Propellant for Descent: 4.4 % Landing Thrust Level: 45.5% Grid Fin Area: 10.8 m^2	Type: none Area: NA m^2 Deployment Altitude :NA	Type: HIAD Area: 47.49 m^2 Altitude: NA km
		Type: Hemisflo Ribbon Parachute Area [m^2]: 2054 m^2 Deployment Altitude : 11.8 km	Type: Ringsail Parachute Area: 8038 m^2 Altitude: 0.94 km

more propellant is need for the second stage which for all cases is near the maximum 21317 kg. Case 1 needs 2 more boosters as compared to the LEO mission. Furthermore only one system is needed for case 2 which is a supersonic parachute which is deployed higher than seen before. However there is one critical element in that case 1 did not fall within all the constraints, the maximum deceleration is more than 10 g even with the large grid fins of 10 m^2 per fin. Case 1 is kept in the tables and figures to compare it but it does not meet the constraints. When comparing the masses once again the significant increase in the landing system can be seen for case 3. This is again due to the increase of the structural mass due to the extra propellant. As in the LEO mission case 2 is the lightest followed by cases 1 and 3. Where for case 3, 162 t of extra propellant is needed for the first stage. The return-flight parameters can be seen in Table 6.22. As already mentioned the maximum deceleration for case 1 is higher than the 10 g limit but the other parameters are comparable to those from the LEO mission. What is interesting is that the maximum deceleration for case 3 is not near the 10 g as compared to the LEO mission. As previously mentioned, in subsection 5.4.2 the objective function will give always give a solution even if this is outside the constraints. This just means that for case 1 there are no solution that are within the constraints that could be found.

Table 6.21: Vehicle Masses overview

Parameter	Expendable Launcher	Reusable Launcher		
		Case 1	Case 2	Case 3
First Stage				
Final Empty Mass [kg]	26390	30269	28454	43337
Structural mass	26390	26390	26390	35994
Landing system [kg]	NA	2752	1613	5363
Grid Fins [kg]		1127		
Hemisflo Ribbon Parachute System [kg]			451	
Ringsail Parachute System [kg]				593
HIAD System [kg]				1387
Propellant Mass [kg]	204000	203940	181882	366479
Propellant Reserve [%]	0	4.4	0	0
Second Stage				
Payload Mass [kg]	4500			
Empty Mass [kg]	3081			
Propellant Mass [kg]	21317	20529	20203	20402
Boosters				
Total Empty Mass [kg]	NA	15143	0	7571
Total Propellant Mass [kg]	NA	118788	0	59394

Table 6.22: Delta IV+ GTO mission re-turn flight parameters

Parameter	Case 1	Case 2	Case 3
Start Landing Burn Altitude [m]	1027	NA	NA
Maximum deceleration [g]	**14.35**	9.4	8.6
Maximum dynamic pressure [kPa]	105	34.5	52.5
First Stage Propellant Left [kg]	545	0	0
Second Stage Propellant Left [kg]	897	30.3	1295

To compare the unit cost, Figure 6.36, a couple of things spring out. First is that the complete stage recovery using non-propulsive means, case 3, is the cheapest to produce after seven reuses even though there is 9t extra of tank mass in the initial cost and two boosters which are used every reuse. It is not cheaper than case 2 where no boosters are used, but just the tank has to be rebuilt every reuse. Secondly, after about 30 reuses case 2, even becomes the most expensive reusable system to produce. Furthermore, the initial unit cost that is needed from both cases 1 and 3 is about 25% higher than for the expendable case. On top of that, the initial unit cost for cases 1 and 3 are about the same, so this means two boosters are about the same cost in production cost as 9t of extra tank mass. A breakdown of the initial production cost can be seen in Table 6.23. The operational cost, Figure 6.37, is by now a very familiar sight. The production cost of the part that is reused

Table 6.23: Initial production cost breakdown for the Delta IV+ reusable launcher for the LEO mission in M€

Part	Expendable	Case 1	Case 2	Case 3
1st stage tank	20.9	20.9	20.9	28.59
1st stage engine	11.8			
1st stage additional reusability cost	NA	2.5	0.1	0.3
2nd stage tank	6.2			
2nd stage engine	3.6			
Assembly Cost	23.8	30.2	24.6	30.3
Boosters	NA	8.7	NA	4.5

determines how high the refurbishment cost is, which is most of the operational cost. So case 1 is cheaper in operation than case 3 for the fact that the boosters are not reused, and case 3 has more tank mass to refurbish.

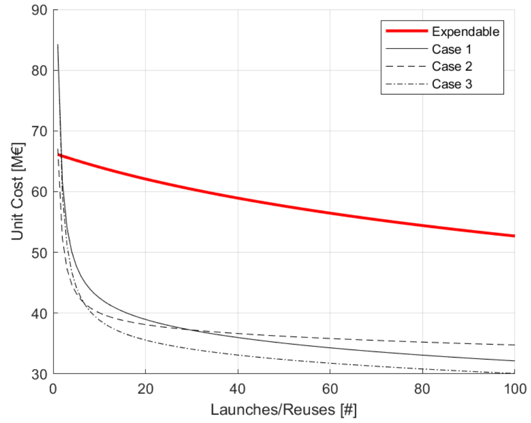

Figure 6.36: Unit cost as a function of the amount of launches

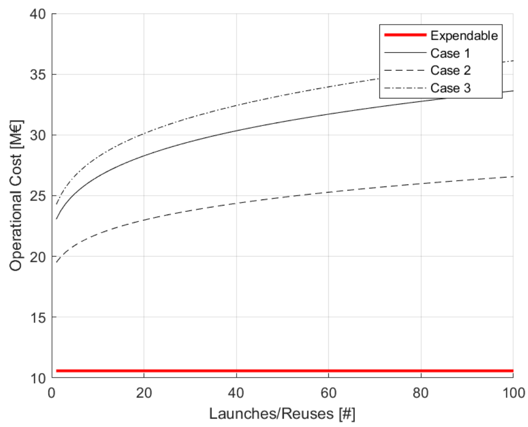

Figure 6.37: Operational cost as a function of the amount of launches

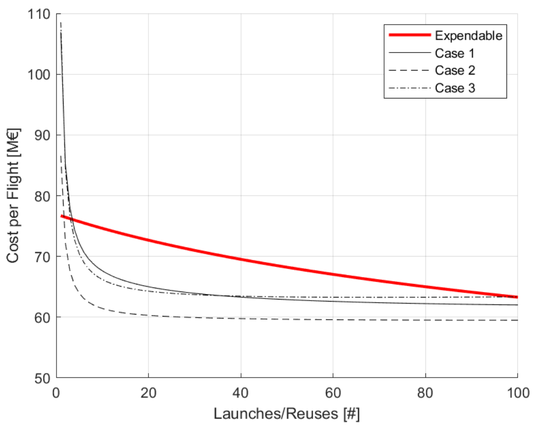

Figure 6.38: Cost per flight as a function of the number of launches

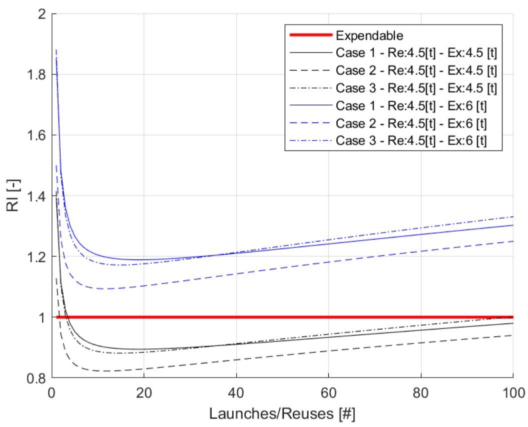

Figure 6.39: Reuse index as a function of the number of launches

The costs per flight in Figure 6.38 however, are deviating a bit from the LEO mission. Case 2 recovering only the engine seems for once to be the cheapest option. Followed by the other two cases which are fairly aligned. Case 3 is slightly cheaper when reusing less than 35 times, and after that, case 1 is slightly cheaper but never more than 2 M€ or 2.5% of the expendable launcher cost. The Reuse-Index, Figure 6.39, has a similar shape as the cost per flight. What is interesting here is that cases 1 and 3 are close to the expendable case close to 100 reuses.

For the final mission case 2 is the cheapest option the trajectory of the case can be seen in Figure 6.40 and Figure 6.41. The altitude in Figure 6.40 shows some interesting behaviour where the second stage ascends in two bounds. What can also be seen is that the final part of the descent from 12 km takes about 500 s. This is due to the fact that the parachute is deployed relatively soon. The range of the engine at touchdown is 1166 km due east from the launch site.

For the acceleration in Figure 6.42 the maximum deceleration occurs during re-entry of the engine section. With the maximum deceleration of the engine during parachute deployment at 6 g, which is the same as the maximum acceleration during the ascent. For the dynamic pressure, Figure 6.43, the maximum dynamic pressure during ascent is half of the limit set. The maximum dynamic pressure during descent is around during re-entry and it is lower than the dynamic pressure during the ascent.

Sensitivity Analysis

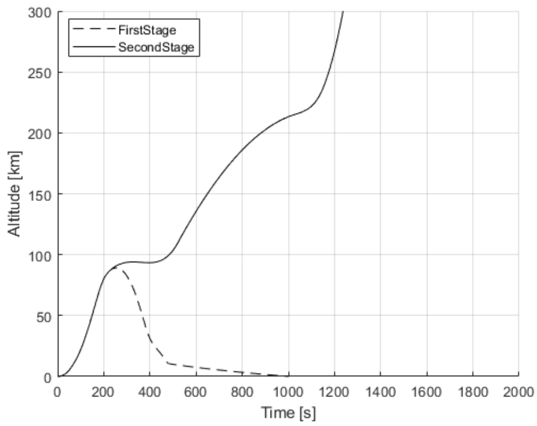

Figure 6.40: The altitude over time for the first and second stages for Case 2

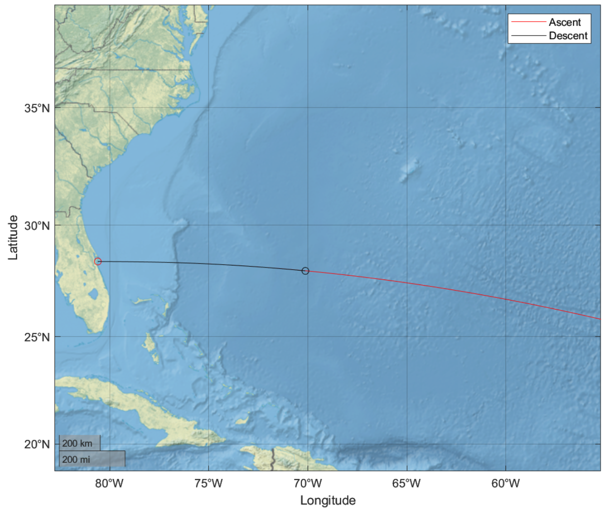

Figure 6.41: Ground track for Case 2

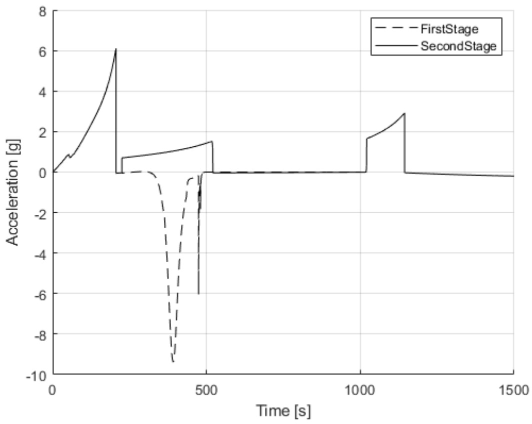

Figure 6.42: The acceleration over time for the first and second stages for Case 2

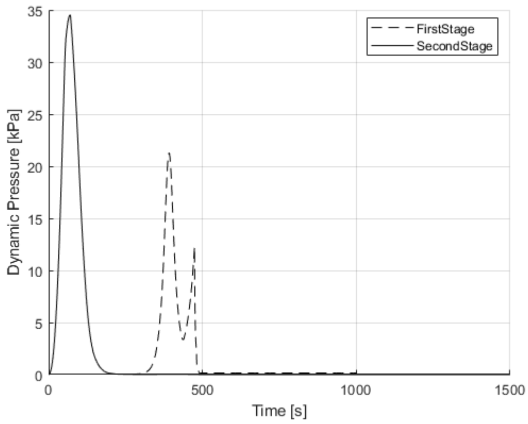

Figure 6.43: The dynamic pressure over time for the first and second stages for Case 2

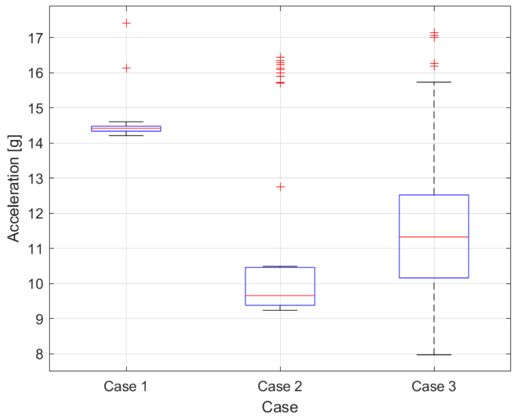

Figure 6.44: Sensitivity of the maximum deceleration during the descent for the Delta IV+ GTO mission

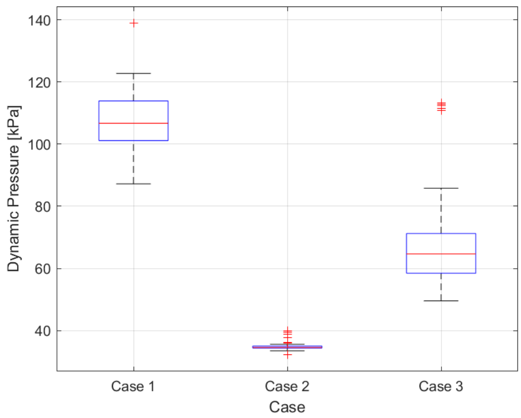

Figure 6.45: Sensitivity of the maximum deceleration during the descent for the Delta IV+ GTO mission

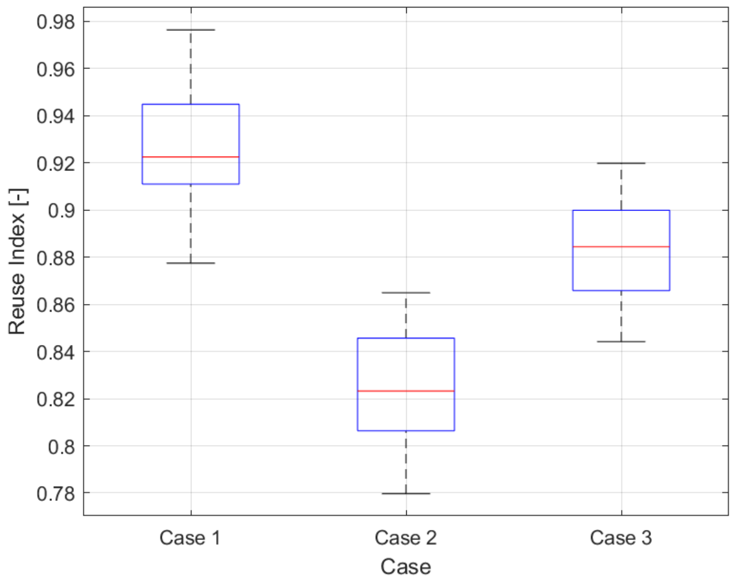

Figure 6.46: Sensitivity of the Reuse-index for the Delta IV+ GTO mission for ten reuses

The sensitivity of the GTO mission provides some interesting results. The dynamic pressure Figure 6.45 has a very narrow range for case 2 whereas the other two cases have a dynamic pressure range of 40 kPa, and case 3 even has some outliers towards with a maximum of 125 kPa.
However, the acceleration, which can be seen in Figure 6.44 is the main limit once again. Although the limits for both the non-propulsive cases (cases 2 and 3) had their maximum deceleration below 10 g, in the sensitivity analysis, the median for both cases are above 10 g. With the sensitivity of case 2 being significant ranging from 9 to 16.5 g and case 3 having a slightly smaller range but it does have some outliers between 16.5 and 17 g. This shows that for the GTO mission the non-propulsive, passive, cases are more sensitive to changes than the propulsive, active, case which even though it has a median at 14.5 g. has a range of less than 1 g.

The sensitivity of the Reuse-Index can be found in Figure 6.46. Here is can be seen that case 1 nearly has a range which goes over an RI of 1, so more expensive than the expendable case. All the other cases produce no interesting results when comparing it to Figure 6.39.

From the sensitivity, it is clear that although for the GTO mission, the non-propulsive manner of recovering the first stage is the cheaper solution. They, as case 1, are sensitive to going over the 10 g deceleration limit. This shows that although it is certainly possible to reuse the first stage for a GTO mission and save approximately 20% of the cost, it is susceptible to cross the 10 g deceleration limit.

6.3.4. Conclusion

For the Delta IV+, the results for the LEO and GTO missions are, as for the Falcon 9, relatively the same. Case 2, which is recovering only the engine, is the cheapest options. Case 2 has for both missions an RI of about 0.8 where the complete stage is around 0.9. The main reason for the engine only options becoming the cheapest is not that the engine only option is getting cheaper as compared to Falcon 9, it does, but this is not the main reason. The main reason that the engine only case is the cheapest is because the others are getting more expensive. This is because boosters are needed for complete stage recovery. Furthermore, because the engine is slightly heavier and therefore also more expensive engine recovery becomes more interesting commercially speaking. Again as was seen for the Falcon 9 when comparing the Reuse-Index for the maximum expendable payload mass, it can be seen that the reusable cases are more expensive than the expendable case.

The best landing method is airbags for non-propulsive. Where for the Falcon 9 launcher the reasons could that the landing distance was not far enough to make a significant distance. Here it could be because the amount of launches performed by ULA yearly is much lower than for SpaceX, 3 versus 11 respectively. This means the more expensive helicopter base cost is not outweighed by the saving on the personal cost for recovery.

As to the deceleration system, the HIAD and Ringsail combination seems to be the favourite again. With a HIAD of about 50-100 m^2 and a Ringsail parachute with an area of 7000-9000 m^2. Interesting is that for the GTO mission propulsive landing is not a viable option anymore. This option is not able to reduce the deceleration to below the limit of 10 g.

The sensitivity for the Delta IV+ has, at least for the deceleration, a larger range than the Falcon 9 case. For most of the cases, the deceleration limit is crossed, and the medians are higher than 10 g. This in part, due to the additions of boosters, and in part because for the Delta IV+ the ascent trajectory makes more of a difference than for the Falcon 9. This is because for the Falcon 9, the separation occurred relatively quickly and the second stage performed most of the work of getting the payload into orbit. However, for the Delta IV+, it is the other way around.

Again comparing this to real-life cases. Both the Vulcan and Ariane 6, which are primarily designed as an expendable launcher with reusability as a secondary objective, both use engine only recovery although in two different forms. The result of HIAD and Ringsail is very close to the HIAD and parafoil options chosen for the Vulcan launcher. A parafoil in rough terms being nothing more than a steerable subsonic parachute, where a Ringsail parachute is a non-steerable subsonic parachute.

6.4. Overall Comparison

Now that both vehicles have been discussed a final comparison can be made between the best solutions for all vehicles and missions. Also some overall comparisons will be made between the different vehicles and missions. To start with in Table 6.24 the best solution from all optimisation are given. Here it can be seen that there is a clear favourite solution this is the HIAD and Ringsail parachute which is used for three of the four missions.

The sizes of the HIAD and the Ringsail are also relatively comparable with the HIAD between 20-60 m^2 and the Ringsail parachute between 6700 and 8400 m^2. The deployment altitude for the parachute varies a little for the Delta IV LEO case but all are in the lower parts of the atmosphere. The Delta IV+ GTO case is deviating from the rest where only one deceleration system is used, a Hemisflo ribbon parachute. This parachute also deploys earlier than the Ringsail parachutes at 11.8 km.

For these cases also some key parameters from their trajectory is given in Table 6.25. Here various parameters from the descent can be found among which are the maximum deceleration, velocity at re-entry interface and down-range distance at landing. What can be seen is that the re-entry velocities for the Delta IV+ cases are almost twice as high as for the Falcon 9 cases. Also the re-entry altitude, which is defined by the altitude where the dynamic pressure reaches 1 kPa, is higher for the Delta IV+ than for the Falcon 9. This is due to the

Table 6.24: The best optimised solutions for the different missions

Optimisation Parameter		Falcon 9 LEO	Falcon 9 GTO	Delta IV+ LEO	Delta IV+ GTO
Engine Separation		No	No	Yes	Yes
1^{st} stage propellant mass [kg]		366097	338452	195077	181882
2^{nd} stage propellant mass [kg]		100544	94525	16485	20203
Landing System		Airbags			
Deceleration System 1	Type	HIAD	HIAD	HIAD	none
	Area [m^2]	62	35	20	NA
	Deployment Altitude [km]	NA	NA	NA	NA
Deceleration System 2	Type	Ringsail Parachute	Ringsail Parachute	Ringsail Parachute	Hemisflo Parachute
	Area [m^2]	6692	8384	6869	2054
	Deployment Altitude [km]	4.3	4.0	1.1	11.8

higher velocities that are achieved by the first stage.
What is the same for all cases is that the deceleration is the leading constraint for all cases. The dynamic

Table 6.25: Overview of the parameters during the descent for the best options for the different missions

Parameter	Falcon 9 LEO	Falcon 9 GTO	Delta IV+ LEO	Dela IV+ GTO
Maximum Deceleration [g]	9.7	6.4	10.0	9.4
Maximum Dynamic Pressure [kPa]	32	58	28	35
Maximum Temperature [K]	294	371	339	334
Re-entry Altitude [km]	58	62	67	66
Velocity at Re-Entry [m/s]	2356	3076	4331	4224
Separation Velocity [m/s]	2383	3157	4363	4274
Landing Distance [km]	754	719	1109	1156

pressure is relatively constant for the cases that use a HIAD. However for non of the optimal solutions was the dynamic pressure near the limit of 200 kPa. For the temperature the same holds as the limit was set at 500 K no temperature was encountered that was higher than 371 K (98C).

As for the cost comparison it is difficult to do a direct comparison as they are different vehicle with different costs associated with them. However, the Reuse-Index is a normalised function which can be compared for any vehicle. This can be seen in Figure 6.47.

Again as for the cases themselves two groups are formed. First is the group below the expendable line this is comparing the cost per flight for the same payload mass as was flown in the reusable case. The other group is the group compared to the maximum expendable payload. The results are interesting as when comparing the same payload mass recovering the complete stage as is done for the Falcon 9 save more than the engine only recovery of the Delta IV+. This is difficult to see but the two lines are are actually four lines in two groups of two which are very close together. What is interesting is when comparing the RI using the maximum expendable payload all the lines fall within the same region. Although all are above a RI of 1, meaning that they are more expensive than the expendable launcher, they are surprisingly close together with the Delta IV+ LEO case being the cheapest and the Falcon 9 GTO case being the most expensive. The slightly different gradients in the RI curves between the Delta IV+ and the Falcon 9 are due to the different initial production numbers. Where the Falcon 9 had 87 previously produced launcher the Delta IV+ only had 40. On top of that the number of launches per year are also different, with 10 launches per year for the Falcon 9 and 3 for the Delta IV+. This leads to the expendable launcher for the Delta IV+ become cheaper faster than the Falcon 9 because of the stronger learning curve effects with the reduced production numbers. An overview of the initial production cost of the best options for all the missions can be found in Table 6.26.

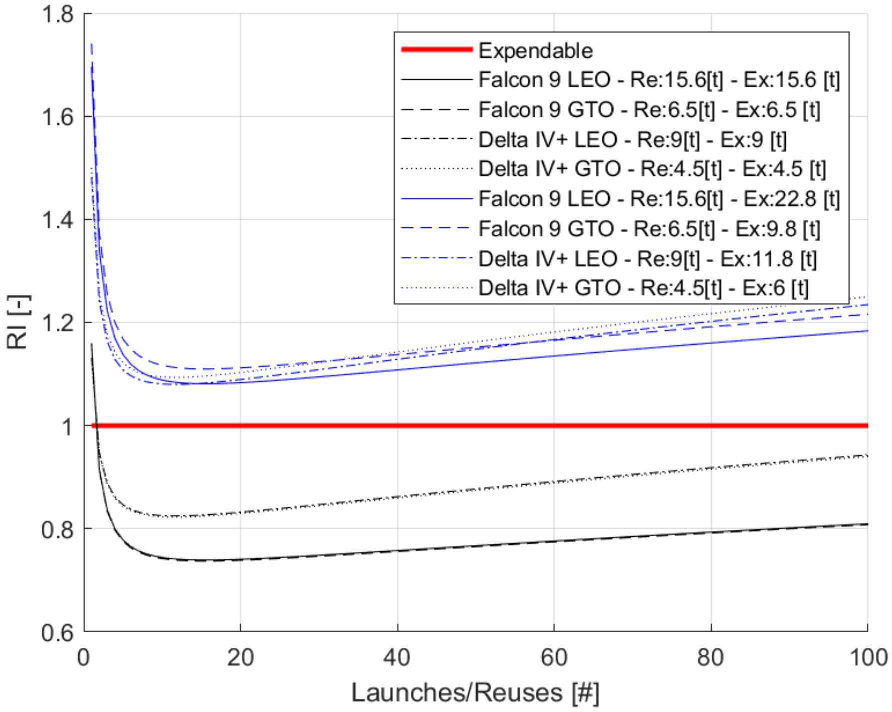

Figure 6.47: Reuse-Index for the different missions

What can be seen in Table 6.26 is that the even if for all the cases the entire stage is recovered this is in

Table 6.26: Initial production cost breakdown for the cheapest reusable launcher options

Part	**Falcon 9 LEO**		**Falcon 9 GTO**		**Delta IV+ LEO**		**Delta IV+ GTO**	
	[M€]	[%]	[M€]	[%]	[M€]	[%]	[M€]	[%]
1st stage tank	11.6	29.7	11.6	30.0	20.9	31.0	20.9	31.1
1st stage engine	5.9	15.1	5.9	15.2	11.8	17.5	11.8	17.6
1st stage additional reusability cost	0.2	0.51	0.2	0.52	0.1	0.14	0.1	0.14
2nd stage tank	5.6	14.3	5.6	14.5	6.2	9.2	6.2	9.2
2nd stage enigne	1.3	3.3	1.3	3.4	3.6	5.3	3.6	5.3
AIT Cost	14.5	37.1	14.1	36.4	24.8	36.8	24.6	36.6

all cases not even 50% of the initial production cost. This is mostly due to the assembly cost, which are in all cases more than 35% of the cost. It might be that some of the AIT costs are not needed when reusing part of the launcher. Although most of the assembly integration and test (AIT) costs are still expected to be needed.

When comparing the LEO missions against the GTO missions no significant difference can be found for one vehicle although the Falcon 9 GTO case has a little bit less propellant than it needs compared to its LEO counterpart. This leads to the conclusion that 6500 kg is not the maximum GTO payload capability for down-range landing for the Falcon 9. This could be the case as the maximum proven payload mass was used and not the maximum payload mass as this is not known for the reusable case. Overall there are almost no differences between the two in costs or the size of the system needed for either a LEO or GTO mission. However less payload is carried into orbit for the GTO missions than for the LEO mission naturally.

7

Conclusion & Recommendations

7.1. Conclusion

During this research two vehicles were optimised to be reusable for two missions. For each combination of vehicle and mission three cases were investigated for their cost and their trajectory. However, the initial question was:

Is it feasible to reduce the launch cost with 30% by recovering the first stage of a launcher, given a launch rate of 10 launches per year?

Reusing the first stage of a launcher is a significant part of making the cost of getting to space cheaper since most of the cost of the launch is spent on the first stage. When looking at reusing the first stage, it is certainly possible to decrease a significant portion of the cost per flight. However, this is dependent on the type of launcher that is being used and what payload mass is used. Nevertheless, on the total cost savings of 20-25% can be achieved. The Falcon 9 cases which were seen in section 6.2 came close to the 30% target set for the main research question but were still below the 30%.
The value of 30% came from Ariane's project for engine only recovery. This seems unfeasible based on the results in this research because non of the engine only recovery cases came below the 20% cost saving. This is mostly due to the production of the tank that has to be done for every reuse. If engine only reusability, or complete stage reusability, is better depends on the type of launcher. For first stages with high separation velocity like for the Delta IV+ case engine only becomes cheaper. However, when the separation velocity is lower, the complete stage is cheaper. This result seems independent of the two orbits used in this research. It should be noted however that this could be due to that the perigees of both orbits are relatively similar, 290 km and 218 km for the LEO and GTO orbits respectively.

For the best method of decelerating the system this is the HIAD/Ringsail combination. This uses the HIAD to help to deal with any re-entry heat and helps to manage the deceleration that occurs during re-entry. However, mostly the HIAD is used to lower the maximum deceleration during the return flight. The reason the deceleration is lower is that it is deployed before the re-entry occurs. Therefore it can already decelerate the system slightly; therefore, instead of a sharp peak, the deceleration is spread more along the trajectory. The decreasing of the deceleration seems to be critical, though since this is the primary constraint for the cases. The dynamic pressure only becomes of interest for thin launchers compared to their weight, as was seen when comparing the Delta IV+ and Falcon 9. That even though Falcon 9 had much lower re-entry velocities and about the same mass as the Delta IV+, the Delta IV+ has lower dynamic pressures during re-entry because the reference area for the drag was larger thereby as for the HIAD spreading the deceleration curve over a larger range.
The extra mass that is needed for decelerating a system to land safely is on average; over all the cases, 15%. This is, however, is split up into two parts. The propulsive landing requires, on average, 30% of the landing mass in extra propellant to land. The non-propulsive cases need, on average, 6% of the landing mass. This shows that propulsive landing needs at least twice the mass to decelerate the system and where for non-propulsive cases this only comes at the cost of increasing the empty mass of the ΔV equation. For the

propulsive case it not only increases the inert mass but also the amount of propellant that can be used for the ascent, so this will decrease the ΔV of the propulsive system. Although this was not examined in this research, this probably means that the payload loss, the loss of payload compared to the expendable launcher should be higher for the propulsive landing than for non-propulsive options.

As for the effect of the number of reuses, the results are fascinating. What is found during the research is that the maximum saving occurs between 8-15 reuses. After this, the savings decrease again for a couple of reasons. First, the decrease in production cost for the expendable case due to the learning curve, as well as the increasing refurbishment cost for the reusable launcher. The two cause that the cost per flight of the reusable case flattens out. However, expendable launcher becomes increasingly cheaper. This would mean that reusing the launcher 100 times, as SpaceX plans, seems not cost-effective using the models in this research.

These conclusions are drawn based on the solutions, trajectories and costs given by the FRT tool. This tool is, of course, not perfect the most significant uncertainty are the costs associated with the deceleration and landing systems for which it was difficult to obtain data. However, even when varying these by 50% all results were cheaper than the expendable. The calculations were done without any wind or atmospheric effects other than the standard drag. This could be an issue when the wind is introduced. When deploying a parachute at higher altitudes, this could cause a significant drift causing extra costs.
The Surrogate optimisation showed a significant improvement in computation time. It reduced the computation time by at least 80% if not more. This made it possible to be more flexible in the ascent trajectory calculation, although this still takes up a significant portion of the computation time for each iteration. Although the surrogate optimisation algorithm gives a significant performance boost, it should be noted that it does introduce an additional uncertainty of 0.5% on the final objective function value. This is the error that was found when comparing the surrogate optimisation with the genetic algorithm.
On the whole significant savings could be achieved, even though the 30% savings could not be achieved 20-25% is still significant based on the fact that the launch cost is in the tens of millions of euros meaning that for the Falcon 9, 8 M€ is saved and for the Delta IV 12 M€. However, when comparing the cost per kilogram of payload, the expendable launcher this same saving could not be achieved. The expendable launcher was cheaper compared to most of the cases because of the chosen payload mass.

7.2. Recommendations

What was found during the ascent optimisation is that the maximum dynamic pressure during ascent is not equal for all launchers, or at least not for the two investigated in this research. The fix here was to set them individually at different values based on sources. However, a better way would be to include them in the main optimisation loop. This could not be achieved due to time constraints. A reason to include it in the main optimisation is not only to manage it more dynamically for the ascent and not be ultimately dependent on sources for this. Another reason is that the maximum dynamic pressure during ascent controls (in)directly the drag losses from the launcher. This control could be used to slow down a launcher at separation without adding more inert mass or removing propellant mass which is beneficial for reusing first stages.

Besides putting the dynamic pressure limit in the main optimisation loop, the ascent optimisation itself could also be put in this loop. This solves the issue of the two loops required first to find the cheapest vehicle and then looking for the best ascent trajectory that leads to the smallest landing distance. The separation between the two was done for the benefit of speed but can, in some cases, lead to slightly different results. However, this is not a simple point to achieve in practice since it seems unlikely that this could be done within MATLAB within a similar computation time-frame as is performed currently.
Finally, the last parameter that could be added to the main optimisation loop is the payload mass itself. However, this is only of interest when looking at the reuse index. In this research, a fixed value was used for all reusable options, but this does not have to be the case. When adding different masses when, for example, comparing engine only and complete stage reusability, the corresponding payload mass does not have to be the same. Again this can only be done when comparing based on the Reuse index, or cost per kilogram payload. This could probably increase the attractiveness of the engine only recovery since there the loss of payload mass should be less than when recovering the complete stage.

Aside from the main optimisation loop, in FRT it is assumed that the structure can take the loads, this, especially for the parachute, does not have to be the case as these introduce a significant load in a small area. Therefore looking into a model to increase the stage mass based on the loads would improve the accuracy of the tool when comparing to real-life cases. The same goes for introducing a wind model in order to incorporate the drift of the stage under a parachute.

Currently, FRT only uses an existing launcher to create a reusable version. However, the change could be made to create an entirely new launcher using the tool. For this, a couple of changes are to be made. First is the conversion of the tank extension model to a tank mass model. This could be combined with the work from Pietrobon. On top of that, a mass model for the engine is needed as this is currently lacking. The thrust model does not need to change, as this is already capable of being used for a design tool. Besides the models, data is needed on the geometry of a launcher in order to produce a realistic design. As very long but slender launcher might be good from a drag point of view but not realistic as if might not be able to handle the required loads. The biggest challenge to make the tool usable for the design of an entire launcher is the drag coefficient. This is currently obtained from a different program RASAero II which is then used as an input. This cannot be done if designing a launcher as changing geometries mean different drag coefficient curves.
What was seen in the sensitivity of the costs is that the refurbishment costs are still a point of interest. For this study, a refurbishment scheme on a conceptual level was used. This model had nothing to do with the complexity of the system and the level of engineering required to get it back into operation. It was a model based on the cost of production with nothing more than a percentage of this being used as the refurbishment cost.

What was seen in the overall costs is that the assembly, integration and test costs are the biggest cost post that is not recovered. If this number could be driven down the reusable case would become even cheaper. This could even drive the cost for the reusable launcher so far down that it would even be cheaper per kilogram payload than the expendable launcher when comparing the maximum payloads. As for the systems, additional research in a HIAD system for earth application is recommended. This proved to be the main decelerator for high altitude deceleration, and smooth entry into the atmosphere. NASA is performing significant research on HIADs for their Mars missions. However, specific research for earth applications might be needed as the atmosphere has a different composition, which could lead to different material requirements due to the heating constraints. This, in turn, could lead to different mass models being needed.

Bibliography

[1] Spaceflight 101. Delta ii 7920h-10, August 2020. URL https://web.archive.org/web/20140714122955/http://www.spaceflight101.com/delta-ii-7920h-10.html. date published: 2011-10-25.

[2] A.G. Ajayakumar, G.P. Vipin, and Sarathchandradas. Structural design and mass optimisation of grid fin for launch vehicles. *International Research Journal of Engineering and Technology*, 5:43–58, 2018.

[3] United Launch Alliance. *Delta IV Launch Services User's Guide*, June 2013.

[4] United Launch Alliance. Atlas v breakdown, October 2017. URL https://twitter.com/torybruno/status/561933155951595520. date published: 2015-02-15.

[5] United Launch Alliance. Delta iv: The 21st century launch solution, April 2017. URL http://www.ulalaunch.com/products_deltaiv.aspx. date published: 2017-04-22.

[6] Jonathan Amos. Airbus unveils 'adeline' re-usable rocket concept, October 2017. URL http://www.bbc.com/news/science-environment-33006056. date published: 2015-06-05.

[7] Astronautix. F-1, May 2020. URL http://www.astronautix.com/f/f-1.html. date published: 2020-05-27.

[8] Astronautix. J-2, September 2020. URL http://astronautix.com/j/j-2.html. date published: 2019.

[9] Astronautix. Kistler k-1, September 2020. URL http://www.astronautix.com/k/kistlerk-1.html. date published: 2019.

[10] Astronautix. Lox/lh2, September 2020. URL http://astronautix.com/l/loxlh2.html. date published: 2019.

[11] Astronautix. Lox/kerosene, September 2020. URL http://www.astronautix.com/l/loxkerosene.html. date published: 2019.

[12] Astronautix. Merlin 1d, May 2020. URL http://www.astronautix.com/m/merlin1d.html. date published: 2020-05-27.

[13] Astronautix. N2o4/udmh, September 2020. URL http://www.astronautix.com/n/n2o4udmh.html. date published: 2020.

[14] Astronautix. Rd-180, May 2020. URL http://www.astronautix.com/r/rd-180.html. date published: 2020-05-27.

[15] Astronautix. Rd-253-11d48, May 2020. URL http://www.astronautix.com/r/rd-253-11d48.html. date published: 2020-05-27.

[16] Astronautix. Viking 5c, May 2020. URL http://www.astronautix.com/v/viking5c.html. date published: 2020-05-27.

[17] Astronautix. Vulcain 2, May 2020. URL http://www.astronautix.com/v/vulcain2.html. date published: 2020-05-27.

[18] Astronautix.com. Centaur iiib, June 2020. URL http://www.astronautix.com/c/centauriiib.html.

[19] Astronautix.com. Centaur ii, June 2020. URL http://www.astronautix.com/c/centaurii.html.

[20] Alliant Techsystems Inc. (ATK). Atk space propulsion products catalog, June 2020. URL https://forum.nasaspaceflight.com/index.php?action=dlattach;topic=31042.0;attach=494063;sess=0. date published: 2008-05-14.

[21] Kim Bhasin. Elon musk: 'if we published patents, it would be farcical', April 2017. URL http://www.businessinsider.com/elon-musk-patents-2012-11?international=true&r=US&IR=T. date published: 2012-11-09.

[22] David M Bose, Richard Winski, Jeremy Shidner, Carlie Zumwalt, Christopher O Johnston, DR Komar, FM Cheatwood, and Stephen J Hughes. The hypersonic inflatable aerodynamic decelerator (hiad) mission applications study. In *AIAA Aerodynamic Decelerator Systems Technology Conference and Seminar, Daytona Beach, FL*, 2013.

[23] R.E. Brackeen. Space shuttle solid rocket booster recovery system definition. Technical Report NASA-CR-120106, NASA, 1973.

[24] Aaron M Brandis and Christopher O Johnston. Characterization of stagnation-point heat flux for earth entry. In *45th AIAA Plasmadynamics and Lasers Conference*, page 2374, 2014.

[25] Arthur E. Bryson. Determination of lift or drag programs to minimize re-entry heating. *Journal of the Aerospace Sciences*, 29(4):420–430, 1962.

[26] Rib Parts BUdding. Neoprene fabric for inflatable boats manufacturing and repairing, July 2020. URL https://www.rib-parts-budding.nl/a-40164480-,3288483/stootstrippen-neoprene-en-pvc/hypalon-neopreen-doek-voor-het-maken-of-herstellen-van-opblaa #description. date published: 2020.

[27] BuyAerogel.com. Pyrogel® xt blanket cut-to-size (5-mm thickness), July 2020. URL http://www.buyaerogel.com/product/pyrogel-5-mm-cut-to-size/. date published: 2020.

[28] D.R. Chapman. An approximate analytical method for studying entry into planeraty atmospheres. Technical Report NACA TN-4276, Ames Aeronautical Lab., Moffett Field, Calif., 1958.

[29] Ian G Clark, Allison L Hutchings, Christopher L Tanner, and Robert D Braun. Supersonic inflatable aerodynamic decelerators for use on future robotic missions to mars. *Journal of Spacecraft and Rockets*, 46(2):340–352, 2009.

[30] CS Hyde Company. Kapton® (polyimide) film - type hn, July 2020. URL https://catalog.cshyde.com/viewitems/films/kapton-polyimide-film-type-hn. date published: 2020.

[31] S Constant. Design and optimization of a small reusable launch vehicle using vertical landing techniques. Masters thesis, TU Delft, 2019.

[32] Rob Coppinger. Airbus' adeline project aims to build reusable rockets and space tugs, October 2017. URL https://www.space.com/29620-airbus-adeline-reusable-rocket-space-tug.html?adbid=10152877135861466&adbpl=fb&adbpr=17610706465. date published: 2015-06-10.

[33] P. B. de Selding. Meet adeline airbus answer to spacex reusability, October 2017. URL http://spacenews.com/meet-adeline-airbus-response-to-reusable-spacex-rocket/. date published: 2015-06-05.

[34] P.B. de Selding. Ula touts mid-air recovery as more cost-effective than spacex's reusability plan, January 2018. URL http://spacenews.com/ula-touts-mid-air-recovery-as-more-cost-effective-than-spacexs-reusability-plan/. date published: 2015-09-30.

[35] Phillip Delurgio. Evolution of the ringsail parachute. In *15th Aerodynamic Decelerator Systems Technology Conference*, page 1700, 1999.

[36] 3M Advanced Materials Division. 3m nextel ceramic fibers and textiles technical reference guide, July 2020. URL https://multimedia.3m.com/mws/media/1327055O/3m-nextel-technical-reference-guide.pdf. date published: 2018.

[37] Hughes Aircraft Company Space Systems Division. Surveyor spacecraft a-21a model description. Technical report, Hughes Aircraft Company, 09 1964. Report was made for the Jet Propulsion Laboratory.

[38] N.T. Drente. Small orbital launch systems, a tentative initial cost estimate. Masters thesis, TU Delft, 2016.

[39] Etienne Dumont, Sven Stappert, Tobias Ecker, Jascha Wilken, Sebastian Karl, Sven Krummen, and Martin Sippel. Evaluation of future ariane reusable vtol booster stages. In *68th International Astronautical Congress (IAC), Adelaide, Australia*, pages 25–29, 2017.

[40] Astrium EADS. Hm-7 and hm-7b rocket engine - thrust chamber, September 2020. URL `https://web.archive.org/web/20120508062948/http://cs.astrium.eads.net/sp/launcher-propulsion/rocket-engines/hm7b-rocket-engine.html`. date published: 2012-05-08.

[41] FAA. Returning from space: Re-entry, Decemeber 2018. URL `https://www.faa.gov/about/office_org/headquarters_offices/avs/offices/aam/cami/library/online_libraries/aerospace_medicine/tutorial/section3/spacecraft_design/`. date published: 2018-04-11.

[42] Edward Fallon, II, Anthony Taylor, and Robert Meyerson. Landing system design summary of the k-1 reusable launch vehicle. In *15th Aerodynamic Decelerator Systems Technology Conference*, page 1720, 1999.

[43] V Finchenko, K Pitchkhadze, A Ivankov, and N Voron. Inflatable re-entry and descent technology for manned martian mission. In *55th International Astronautical Congress of the International Astronautical Federation, the International Academy of Astronautics, and the International Institute of Space Law*, pages I–6, 2004.

[44] Reinald G Finke. Calculation of reentry-vehicle temperature history. Technical report, INSTITUTE FOR DEFENSE ANALYSES ALEXANDRIA VA, 1990.

[45] T. Haex. Dawn aerospace mk-iii, August 2020. URL `https://repository.tudelft.nl/islandora/object/uuid%3A1a3bcc22-4b92-41c1-ae21-55bf4de3d259`. date published: 2020-07-02.

[46] Todd Herrmann and David Akin. A critical parameter optimization of launch vehicle costs. In *Space 2005*, page 6680. American Institute of Aeronautics and Astronautics, 2005.

[47] Elizabeth Howell. Ariane 5 rocket lofts 2 satellites on milestone 100th launch, August 2020. URL `https://www.space.com/41936-ariane-5-rocket-aces-100th-launch.html`. date published: 2018-09-26.

[48] Mark C Ivanov, Eric M Blood, Brant T Cook, Louis R Giersch, Myron R Grover, Julie K Jakobowski, Tommaso P Rivellini, Robbie P Su, Jamshid A Samareh, Thomas A Zang, et al. Entry, descent and landing systems analysis study: Phase 2 report on mars science laboratory improvement. Technical report, Pasadena, CA: Jet Propulsion Laboratory, National Aeronautics and Space ..., 2011.

[49] John D. Anderson Jr. *Fundamentals of Aerodynamics, 5th Edition*. McGraw-Hill Science/Engineering/-Math, New York, 5th edition edition, 02 2010. ISBN 9780073398105.

[50] Chris D Karlgaard, Jake Tynis, and Clara O'Farrell. Reconstruction of the advanced supersonic parachute inflation research experiment sounding rocket flight test. In *2018 Atmospheric Flight Mechanics Conference*, page 3624, 2018.

[51] Jacob Kim. How much do the landing legs on spacex f9 rockets weigh?, September 2020. URL `https://www.quora.com/How-much-do-the-landing-legs-on-SpaceX-F9-rockets-weigh`. date published: 10-2017.

[52] T.W. Knacke. *Parachute Recovery Systems Design Manual*. Para Publishing, 1992.

[53] TW Knacke and LI DIMMICK. Design analysis of final recovery parachutes b-70 encapsulated seat and the usd-5 drone. Technical report, SPACE RECOVERY SYSTEMS INC EL SEGUNDO CA, 1962.

[54] Ltd. Kuraray Co. Vectran: Development of high-functionality fiber and its applications at kuraray co., ltd., July 2020. URL `http://hermes-ir.lib.hit-u.ac.jp/rs/bitstream/10086/26905/1/070iirWP14-06.pdf`. date published: 10-2014.

[55] Ed Kyle. 2019 space launch report, August 2020. URL `https://www.spacelaunchreport.com/log2019.html`. date published: 2019-12-27.

[56] D. E. Kölle. The transcost-model for launch vehicle cost estimation and its application to future systems analysis. *Acta Astronautica*, 11, 1984.

[57] Dietrich E Kölle. *Handbook of Cost Engineering for Space Transportation Systems: Including TRANSCOST 8.2 Statistical-analytical Model for Cost Estimation and Economical Optimization of Launch Vehicles*. TransCostSystems, 2013.

[58] A.C. Lambers. Development of surrogate-based multidisciplinary optimization methodology with flutter constraints for aircraft conceptual design. Masters thesis, TU Delft, 2016.

[59] J Lingard. The effects of added mass on parachute inflation force coefficients. In *13th Aerodynamic Decelerator Systems Technology Conference*, page 1561, 1995.

[60] J S Lingard, Arrun Saunders, John C Underwood, Steven Rogers, James Merrifield, and Luca Ferracina. Supersonic parachute testing using a maxus sounding rocket piggy-back payload. In *24th AIAA Aerodynamic Decelerator Systems Technology Conference*, page 3724, 2017.

[61] Isidoro Martínez. Vapour pressure for liquid-vapour equilibrium, September 2020. URL `http://webserver.dmt.upm.es/~isidoro/dat1/ePv.pdf`. date published: 2020.

[62] Mathworks. ode113, October 2020. URL `https://www.mathworks.com/help/matlab/ref/ode113.html`. date published: 10-2020.

[63] Mathworks. ode15s, October 2020. URL `https://www.mathworks.com/help/matlab/ref/ode15s.html`. date published: 10-2020.

[64] Mathworks. ode45, October 2020. URL `https://www.mathworks.com/help/matlab/ref/ode45.html`. date published: 10-2020.

[65] Mathworks. surrogateopt, October 2020. URL `https://www.mathworks.com/help/gads/surrogateopt.html`. date published: 10-2020.

[66] Mathworks. Surrogate optimization algorithm, June 2020. URL `https://nl.mathworks.com/help/gads/surrogate-optimization-algorithm.html`. date published: 2020-06-03.

[67] MatWeb. Aluminum 7075-t6; 7075-t651, September 2020. URL `http://www.matweb.com/search/DataSheet.aspx?MatGUID=4f19a42be94546b686bbf43f79c51b7d&ckck=1`. date published: 09-2020.

[68] F. Miranda. Design optimization of ground and air-launched hybrid rockets. Masters thesis, TU Delft, 2015.

[69] J.A. Mulder, W.H.J.J. van Staveren, J.C. van der Vaart, E. de Weerdt, C.C. de Visser, A.C. in 't Veldt, and E. Mooij. *Lecture Notes AE3202- Flight Dynamics*. Delft University of Technology, 2013.

[70] Suman Muppidi, Clara O'Farrell, Christopher Tanner, John W Van Norman, and Ian G Clark. Modeling and flight performance of supersonic disk-gap-band parachutes in slender body wakes. In *2018 Atmospheric Flight Mechanics Conference*, page 3623, 2018.

[71] Declan Murphy. Flight club, September 2020. URL `https://flightclub.io/result/telemetry?id=1064d9c3-6d80-4173-9f5b-6b115ae03d33`. date published: 09-2020.

[72] Elon Musk. Tweet from elon musk, August 2020. URL `https://twitter.com/elonmusk/status/726216836069515264`. date published: 2016-04-30.

[73] NASA. Earth fact sheet, September 2020. URL https://nssdc.gsfc.nasa.gov/planetary/factsheet/earthfact.html. date published: 04-2020.

[74] United States Government Accountability Office. Surplus missile motors: Sale price drives potential effects on dod and commercial launch providers, August 2020. URL https://www.gao.gov/assets/690/687571.pdf. date published: 2017-08-16.

[75] Blue Origin. New glenn, February 2018. URL https://www.blueorigin.com/new-glenn. date published: 2018-02-14.

[76] Karl S Orthner. Aerodynamic analysis of lattice grid fins in transonic flow. Technical report, AIR FORCE INSTITUTE OF TECHNOLOGY, 2004.

[77] L Pepermans. Development of a multidisciplinary design optimisation tool to determine the feasibility of upper stage reusability. Masters thesis, TU Delft, 2019.

[78] L. Pepermans, M. Rozemeijer, R. Gurumoorthy, E. Menting, N. Suard, S. Khurana, T. Britting, and M. Serman. Flight simulations of the stratos iii parachute recovery system. In *69th International Astronautical Congress*, 2018.

[79] L. Pepermans, E. Menting, M. Rozemeijer, T. Britting, and P.J. Derks. Trajectory simulations and sensitivity for the spear parachute test vehicle. In *70th International Astronautical Congress*, 2019.

[80] Lars Pepermans, Mark Rozemeijer, Esmée Menting, Noah Suard, and Sayyam Khurana. Systematic design of a parachute recovery system for the stratos iii student built sounding rocket. In *2018 Atmospheric Flight Mechanics Conference*, page 3626, 2018.

[81] Steven S Pietrobon. Analysis of propellant tank masses. *Submitted to Review of US Human Space Flight Plans Committee*, 6, 2009.

[82] NASA Commercial Crew Program. Starliner performs well in airbag testing, March 2019. URL https://blogs.nasa.gov/commercialcrew/2016/02/17/starliner-performs-well-in-airbag-testing/. date published: 2016-02-17.

[83] M.M. Ragab, F. McNeil Cheatwood, S.J. Hughes, and A. Lowry. Launch vehicle recovery and reuse. In *AIAA Space 2015 Conference & Exposition*, 2015.

[84] Eric Ralph. Spacex hits new falcon 9 reusability milestone, retracts all four landing legs, September 2020. URL https://www.teslarati.com/spacex-starts-falcon-9-landing-leg-retraction/#:~:text=Put%20simply%2C%20after%20rapidly%20deploying,ft)%20from%20hinge%20to%20tip. date published: 05-2019.

[85] Space Launch report. Space launch report: Delta iii data sheet, June 2020. URL https://www.spacelaunchreport.com/delta3.html. date published: 2010-09-05.

[86] Space Launch report. Space launch report: Delta iv data sheet, June 2020. URL http://www.spacelaunchreport.com/delta4.html. date published: 2019-08-22.

[87] Space Launch Report. Space launch report: Falcon 9 v1.2 data sheet, June 2020. URL http://www.spacelaunchreport.com/falcon9ft.html. date published: 2020-06-13.

[88] Space Launch Report. Space launch report: Chang zheng data sheet, June 2020. URL https://www.spacelaunchreport.com/cz.html. date published: 2020-06-23.

[89] Aerojet Rocketdyne. Rl10 engine, September 2020. URL https://www.rocket.com/space/liquid-engines/rl10-engine. date published: 2020-09-25.

[90] Aerojet Rocketdyne. Rs-28 engine, May 2020. URL https://www.rocket.com/space/liquid-engines/rs-25-engine. date published: 2020-05-27.

[91] Aerojet Rocketdyne. Rs-68 engine, May 2020. URL https://www.rocket.com/space/liquid-engines/rs-68a. date published: 2020-05-27.

[92] Charles E. Rogers and David Cooper. Ras aero, September 2020. URL http://www.rasaero.com/. date published: 2008.

[93] William F. Rogers. Apollo experience report - lunar module landing gear subsystem. Technical report, NASA, 07 1972.

[94] Reinhard Roll, Lars Witte, and Walter Arnold. Rosetta lander philae–soil strength analysis. *Icarus*, 280: 359–365, 2016.

[95] M D Rozemeijer. First stage recovery, a literature study for the concepts of first stage recovery. literature study, TU Delft, 2018. not published.

[96] Jamshid Samareh and D Komar. Parametric mass modeling for mars entry, descent and landing system analysis study. In *49th AIAA Aerospace Sciences Meeting including the New Horizons Forum and Aerospace Exposition*, page 1038, 2011.

[97] Jamshid A Samareh. Estimating mass of inflatable aerodynamic decelerators using dimensionless parameters. In *8th International Planetary Probe Workshop 2011 (IPPW-8)*, 2011.

[98] Martin Sippel, Sven Stappert, Leonid Bussler, and Etienne Dumont. Systematic assessment of reusable first-stage return options. In *68th International Astronautical Congress, IAC-17-D2*, volume 4, 2017.

[99] M Snijders. Cost effectiveness of the first stage recovery of a small satellite launcher. Masters thesis, TU Delft, 2017.

[100] SpaceX. Reusability: The key to making human life multi-planetary, March 2017. URL http://www.spacex.com/news/2013/03/31/reusability-key-making-human-life-multi-planetary. date published: 2014-06-10.

[101] SpaceX. Capabilities & services, April 2017. URL http://www.spacex.com/about/capabilities. date published: 2017-04-13.

[102] SpaceX. Falcon 9 user guide, May 2020. URL https://www.spacex.com/media/falcon_users_guide_042020.pdf. date published: 2020-05-04.

[103] Sven Stappert, Jascha Wilken, Leonid Bussler, and Martin Sippel. A systematic comparison of reusable first stage return options. In *8th European Conference for Aeronautics and Space Sciences (EUCASS)*, 2019.

[104] P.V. Tartabini, J.R. Beaty, R.A. Lepsch, and M.G. Gilbert. Payload performance analysis for a reusable two-stage-to-orbit vehicle. Technical Report NASA TM-2015-218760, NASA, 2015.

[105] Pascal Tatiossian, Jean Desmariaux, and Matthieu Garcia. Callisto project-reusable first stage rocket demonstrator. In *7th European Conference for Aeronautics and Space Sciences, Milano, Italy, DOI*, volume 10, 2017.

[106] Tesla. Model s, September 2020. URL https://www.tesla.com/nl_nl/models. date published: 09-2020.

[107] The Engineering Toolbox. Surface - radiation absorptivity, September 2020. URL https://www.engineeringtoolbox.com/radiation-surface-absorptivity-d_1805.html. date published: 2003.

[108] The Engineering Toolbox. Emissivity coefficients materials, September 2020. URL https://www.engineeringtoolbox.com/emissivity-coefficients-d_447.html. date published: 2011.

[109] Olga Trivailo, Martin Sippel, and Y Ahmet Şekercioğlu. Review of hardware cost estimation methods, models and tools applied to early phases of space mission planning. *Progress in Aerospace Sciences*, 53: 1–17, 2012.

[110] ULA. Rocketbuilder, August 2020. URL https://web.archive.org/web/20161203124622/https://www.rocketbuilder.com/start/configure. date published: 2016-12-03.

[111] ULA. Smart reuse, August 2020. URL https://spaceflightnow.com/wp-content/uploads/2015/04/NC3_SMARTReuse413201561546PM63.jpg. date published: 2020-08-17.

[112] M.W. van Kesteren. Air launch versus ground launch: a multidisciplinary design optimization study of expendable launch vehicles on cost and performance. Masters thesis, TU Delft, 2013.

[113] A. Vishnyak. Parachute simulations for ariane-5 booster recovery system design. *American Institute of Aeronautics and Astronautics*, 1995.

[114] D Webb and L Palm. Development of a nylon-kevlar recovery system for the cl-289/an/usd502/surveillance drone. In *7th Aerodynamic Decelerator and Balloon Technology Conference*, page 1952, 1981.

[115] NIST Chemistry Webbook. Hydrogen, September 2020. URL https://webbook.nist.gov/cgi/cbook.cgi?ID=C1333740&Units=SI&Mask=4&Type=ANTOINE&Plot=on#ANTOINE. date published: 2018.

[116] NIST Chemistry Webbook. Oxygen, September 2020. URL https://webbook.nist.gov/cgi/cbook.cgi?ID=C7782447&Units=SI&Mask=4#Thermo-Phase. date published: 2018.

[117] NIST Chemistry Webbook. Octane, September 2020. URL https://webbook.nist.gov/cgi/cbook.cgi?ID=C111659&Mask=4#Thermo-Phase. date published: 2018.

[118] NIST Chemistry Webbook. Hydrazine, 1,1-dimethyl-, September 2020. URL https://webbook.nist.gov/cgi/cbook.cgi?ID=C57147&Mask=4&Type=ANTOINE&Plot=on. date published: 2018.

[119] James R Wertz. Economic model of reusable vs. expendable launch vehicles. In *IAF, International Astronautical Congress, 51 st, Rio de Janeiro, Brazil*, 2000.

[120] James R. Wertz, David F. Everett, and Jeffery J. Puschell. *Space Mission Engineering: The New SMAD*. Microcosm Press, 1st edition, 2011.

[121] Wikipedia. Spacex merlin, May 2020. URL https://en.wikipedia.org/wiki/SpaceX_Merlin#Merlin_1D. date published: 2020-05-24.

[122] Wikipedia. surrogateopt, October 2020. URL https://en.wikipedia.org/wiki/Sikorsky_CH-53E_Super_Stallion#Specifications_(CH-53E). date published: 16-08-2020.

[123] Ding Yang, Yimin Sun, Danilo Di Stefano, Michela Turrin, and Sevil Sariyildiz. Impacts of problem scale and sampling strategy on surrogate model accuracy: An application of surrogate-based optimization in building design. In *2016 IEEE congress on evolutionary computation (CEC)*, pages 4199–4207. IEEE, 2016.

[124] B.T.C Zandbergen. *Thermal Rocket Propulsion*. Delft University of Technology, 2.04 edition, 2010.

[125] Yan Zeng, Jinsheng Cai, Marco Debiasi, and Tat Loon Chng. Numerical study on drag reduction for grid-fin configurations. In *47th AIAA aerospace sciences meeting including the new horizons forum and aerospace exposition*, page 1105, 2009.

A

FRT Inputs & Outputs

FRT requires several inputs to create a range of outputs. These inputs and outputs will be given here

A.1. Inputs

FRT uses existing launcher and coverts them into reusable launchers. This requires the tool to be able to run on a limited amount of information since any detailed information might be hard to acquire. This could be either due to that these inputs are commercially important as for the actual flight cost of the launcher or could be used to redesign the system by for example releasing a detailed mass breakdown. Therefore FRT has to make due with the minimal amount of inputs. The inputs that are required start with the mission to be flown and the initial conditions:

- Payload mass
- Target orbit
  - Apogee altitude
  - Perigee altitude
  - inclination or launch heading
- Initial location
  - latitude & longitude
  - altitude
  - velocity
  - orientation (azimuth and heading)

Since FRT is aimed to alter existing vehicles in order to make them reusable after the mission the vehicle has to be defined

- Sizing and mass for the individual stages & boosters
  - Empty mass
  - Propellant mass
  - Engine mass
  - Stage diameter
  - Stage length
  - Nosetip radius (required for re-entry heating)
- Engine specifications
  - Nozzle geometry

  - chamber pressure
  - thrust limit
  - real-life correction factors for either sea-level or vacuum conditions (optional)
  - Thrust curve (in-case of solid boosters)

- Drag coefficient as a function of Mach number.

Currently FRT can only accept two full stages of which the first can accept an unlimited amount of booster. However all boosters are separate, they can either be solid or liquid but when liquid no cross-feeding is available Besides the vehicle and the mission inputs are required for the reusability

- Which Types of decelerators are allowed
- Which Landing Systems are allowed
- Amount of previously produced stages
- Amount of launches performed per year
- The usage of booster and if boosters are always symmetrical
- The acceleration, dynamic pressure and temperature constraints
- The production for the 1st and 2nd stages
- Whether separating the engine is allowed

A.2. Outputs

The outputs from the tool are numerous so they are divided into a couple of categories. Most of the parameters have todo with the trajectory that is flown

A.2.1. Points of interest

Ther points of interest are the points withtin the trajectory which correspond to an event or something of interest

- 1st stage throttle down
- 1st stage throttle up
- Main Engine Cut-Off (MECO)
- Apogee Burn
- Second Engine Cut-Off (SECO) 1
- SECO 2
- Reentry
- Touchdown

A.2.2. Trajectory Outputs

The trajectory contributes the most to the total amount of outputs. The following outputs are saved.

- time
- location in inertial frame
- location in earth frame
- distance to center of the earth
- Altitude above surface

- Latitude
- Longitude
- Arc along the earth surface travelled
- Distance from starting point along the earth surface
- Velocity vector in inertial frame
- Velocity magnitude in inertial frame
- velocity parallel to the surface of the earth
- velocity magnitude in local plane
- atmosphere data along trajectory (density, pressure, temperature, speed of sound)
- dynamic pressure along the trajectory
- flight path angle
- heading angle
- acceleration

A.2.3. Keplerian Elements

Although almost all the keplerian elements are calculated the following are saved for further use.

- apogee altitude
- perigee altitude
- error in apogee altitude to target orbit
- error in perigee altitude to target orbit

A.2.4. Vehicle Outputs

For the vehicle the following outputs are saved for further use:

- 1st stage propellant
- 2nd stage propellant
- Thrust produced
- Vehicle Drag
- Deceleration system drag
- Recovery system mass
- Landing system mass
- Final empty stage mass
- Final stage length
- Sizes of the deceleration systems used
- Deployment altitudes of the deceleration systems (non-propulsive only)
- Propellant reserves kept for the descent (propulsive only)
- Chosen re-entry velocity (propulsive only)

A.2.5. Cost Outputs

Finally the outputs for the costs:

- Average unit cost
- Development cost
- Operational cost
- Cost per flight
- Reuse-Index
- Turnaround cost (retrieval + refurbishment cost)
- Recovery system cost
- A cost breakdown for the initial production cost. this includes
  - Tank cost
  - Engine cost
  - Recovery systems production cost
  - Assembly, Integration & Testing Cost

B

Ideal Rocket Theory Validation

As mentioned in section 3.4 the validation of the ideal rocket theory model is used to correct the model if no specific correction can be applied. The inputs for this validation effort can be seen in Table B.2. The results using the model described in section 3.4 without any correction can be found in Table B.3, all values for the engine are taken at vacuum conditions. This is done to omit any possible error in the atmospheric model that is used. In Table B.3 the values as well as the error is given for each of the three parameters. As can be seen the specific impulse is relatively accurate with a mean error of 2.5% and a standard deviation of 3.0%. However the thrust has an average error of 10% with a standard deviation of 12.5%. In order to adjust this a correction factor is applied to both the mass flow and the specific impulse, the correction factor is calculated from the average errors calculated. The correction factors can be found in Table B.1.

Table B.1: Correction factors to be applied in the thrust model

Correction Factor	Value
Specific Impulse	0.976428709
Mass flow	0.946562396
Thrust (Overall)	0.917947794

The correction factor for the thrust is the product of the two other correction factors.

Table B.2: Data used for the thrust model validation

Engine					Actual Data		
Name	D_e [m]	A_e/A_t [-]	P_c [bar]	Propellant	F_T [kN]	I_sp [s]	$\dot{m}$[kg/s]
Merlin 1D [12, 102, 121]	1.25	16	97	LOX/RP1	981	311	322
Rocketdyne F1 [7]	3.7	16	70	LOX/RP1	7770	304	2605
RS-68A [91]	2.44	21.5	108.9	LOX/LH2	3558	411	883
J-2 [8]	2.1	27.5	52.6	LOX/LH2	1033	421	250
RL-10B-2 [89]	2.21	280	44.12	LOX/LH2	110	466	24
RD-180 [14]	2x 1.575	36.87	267	LOX/RP1	4150	338	1252
Vulcain-2 [17]	2.09	58.2	117	LOX/LH2	1359	429	323
RS-25 [90]	2.4	69	206	LOX/LH2	2278	452	514
Viking 5C [16]	0.99	11	55	UDMH/N2O4	758	278	278
RD-253 [15]	1.5	26.2	147	UDMH/N2O4	1630	316	526
HM7B [40]	0.99	83.1	37	LOX/LH2	65	446	15

Table B.3: Results of the ideal rocket theory model

Engine	Actual Data			Ideal Rocket Theory					
				Thurst		Specific Impulse		Mass flow	
	F_T [kN]	I_{sp} [s]	$\dot{m}$ [kg/s]	F_T [kN]	Error [%]	I_{sp} [s]	Error [%]	$\dot{m}$ [kg/s]	Error [%]
Merlin 1D	981	311	322	1316	34.1	314	1.1	427	32.7
Rocketdyne F1	7770	304	2605	8318	7.1	314	3.4	2697	3.5
RS-68A	3559	411	883	4212	18.4	433	5.4	991	12.3
J2	1033	421	250	1192	15.4	438	4.0	278	10.9
RL-10B-2	110.1	466	24	116	5.5	468	0.5	26	9.2
RD-180	4150	338	1252	5190	25.1	327	-3.3	1618	29.3
Vulcain 2	1359	429	323	1278	-5.9	450	4.9	290	-10.3
RS-25	2278	452	514	2515	10.4	452	0.1	567	10.3
Viking 5C	758	278	278	685	-9.6	302	8.5	232	-16.7
RD-253	1630	316	526	1870	14.7	320	1.1	597	13.4
HM7B	65	446	15	64	-1.2	455	2.0	13	-9.8
Mean					10.4		2.5		7.7
Standard Deviation					12.5		3.0		14.8

C

Standard Sensitivity Analysis Results

In order to judge the robustness of the solutions found in chapter 6, a Monte Carlo analysis is run. This is done to see the variations in the solution as well as in the constraints. However, with Monte Carlo analysis, it is not easy to distinguish which parameter contributes the most to the deviation from the nominal case. This is where the once-at-a-time or "standard" analysis comes in. Here one and only one parameter is changed at a time to see what the results would be. As with the cases, the sensitivity analysis will be given per vehicle and per mission, as was done in chapter 6.

C.1. Sensitivity Values

For this sensitivity analysis, the same maximum and minimum errors are used as for the Monte Carlo analysis. However here no distribution is used. The parameter is varied by the both maximum and minimum separately. This means that for each entry in Table C.1 two cases are run. Also, to cut back on unnecessary cases, models which are not used in the vehicle will not be varied. So, for example, the HIAD mass model will not be varied if only parachutes are used. For the analysis the following parameters are investigated to how they change:

Table C.1: Variations of the various models/inputs for the sensitivity analysis

System	Category	Bounds	(Sub)Section
Parachute Models	Mass	$-2.5\%, 25\%$	subsection 3.3.2
	Cost	$\pm 50\%$	section 4.3
HIAD Models	Mass	$0\%, 10\%$	subsection 3.3.3
	Cost	$\pm 50\%$	section 4.3
Airbag Models	Mass	$-30\%, 30\%$	subsection 3.2.2
	Cost	$\pm 50\%$	section 4.3
Flotation Device Models	Mass	$\pm 20\%$	subsection 3.2.3
	Cost	$\pm 50\%$	section 4.3
Landing Legs	Mass	$\pm 10\%$	subsection 3.2.1
Refurbishment	Cost	$-10\%, +30\%$	subsection 4.2.3
Added Tank Mass	Mass	$-10\%, +8\%$	subsection 3.1.2
Thrust Model	Trajectory	$-1\%, +5\%$	subsection 3.4.2
Grid Fins	Mass	$\pm 50\%$	subsection 3.3.1
CD Total Launcher	Trajectory	$\pm 10\%$	section 3.5
CD First Stage	Trajectory	$\pm 10\%$	section 3.5
Empty Mass	Initial Condition	$\pm 10\%$	subsection 6.1.3

- **a** - The maximum deceleration of the first stage during the descent
- **q** - The maximum dynamic pressure of the first stage during the descent

- **T** - The maximum temperature of the first stage during descent
- **CpF** - The cost per flight when reusing 10 times
- **RI** - The Reuse-Index when reusing 10 times

For the changes the value as well as the difference to the original case will be given. If nothing changes the differences will be 0%. If changes are smaller than ±0.005% the change will be denoted as ≈ ±0%. This is done to show that are is an influence although it is very small.

C.2. Falcon9

C.2.1. LEO Mission

Table C.2: Standard sensitivity analysis results for the complete stage recovery using propulsive means, case 1, for the Falcon 9 LEO mission

Parameter	Var.	Acceleration		Dyn. Pres.		Temperature		CpF		RI	
		[g]	[%]	[kPa]	[%]	[K]	[%]	[M €]	[%]	[-]	[%]
Original	0%	9.80	0	132.8	0	292.9	0	32.9	0	0.748	0
Landing Legs Mass Model	-10%	9.87	0.71	131.8	-0.78	292.8	-0.01	32.8	-0.19	0.747	-0.19
	10%	9.73	-0.70	134.0	0.88	292.9	0.01	33.0	0.19	0.750	0.19
Refurbishment Cost	-10%	9.80	0	132.8	0	292.9	0	32.2	-2.05	0.733	-2.05
	30%	9.80	0	132.8	0	292.9	0	35.0	6.16	0.794	6.16
Thrust Model	-1%	9.81	0.08	132.7	-0.03	292.9	≈-0	32.9	≈0	0.748	≈0
	5%	9.77	-0.35	133.3	0.37	292.8	-0.01	32.9	-0.01	0.748	-0.01
C_D Entire Launcher	-10%	9.81	0.08	132.9	0.08	292.9	≈-0	32.9	≈0	0.748	≈0
	10%	9.79	-0.07	132.9	0.12	292.8	-0.02	32.9	≈-0	0.748	≈-0
C_D First Stage	-10%	9.92	1.21	148.3	11.71	293.4	0.17	32.9	≈0	0.748	≈0
	10%	9.70	-1.04	120.3	-9.38	292.4	-0.15	32.9	≈-0	0.748	≈-0
Empty Mass	-10%	10.63	8.43	121.3	-8.67	292.4	-0.16	31.8	-3.32	0.723	-3.32
	10%	9.10	-7.18	144.9	9.15	293.3	0.15	33.9	3.18	0.772	3.18

What can be seen in Table C.2 is that the values that come from the trajectory are most influenced by changes in initial empty mass and the C_D of the first stage. The dynamic pressure is the most sensitive with changes of -9% to +12%. The maximum temperature seems to be unaffected. For the cost, changes in the refurbishment produce the biggest deviation. This make sense since this is one of the major costs of a reusable launcher. Furthermore the empty mass again produces significant differences of ±3%.

For the sensitivity results of case 2, Table C.3, different rows are added as the recovered system had different elements. As this case used Mid-Air Recovery (MAR), no landing system can be varied. In Table C.3 the same trend can be seen as for case 1, with the drag coefficient, this time from the entire launcher and the initial empty mass causing the biggest changes. However, here also changes to the thrust model can create significant differences. This could either be because the engine section is much lighter, so if the first stage can produce more thrust, it goes faster, which leads to higher drag loads during re-entry. However, another reason could have to do with the tool. The tool, for the sensitivity analysis, first checks the original ascent trajectory. If this ascent trajectory does not satisfy the requirements, lower than 2.5% error in the final orbit, it starts searching for a new trajectory. This new trajectory could also cause these differences. For the costs, the same can be said as for case 1, where changes in the refurbishment costs and the empty mass cause the biggest changes in the final cost. It should be said that even if the costs go up by 5%, the savings are still more than 10%. This can be said when looking at the RI.

In Table C.4, besides the trends seen in Table C.2 and Table C.3 is that the airbag mass becomes a relevant parameter to keep an eye on, as it can vary the dynamic pressure by almost 2%. For the remainder of the variations are the empty mass and drag of the vehicle.

Table C.3: Standard sensitivity analysis results for the enigne only recovery using non-propulsive means, case 2, for the Falcon 9 LEO mission

Parameter	Var.	Acceleration		Dyn. Pres.		Temperature		CpF		RI	
		[g]	[%]	[kPa]	[%]	[K]	[%]	[M €]	[%]	[-]	[%]
Original	0%	7.30	0	20.5	0	290.1	0	37.3	0	0.848	0
Refurbishment Cost	-10%	7.30	0	20.5	0	290.1	0	36.9	-1.06	0.839	-1.06
	30%	7.30	0	20.5	0	290.1	0	38.5	3.19	0.875	3.19
Thrust Model	-1%	7.31	0.19	20.5	0.11	290.0	-0.05	37.3	≈0	0.848	≈0
	5%	8.84	21.08	20.4	-0.37	287.0	-1.09	37.3	≈0	0.848	≈0
C_D Entire Launcher	-10%	7.36	0.90	20.6	0.24	290.2	0.04	37.3	≈0	0.848	≈0
	10%	8.87	21.58	20.5	-0.21	287.3	-1.00	37.3	≈0	0.848	≈-0
Empty Mass	-10%	9.18	25.81	20.8	1.38	287.8	-0.81	35.6	-4.56	0.809	-4.56
	10%	7.14	-2.13	20.3	-1.10	289.2	-1.10	38.9	4.36	0.885	4.36
HIAD Mass	10%	7.30	0.02	20.5	≈0	290.2	0.01	37.3	0.01	0.848	0.01
HIAD Cost	-50%	7.30	0	20.5	0	290.1	0	37.3	-0.08	0.847	-0.08
	50%	7.30	0	20.5	0	290.1	0	37.3	0.08	0.849	0.08
Parachute Mass	-2.5%	7.30	-0.01	20.5	≈0	290.2	≈0	37.3	≈-0	0.848	≈-0
	25%	7.30	0.09	20.5	-0.01	290.2	0.01	37.3	0.04	0.848	0.05
Parachute Cost	-50%	7.30	0	20.5	0	290.1	0	37.3	-0.01	0.848	-0.01
	50%	7.30	0	20.5	0	290.1	0	37.3	0.01	0.848	0.01
Retrieval Cost	-50%	7.30	0	20.5	0	290.1	0	37.3	-0.09	0.847	-0.09
	50%	7.30	0	20.5	0	290.1	0	37.3	0.09	0.849	0.09

C.2.2. GTO Misson

In Table C.5, Table C.6 and Table C.7 The results for the standard sensitivity analysis can be seen. the results follow the same trend as the results fro the LEO mission. Variations in the drag coefficient and the Emtpy mass are critical for the parameters associated with the trajectory. For the cost the refurbishment and the empty mass are key. This shows that for the Falcon 9 the finding a correct empty mass should be the first priority as this set most of the errors.

C.3. Delta IV+

C.3.1. LEO Mission

The results of the standard sensitivity analysis for the Delta IV+ LEO mission can be found in Table C.8, Table C.9 and Table C.10. For the Delta IV+, although this is a different vehicle, the same trends can be found once more. Changes in the initial empty mass and the drag for either the entire vehicle or the first stage produce the biggest deviation for the parameter associated with the trajectory. Here also one extra parameter come forward that was not used for the Falcon 9, and this is the added tank mass. This can cause significant changes in the mass and the cost. For the cost changes in the refurbishment cost and the empty mass cause the biggest changes in the cost.

Besides the input and the variations, one other element comes forward in this analysis, and that is the ascent trajectory. Changing the ascent trajectory can cause significant changes in the trajectory elements. So finding a robust ascent trajectory is also crucial. However, this is difficult to achieve as these are very sensitive with small changes already leading to a different ascent trajectory in FRT.

C.3.2. GTO Mission

The results of the standard sensitivity analysis for the Delta IV+ GTO mission can be found in Table C.11, Table C.12 and Table C.13. Here again, the same trends can be seen as before. A couple of things stand out. The first is the impact of change in the thrust model in case 3 to the trajectory causes a larger change than observed before. This could be because the lift-off mass is much higher for these as opposed to the other two cases for this mission.

In Table C.12 a couple of noticeable deviation can be seen. These are for the thrust model, drag of the entire launcher and the airbag mass. These are due to the different trajectory that is flown for those cases.

Table C.4: Standard sensitivity analysis results for the complete stage recovery using non-propulsive means, case 3, for the Falcon 9 LEO mission

Parameter	Var.	Acceleration [g]	Acceleration [%]	Dyn. Pres. [kPa]	Dyn. Pres. [%]	Temperature [K]	Temperature [%]	CpF [M€]	CpF [%]	RI [-]	RI [%]
Original	0%	9.66	0	31.62	0	292.6	0	32.7	0	0.744	0
Refurbishment Cost	-10%	9.66	0	31.6	0	292.6	0	32.1	-2.02	0.729	-2.02
	30%	9.66	0	31.6	0	292.6	0	37.7	6.06	0.790	6.06
Thrust Model	-1%	9.69	0.30	31.7	0.29	292.7	0.01	32.7	≈0	0.744	≈0
	5%	9.52	-1.50	31.2	-1.4	292.5	-0.04	32.7	-0.01	0.744	-0.01
C_D Entire Launcher	-10%	9.73	0.76	31.8	0.72	292.7	0.02	32.7	≈0	0.744	≈0
	10%	9.58	-0.80	31.4	-0.75	292.6	-0.01	32.7	≈0	0.744	≈-0
Empty Mass	-10%	11.03	14.15	31.8	0.66	292.3	-0.10	31.6	-3.25	0.720	-3.25
	10%	9.40	-2.72	34.5	9.07	292.3	-0.11	33.8	3.18	0.768	3.18
HIAD Mass	10%	9.65	-0.08	31.7	0.28	292.6	-0.01	32.7	0.07	0.745	0.07
HIAD Cost	-50%	9.66	0	31.6	0	292.6	0	32.7	-0.14	0.743	-0.14
	50%	9.66	0	31.6	0	292.6	0	32.8	0.14	0.745	0.14
Parachute Mass	-2.5%	9.66	0.01	31.6	-0.04	292.6	≈0	32.7	-0.01	0.744	-0.01
	25%	9.65	-0.12	31.7	0.42	292.7	0.01	32.8	0.10	0.745	0.10
Parachute Cost	-50%	9.66	0	31.6	0	292.6	0	32.7	-0.03	0.744	-0.03
	50%	9.66	0	31.6	0	292.6	0	32.7	0.03	0.745	0.03
Airbag Mass	-30%	9.71	0.47	31.0	-1.87	292.6	-0.02	32.7	-0.04	0.744	-0.04
	30%	9.61	-0.53	32.2	1.79	292.6	≈-0	32.7	0.04	0.745	0.04
Airbag Cost	-50%	9.66	0	31.6	0	292.6	0	32.7	-0.07	0.744	-0.07
	50%	9.66	0	31.6	0	292.6	0	32.8	0.07	0.745	0.07
Flotation System Mass	-20%	9.67	0.05	31.5	-0.22	292.6	≈-0	32.7	≈0	0.744	≈0
	20%	9.66	-0.06	31.7	0.21	292.6	-0.01	32.7	≈-0	0.744	≈-0
Flotation System Cost	-50%	9.66	0	31.6	0	292.6	0	32.7	-0.01	0.744	-0.01
	50%	9.66	0	31.6	0	292.6	0	32.7	0.01	0.744	0.01
Retrieval Cost	-50%	9.66	0	31.6	0	292.6	0	32.6	-0.43	0.741	-0.43
	50%	9.66	0	31.6	0	292.6	0	32.9	0.43	0.748	0.43

Where for the original trajectory, the first stage does not have an apogee around 80 km, these two cases have an apogee around 180 km. This means that the original trajectory goes horizontal faster than the one used for the drag and thrust increases. This means in the original case, more drag losses occur, and the re-entry velocity is lower than for the deviations. This leads to higher maximum deceleration for these cases.
The other interesting case, although not as noticeable is that the trajectory values for the empty mass increase are identical to the original case. This can also be explained. Since this case recovers only the engine the mass that re-enters is identical to the original case. It also has the same drag coefficient as the original case. This leads to an identical trajectory.

Table C.5: Standard sensitivity analysis results for the complete stage recovery using propulsive means, case 1, for the Falcon 9 GTO mission

Parameter	Var.	Acceleration		Dyn. Pres.		Temperature		CpF		RI	
		[g]	[%]	[kPa]	[%]	[K]	[%]	[M €]	[%]	[-]	[%]
Original	0%	9.01	0	119.4	0	344.6	0	32.8	0	0.746	0
Landing Legs Mass Model	-10%	9.07	0.56	118.9	-0.44	344.8	0.06	32.7	-0.19	0.745	-0.19
	10%	8.97	-0.56	119.9	0.42	344.9	0.07	32.9	0.19	0.748	0.19
Refurbishment Cost	-10%	9.01	0	119.4	0	344.6	0	32.1	-2.06	0.731	-2.06
	30%	9.01	0	119.4	0	344.6	0	34.8	6.18	0.792	6.18
Thrust Model	-1%	9.02	0.01	119.6	0.19	344.9	0.08	32.8	≈0	0.746	≈0
	5%	9.01	-0.06	117.9	-1.28	334.4	-0.06	32.8	-0.01	0.746	-0.01
C_D Entire Launcher	-10%	9.02	0.04	120.6	1.01	345.0	0.10	32.8	≈0	0.746	≈0
	10%	9.01	-0.03	118.2	-1.05	344.7	0.04	32.8	≈-0	0.746	≈-0
C_D First Stage	-10%	11.0	21.44	133.6	11.89	347.0	0.69	32.8	≈0	0.746	≈0
	10%	8.88	-1.50	107.8	-9.77	342.5	-0.60	32.8	≈-0	0.746	≈-0
Empty Mass	-10%	9.61	6.61	113.6	-4.85	343.8	-0.25	31.7	-3.33	0.721	3.33
	10%	9.27	2.81	172.6	44.53	337.1	-2.17	33.90	3.33	0.771	3.33

Table C.6: Standard sensitivity analysis results for the enigne only recovery using non-propulsive means, case 2, for the Falcon 9 GTO mission

Parameter	Var.	Acceleration		Dyn. Pres.		Temperature		CpF		RI	
		[g]	[%]	[kPa]	[%]	[K]	[%]	[M €]	[%]	[-]	[%]
Original	0%	5.86	0	50.2	0	342.3	0	37.3	0	0.849	0
Refurbishment Cost	-10%	5.86	0	50.2	0	342.3	0	36.9	-1.06	0.840	-1.06
	30%	5.86	0	50.2	0	342.3	0	38.5	3.19	0.876	3.19
Thrust Model	-1%	5.88	0.31	50.2	0.12	342.4	0.04	37.3	≈0	0.849	≈0
	5%	5.77	-1.45	50.3	0.22	341.5	-0.22	37.3	≈-0	0.849	≈-0
C_D Entire Launcher	-10%	5.95	1.55	50.6	0.89	342.4	0.05	37.3	≈0	0.849	≈0
	10%	5.77	-1.54	50.0	-0.29	341.9	-0.12	37.3	≈-0	0.848	≈-0
Empty Mass	-10%	6.09	3.97	50.5	0.73	343.4	0.33	35.6	-4.55	0.810	-4.55
	10%	5.63	-3.84	50.3	0.19	340.9	-0.39	38.9	4.35	0.885	4.35
HIAD Mass	10%	5.86	≈0	50.2	≈-0	342.3	≈0	37.3	≈0	0.849	≈0
HIAD Cost	-50%	5.86	0	50.2	0	342.3	0	37.3	-0.02	0.848	-0.02
	50%	5.86	0	50.2	0	243.3	0	37.3	0.02	0.849	0.02
Parachute Mass	-2.5%	5.86	-0.01	50.5	0.57	243.0	-0.08	37.3	-0.01	0.849	-0.01
	25%	5.87	0.13	50.2	0.04	342.5	0.07	37.3	0.10	0.849	0.10
Parachute Cost	-50%	5.86	0	50.2	0	342.3	0	37.3	-0.02	0.848	-0.02
	50%	5.86	0	50.2	0	342.3	0	37.3	0.02	0.849	0.02
Retrieval Cost	-50%	5.86	0	50.2	0	342.3	0	37.3	-0.09	0.848	-0.09
	50%	5.86	0	50.2	0	342.3	0	37.3	0.09	0.849	0.09

Table C.7: Standard sensitivity analysis results for the complete stage recovery using non-propulsive means, case 3, for the Falcon 9 GTO mission

Parameter	Var.	Acceleration [g]	Acceleration [%]	Dyn. Pres. [kPa]	Dyn. Pres. [%]	Temperature [K]	Temperature [%]	CpF [M€]	CpF [%]	RI [-]	RI [%]
Original	0%	6.42	0	58.1	0	360.8	0	32.6	0	0.742	0
Refurbishment Cost	-10%	6.42	0	58.1	0	360.8	0	32.0	-2.03	0.727	-2.03
	30%	6.42	0	58.1	0	360.8	0	34.6	6.09	0.787	6.09
Thrust Model	-1%	6.44	0.31	58.3	0.33	360.7	-0.02	32.6	≈0	0.742	≈0
	5%	6.30	-1.84	57.5	-0.98	360.4	-0.11	32.6	-0.01	0.742	-0.01
C_D Entire Launcher	-10%	6.51	1.49	58.5	0.76	360.6	-0.04	32.6	≈0	0.742	≈0
	10%	6.30	-1.84	57.5	-0.98	360.4	-0.11	32.6	-0.01	0.742	-0.01
Empty Mass	-10%	6.63	3.23	58.1	0.04	361.0	0.07	31.5	-3.32	0.748	-3.32
	10%	6.91	7.71	55.8	-3.83	357.7	-0.85	33.7	3.20	0.766	3.20
HIAD Mass	10%	6.41	-0.11	58.2	0.22	360.8	≈-0	32.6	0.06	0.743	0.06
HIAD Cost	-50%	6.42	0	58.0	0	360.8	0	32.6	-0.08	0.0742	-0.08
	50%	6.42	0	58.1	0	360.8	0	32.7	0.08	0.743	0.08
Parachute Mass	-2.5%	6.42	0.02	58.2	0.28	360.8	≈-0	32.6	-0.01	0.742	-0.01
	25%	6.40	-0.23	58.1	0.09	360.7	-0.03	32.7	0.12	0.743	0.12
Parachute Cost	-50%	6.42	0	58.1	0	360.8	0	32.6	-0.03	0.742	-0.03
	50%	6.42	0	58.1	0	360.8	0	32.6	0.03	0.742	0.03
Airbag Mass	-30%	6.45	0.48	58.1	0.12	360.7	-0.03	32.6	-0.02	0.742	-0.02
	30%	6.42	-0.06	58.1	0.08	360.6	-0.05	32.6	0.02	0.742	0.02
Airbag Cost	-50%	6.42	0	58.1	0	360.8	0	32.6	-0.05	0.742	-0.05
	50%	6.42	0	58.1	0	360.8	0	32.6	0.05	0.743	0.05
Flotation System Mass	-20%	6.42	0.09	57.9	-0.22	360.5	-0.09	32.6	≈0	0.742	≈0
	20%	6.41	-0.10	58.2	0.21	360.8	≈-0	32.6	≈-0	0.742	≈-0
Flotation System Cost	-50%	6.42	0	58.1	0	360.8	0	32.6	-0.01	0.742	-0.01
	50%	6.42	0	58.1	0	360.8	0	32.6	0.01	0.742	0.01
Retrieval Cost	-50%	6.42	0	58.1	0	360.8	0	32.5	-0.38	0.739	-0.38
	50%	6.42	0	58.1	0	360.8	0	32.8	0.38	0.745	0.38

Table C.8: Standard sensitivity analysis results for the complete stage recovery using propulsive means, case 1, for the Delta IV+ LEO mission

Parameter	Var.	Acceleration [g]	Acceleration [%]	Dyn. Pres. [kPa]	Dyn. Pres. [%]	Temperature [K]	Temperature [%]	CpF [M€]	CpF [%]	RI [-]	RI [%]
Original	0%	9.91	0	79.1	0	295.1	0	61.8	0	0.828	0
Landing Legs Mass Model	-10%	9.92	0.13	78.56	-0.72	295.0	-0.02	61.7	-0.20	0.826	-0.20
	10%	9.88	-0.27	79.58	0.57	295.1	0.03	61.9	0.20	0.830	0.20
Refurbishment Cost	-10%	9.91	0	79.1	0	295.1	0	60.5	-2.06	0.811	-2.06
	30%	9.91	0	79.1	0	295.1	0	65.6	6.17	0.879	6.17
Thrust Model	-1%	9.87	-0.35	79.0	-0.22	295.1	0.01	61.8	≈0	0.828	≈0
	5%	9.97	0.69	79.9	0.91	295.0	-0.03	61.8	-0.01	0.828	-0.01
Grid Fins Mass	-50%	9.89	-0.12	79.0	-0.13	295.0	≈-0	61.8	-0.05	0.828	-0.05
	50%	9.89	-0.12	79.2	0.06	295.0	-0.01	61.8	0.05	0.828	0.05
C_D Entire Launcher	-10%	9.82	-0.84	78.4	-0.99	295.2	0.03	61.8	0.01	0.828	0.01
	10%	9.97	0.64	79.8	0.89	295.0	-0.03	61.8	-0.01	0.828	-0.01
C_D First Stage	-10%	9.96	0.52	88.4	11.69	295.6	0.18	61.8	≈0	0.828	≈0
	10%	9.83	-0.80	71.3	-9.95	294.6	-0.16	61.8	≈-0	0.828	≈-0
Empty Mass	-10%	16.4	65.9	176.0	122.4	327.1	10.86	59.6	-3.47	0.799	-3.47
	10%	9.91	0	79.133	0	295.1	0	63.8	3.26	0.855	3.26

Table C.9: Standard sensitivity analysis results for the engine only recovery using non-propulsive means, case 2, for the Delta IV+ LEO mission

Parameter	Var.	Acceleration [g]	Acceleration [%]	Dyn. Pres. [kPa]	Dyn. Pres. [%]	Temperature [K]	Temperature [%]	CpF [M€]	CpF [%]	RI [-]	RI [%]
Original	0%	9.99	0	27.6	0	334.3	0	61.6	0	0.826	0
Refurbishment Cost	-10%	9.99	0	27.6	0	334.3	0	60.7	-1.41	0.814	-1.41
	30%	9.99	0	27.6	0	334.3	0	64.2	4.24	0.861	4.24
Thrust Model	-1%	10.0	0.26	27.6	0.25	334.5	0.05	61.6	≈0	0.826	≈0
	5%	9.87	-1.22	27.2	-1.18	333.9	-0.11	61.6	-0.01	0.826	-0.01
C_D Entire Launcher	-10%	10.2	2.30	28.2	2.26	333.8	-0.13	61.6	0.01	0.826	0.01
	10%	9.77	-2.29	27.0	-2.25	334.8	0.15	61.6	-0.01	0.826	-0.01
Empty Mass	-10%	10.64	6.42	29.3	6.25	336.9	0.77	58.3	-5.34	0.782	-5.34
	10%	16.19	62.00	44.7	61.99	315.8	-5.52	64.9	5.37	0.870	5.37
HIAD Mass	10%	9.99	≈-0	27.6	0.07	334.3	≈0	61.6	0.01	0.826	0.01
HIAD Cost	-50%	9.99	0	27.6	0	334.3	0	61.6	-0.03	0.825	-0.03
	50%	9.99	0	27.6	0	334.3	0	61.6	0.03	0.826	0.03
Parachute Mass	-2.5%	10.00	0.01	27.5	-0.15	334.3	0.01	61.6	-0.02	0.825	-0.02
	25%	9.98	-0.10	280	1.45	334.6	0.08	61.7	0.20	0.827	0.20
Parachute Cost	-50%	9.99	0	27.6	0	334.3	0	61.6	-0.02	0.826	-0.02
	50%	9.99	0	27.6	0	334.3	0	61.6	0.02	0.826	0.02
Airbag Mass	-30%	10.00	0.02	24.5	-0.42	334.2	-0.02	61.6	≈-0	0.826	≈-0
	30%	9.99	-0.02	27.7	0.42	334.4	0.03	61.6	≈0	0.826	≈0
Airbag Cost	-50%	9.99	0	27.6	0	334.3	0	61.6	≈-0	0.826	≈-0
	50%	9.99	0	27.6	0	334.3	0	61.6	≈0	0.826	≈0
Flotation System Mass	-20%	10.00	0.02	27.5	-0.30	334.3	≈-0	61.6	-0.01	0.826	-0.01
	20%	9.99	-0.02	27.7	0.30	334.4	0.03	61.6	0.01	0.826	0.01
Flotation System Cost	-50%	9.99	0	27.6	0	334.3	0	61.6	≈0	0.826	≈0
	50%	9.99	0	27.6	0	334.3	0	61.6	≈-0	0.826	≈-0
Retrieval Cost	-50%	9.99	0	27.6	0	334.3	0	61.3	-0.48	0.822	-0.48
	50%	9.99	0	27.6	0	334.3	0	61.9	0.48	0.830	0.48

Table C.10: Standard sensitivity analysis results for the complete stage recovery using non-propulsive means, case 3, for the Delta IV+ LEO mission

Parameter	Var.	Acceleration		Dyn. Pres.		Temperature		CpF		RI	
		[g]	[%]	[kPa]	[%]	[K]	[%]	[M €]	[%]	[-]	[%]
Original	0%	10.00	0	15.6	0	327.1	0	67.4	0	0.903	0
Refurbishment Cost	-10%	10.00	0	15.6	0	327.1	0	65.9	-2.20	0.883	-2.20
	30%	10.00	0	15.6	0	327.1	0	71.8	6.61	0.962	6.61
Added Tank Mass	-10%	12.12	21.22	16.18	3.68	323.6	-1.08	66.1	-1.80	0.886	-1.80
	8%	14.13	41.38	14.6	-6.46	310.6	-5.06	68.5	1.62	0.917	1.62
Thrust Model	-1%	10.11	1.17	15.6	0.011	327.0	-0.04	67.4	0.01	0.903	0.01
	5%	9.47	-5.29	15.5	-0.49	330.7	1.07	67.3	-0.04	0.902	-0.04
C_D Entire Launcher	-10%	10.17	1.72	15.6	0.16	326.7	-0.15	67.4	0.01	0.903	0.01
	10%	9.84	-1.59	15.6	-0.15	327.4	0.07	67.3	-0.01	0.902	-0.01
Empty Mass	-10%	12.97	29.78	16.4	5.12	323.1	-1.23	65.0	-3.56	0.870	-3.56
	10%	12.76	27.60	13.9	-10.65	310.5	-5.09	69.8	3.67	0.936	3.66
HIAD Mass	10%	9.73	-2.68	15.5	-0.39	328.6	0.45	67.5	0.18	0.904	0.18
HIAD Cost	-50%	10.00	0	15.6	0	327.1	0	67.1	-0.32	0.900	-0.32
	50%	10.00	0	15.6	0	327.1	0	67.6	0.32	0.905	0.32
Parachute Mass	-2.5%	10.01	0.16	15.6	0.02	327.2	≈0	67.3	-0.01	0.903	-0.01
	25%	9.89	-1.02	15.6	-0.20	327.6	0.15	67.4	0.10	0.903	0.10
Parachute Cost	-50%	10.00	0	15.6	0	327.1	0	67.3	-0.02	0.902	-0.02
	50%	10.00	0	15.6	0	327.1	0	67.4	0.02	0.903	0.02
Airbag Mass	-30%	10.65	6.55	15.8	1.08	325.4	-0.55	67.4	0.02	0.903	0.02
	30%	15.16	51.70	15.0	-4.20	310.9	-4.98	67.4	0.19	0.904	0.19
Airbag Cost	-50%	10.00	0	15.6	0	327.1	0	67.3	-0.06	0.902	-0.06
	50%	10.00	0	15.6	0	327.1	0	67.4	0.06	0.903	0.06
Flotation System Mass	-20%	10.06	0.68	15.6	0.10	327.1	-0.03	67.4	0.01	0.903	0.01
	20%	10.06	0.68	15.6	0.10	327.1	-0.03	67.4	-0.01	0.903	-0.01
Flotation System Cost	-50%	10.00	0	15.6	0	327.1	0	67.4	≈-0	0.903	≈-0
	50%	10.00	0	15.6	0	327.1	0	67.4	≈0	0.903	≈0
Retrieval Cost	-50%	10.00	0	15.6	0	327.1	0	67.0	-0.59	0.897	-0.59
	50%	10.00	0	15.6	0	327.1	0	67.8	0.59	0.908	0.59

Table C.11: Standard sensitivity analysis results for the complete stage recovery using propulsive means, case 1, for the Delta IV+ GTO mission

Parameter	Var.	Acceleration		Dyn. Pres.		Temperature		CpF		RI	
		[g]	[%]	[kPa]	[%]	[K]	[%]	[M €]	[%]	[-]	[%]
Original	0%	14.34	0	105.3	0	334.8	0	67.6	0	0.906	0
Landing Legs Mass Model	-10%	14.36	0.15	104.36	-0.98	334.6	-0.06	67.5	-0.19	0.905	-0.19
	10%	14.37	0.25	106.3	0.92	334.9	0.05	67.8	0.19	0.908	0.19
Refurbishment Cost	-10%	14.34	0	105.3	0	334.8	0	66.3	-1.92	0.889	-1.92
	30%	14.34	0	105.3	0	334.8	0	71.5	5.75	0.958	5.75
Thrust Model	-1%	14.36	0.16	105.2	-0.07	334.8	0.01	67.6	≈0	0.906	≈0
	5%	14.41	0.48	106.2	0.83	334.8	≈-0	67.6	-0.01	0.906	-0.01
Grid Fins Mass	-50%	14.34	0.02	102.9	-2.33	334.3	-0.16	67.3	-0.43	0.902	-0.43
	50%	14.39	0.38	107.9	2.43	335.3	0.15	67.9	0.42	0.910	0.42
C_D Entire Launcher	-10%	14.46	0.85	105.7	0.37	334.6	-0.06	67.6	0.01	0.906	0.01
	10%	14.2	-0.44	105.0	-0.33	335.0	0.05	67.6	-0.01	0.906	-0.01
C_D First Stage	-10%	14.45	0.81	116.6	10.69	337.1	0.69	67.6	≈0	0.906	≈0
	10%	14.28	-0.39	95.9	-8.94	332.7	-0.61	67.6	≈-0	0.906	≈-0
Empty Mass	-10%	14.25	-0.65	93.8	-10.9	332.6	-0.66	65.6	-3.05	0.879	-3.05
	10%	14.52	1.28	118.0	12.00	336.9	0.63	69.6	2.90	0.933	2.90

Table C.12: Standard sensitivity analysis results for the engine only recovery using non-propulsive means, case 2, for the Delta IV+ GTO mission

Parameter	Var.	Acceleration		Dyn. Pres.		Temperature		CpF		RI	
		[g]	[%]	[kPa]	[%]	[K]	[%]	[M€]	[%]	[-]	[%]
Original	0%	9.38	0	34.5	0	329.8	0	61.4	0	0.823	0
Refurbishment Cost	-10%	9.38	0	34.5	0	329.8	0	60.6	-1.41	0.812	-1.41
	30%	9.38	0	34.5	0	329.8	0	64.0	4.23	0.858	4.23
Thrust Model	-1%	9.42	0.43	34.6	0.11	329.8	0.01	61.4	≈0	0.823	≈0
	5%	16.30	73.70	36.9	6.89	313.6	-4.89	61.6	0.33	0.826	0.33
C_D Entire Launcher	-10%	9.64	2.69	35.2	1.99	329.3	-0.13	61.4	0.01	0.823	0.01
	10%	16.31	73.84	36.9	6.90	313.8	-4.83	61.6	0.33	0.826	0.33
C_D First Stage	-10%	9.54	1.66	34.5	0	332.1	0.70	61.4	≈0	0.823	≈0
	10%	9.23	-1.68	34.5	0	327.7	-0.61	61.4	≈-0	0.823	≈-0
Empty Mass	-10%	10.19	8.59	34.4	-0.27	331.1	0.41	58.1	-5.37	0.779	-5.37
	10%	9.38	0	34.5	0	329.8	0	64.6	5.15	0.866	5.15
Parachute Mass	-2.5%	10.00	6.58	34.7	0.43	327.7	-0.63	61.5	0.03	0.823	0.03
	25%	12.80	36.39	33.5	-3.02	318.6	-3.38	61.7	0.36	0.826	0.36
Parachute Cost	-50%	9.38	0	34.5	0	329.8	0	61.4	-0.01	0.823	-0.01
	50%	9.38	0	34.5	0	329.8	0	61.4	0.01	0.823	0.01
Airbag Mass	-30%	9.45	0.69	34.5	-0.05	329.0	-0.22	61.4	-0.01	0.823	-0.01
	30%	16.43	75.12	39.0	12.88	314.2	-4.72	61.6	0.35	0.826	0.35
Airbag Cost	-50%	9.38	0	34.5	0	329.8	0	61.4	-0.03	0.823	-0.03
	50%	9.38	0	34.5	0	329.8	0	61.4	0.03	0.823	0.03
Flotation System Mass	-20%	9.39	0.05	34.5	0.01	329.5	-0.07	61.4	≈0	0.823	≈0
	20%	9.99	6.58	34.7	0.45	327.8	-0.60	61.5	0.05	0.824	0.05
Flotation System Cost	-50%	9.38	0	34.5	0	329.8	0	61.4	≈-0	0.823	≈-0
	50%	9.38	0	34.5	0	329.8	0	61.4	≈0	0.823	≈0
Retrieval Cost	-50%	9.38	0	34.5	0	329.8	0	61.1	-0.47	0.819	-0.47
	50%	9.38	0	34.5	0	329.8	0	61.7	0.47	0.827	0.47

Table C.13: Standard sensitivity analysis results for the entire stage recovery using non-propulsive means, case 3, for the Delta IV+ GTO mission

Parameter	Var.	Acceleration		Dyn. Pres.		Temperature		CpF		RI	
		[g]	[%]	[kPa]	[%]	[K]	[%]	[M€]	[%]	[-]	[%]
Original	0%	8.58	0	52.6	0	424.2	0	66.2	0	0.887	0
Refurbishment Cost	-10%	8.58	0	52.6	0	424.2	0	64.7	-2.19	0.868	-2.19
	30%	8.58	0	52.6	0	424.2	0	70.6	6.58	0.945	6.58
Added Tank Mass	-1%	11.39	32.69	62.7	19.28	415.3	-2.11	65.0	-1.80	0.871	-1.80
	5%	12.30	43.35	81.6	55.28	346.0	-18.42	67.3	1.62	0.701	1.62
Thrust Model	-1%	8.72	1.64	53.4	1.65	425.0	0.18	66.2	0.01	0.887	0.01
	5%	7.94	-7.45	48.7	-7.4	417.9	-1.47	66.2	-0.05	0.887	-0.05
C_D Entire Launcher	-10%	8.87	3.39	54.3	3.34	426.8	0.61	66.2	0.02	0.887	0.02
	10%	8.30	-3.33	50.8	-3.27	420.7	-0.82	66.2	-0.02	0.887	-0.02
Empty Mass	-10%	12.41	44.64	65.4	24.37	404.8	-4.56	63.8	-3.59	0.855	-3.59
	10%	15.90	85.30	111.8	112.78	339.7	-19.92	68.8	3.92	0.922	3.92
HIAD Mass	10%	8.44	-1.65	51.9	-1.24	423.2	-0.24	66.2	0.08	0.888	0.08
HIAD Cost	-50%	8.58	0	52.6	0	424.2	0	66.2	-0.05	0.887	-0.05
	50%	8.58	0	52.6	0	424.2	0	66.2	0.05	0.888	0.05
Parachute Mass	-2.5%	8.60	0.17	52.6	0.12	424.1	-0.02	66.2	-0.01	0.887	-0.01
	25%	8.43	-1.77	51.9	-1.34	423.0	-0.28	66.3	0.08	0.888	0.08
Parachute Cost	-50%	8.58	0	62.6	0	424.2	0	66.2	-0.02	0.887	-0.02
	50%	8.58	0	52.6	0	424.2	0	66.2	0.02	0.887	0.02
Airbag Mass	-30%	9.59	11.76	56.7	7.95	426.1	0.45	66.2	0.04	0.887	0.04
	30%	11.30	31.69	71.4	35.75	395.4	-6.80	66.3	0.22	0.889	0.22
Airbag Cost	-50%	8.58	0	52.6	0	424.2	0	66.1	-0.08	0.886	-0.08
	50%	8.58	0	52.6	0	424.2	0	66.2	0.08	0.888	0.08
Flotation System Mass	-20%	8.66	0.97	52.9	0.64	424.6	0.09	66.2	0.01	0.887	0.01
	20%	8.49	-1.05	52.1	-0.80	423.7	-0.12	66.2	-0.01	0.887	-0.01
Flotation System Cost	-50%	8.58	0	52.6	0	424.2	0	66.2	≈-0	0.887	≈-0
	50%	8.58	0	52.6	0	424.2	0	66.2	≈0	0.887	≈0
Retrieval Cost	-50%	8.58	0	52.6	0	424.2	0	65.9	-0.51	0.883	-0.51
	50%	8.58	0	52.6	0	424.2	0	66.5	0.51	0.892	0.51